CMI Graduate Student Projects: Volume 5

The Importance of Seaweed Wrack as Habitat and Resource in Cook Inlet
Brian Ulaski*

Subtidal Habitat Mapping in Lower Cook Inlet for Current and Predictive Sea Otter Habitat Associations
Elizabeth Hasan*

Acoustics of Cook Inlet Beluga Whales and Anthropogenic Noise in the Kenai River, Alaska
Sonia Kumar*

Feeding Ecology of Nearshore Fishes along a Gradient of Glacially-influenced Watersheds in Kachemak Bay, Alaska
Lindsey Stadler*

*College of Fisheries and Ocean Sciences, University of Alaska Fairbanks

September 2022
Final Reports
OCS Study BOEM 2022-054

Contact Information:

Email: UAF-CMI@alaska.edu

Coastal Marine Institute
College of Fisheries and Ocean Sciences
University of Alaska Fairbanks
P. O. Box 757220
Fairbanks, AK 99775-7220

These studies were funded in part by the U.S. Department of the Interior, Bureau of Ocean Energy Management (BOEM) under cooperative agreement M19AC00008 between BOEM Alaska Outer Continental Shelf Region and the University of Alaska Fairbanks. This report, BOEM 2022-054 is available through the Coastal Marine Institute, select federal depository libraries, and electronically from https://www.boem.gov/akpubs

The Importance of Seaweed Wrack as Habitat and Resource in Cook Inlet

Brian Ulaski

Subtidal Habitat Mapping in the Cook Inlet Lease Area for Current and Predictive Sea Otter Habitat Associations

Elizabeth Hasan

Acoustics of Cook Inlet Beluga Whales and Anthropogenic Noise in the Kenai River, Alaska

Sonia Kumar

Feeding Ecology of Nearshore Fishes along a Gradient of Glacially-influenced Watersheds in Kachemak Bay, Alaska

Lindsey Stadler

Brian Ulaski

The Importance of Seaweed Wrack as Habitat and Resource in Cook Inlet

Contents

List of Figures

List of Tables

Abstract

Seaweeds maintain their functional role as foundation species across near-subtidal and intertidal zones, including when detached and cast ashore as wrack where they are foraged by shorebirds, harvested by humans, and inhabited by many invertebrates. This study took place in Lower Cook Inlet, where seaweed harvesting is tightly regulated by the Alaska Department of Fish and Game. To determine the ecological importance of wrack, the composition and relative abundance of macroinvertebrates (direct impact) and shorebirds (indirect impact) using wrack were quantified monthly and compared to non-wrack areas. Macroinvertebrate communities in beach-cast wrack, drifting wrack, and bare sediment habitats were notably different. Beach-cast wrack generally had more biomass and abundance of coleopteran beetles and dipteran flies. Drifting wrack had more amphipods, snails, mussels, and polychaete worms. Bare sediment communities were primarily nematode worms. Total macroinvertebrate biomass and abundance were positively correlated with total wrack biomass and, in some cases, the tidal height of the wrack line. Aged wrack that had been cast ashore for 3-24 days harbored diverse and changing macroinvertebrate communities, with amphipods and dipterans being early colonizers, and coleopterans and hymenopterans arriving later. Bird assemblages were similar on and off the beach-cast wrack line, revealing the viable option of wrack as foraging grounds for local and migrating species. This research offers resource managers important information on the ecological roles of wrack on beaches in Alaska. Understanding this unique and ecologically important habitat will be useful for informing decisions to better protect the environment, including planning for oil spill response, as contaminated wrack likely influences macroinvertebrate community structure, higher trophic level consumers, and key ecological processes on beaches.

Introduction

The intertidal zone is a highly complex system with various energy pathways that transition across its interface. This ecotone receives energy and nutrients from multiple donor systems, supporting unique macrofaunal communities that rely on the allochthonous input of organic subsidies (Jaramillo et al. 2006). Effects of these cross-boundary subsidies (Polis et al. 1997) are seen in the productivity of intertidal food webs. Soft-sediment beaches, for example, are generally low in autochthonous primary production given the frequent disturbances of wave action, substrate instability, and exchanging of tides. Macrofauna at the fringe of the tide line on a beach are tolerant to these harsh conditions and increase productivity where macroalgal and terrestrial subsidies accumulate to form patches of habitat (Jaramillo et al. 2006). Nearshore reefs and inland riparian donor systems are sources of exported detritus that form habitat when deposited on beaches (Ulaski et al. in prep.).

Cumulatively, the organic debris that collects onshore is known as beach-cast wrack. Beach-cast wrack is mostly composed of macroalgae and terrestrial debris. It supports intertidal macroinvertebrates and higher trophic level consumers and forms an important habitat on beaches around the world in regions where macroalgae are found. Ecologically, wrack is key for maintaining diversity (Harris et al. 2014) and function (Defeo et al. 2009, Barreiro et al. 2011) on beaches by increasing macrofaunal biomass and species richness (Dugan et al. 2000, MacMillan and Quijón 2012, Ruiz-Delgado et al. 2015, Vieira et al. 2016). The unique assemblages of macroinvertebrates that converge and persist in beach-cast wrack feed higher trophic level consumers, including birds, mammals, and reptiles (Dugan et al. 2003, Mellbrand et al. 2011, Fox et al. 2014). Along the southwestern coasts of California and South Africa, where nearshore kelp beds are expansive, abundance of wintering shorebirds is positively correlated with beach-cast wrack cover and abundance of associated prey (Tarr and Tarr 1987, Hubbard and Dugan 2003, Dugan et al. 2003). This positive correlation may indicate that wrack can be a critical foraging resource for migrating shorebirds. Detached macroalgae and terrestrial debris can drift hundreds of kilometers in the ocean before washing ashore by tides, winds, and storms (Krumhansl and Scheibling 2012). As a precursor to beach-cast wrack, drifting wrack creates a unique habitat in the nearshore water column and benthos where macroinvertebrates and fish find refuge and forage among the loose organic debris (Baring et al. 2018).

Biotic conditions of macroalgal composition can influence the structure of associated macrofaunal communities, which, in turn, can affect the persistence of wrack on beaches. Morphological differences among macroalgae that contribute to beach-cast wrack can determine the complexity and appeal of the habitat for intertidal consumers (MacMillan and Quijon 2012). For example, some consumers prefer kelp wrack over seagrass or rockweed wrack due to more mucus secretion and lower concentrations of phenols in kelps (Mews et al. 2006, Michaud et al. 2019). Seasonality of macroalgal growth and general temporal oscillations of macroinvertebrate abundances (Ely et al. 2018) may be exemplified in the communities that develop in wrack over time. Abiotic factors also affect the structure of wrack communities. Variability in wrack supply can be explained by interactions of wave exposure, substrate type, and seasonality (Barreiro et al.

2011, Wickham et al. 2020). Beach slope is negatively correlated with the accumulation of beach-cast wrack (Harris et al. 2014, Wickham et al. 2020, Ulaski et al. in prep.) and species richness of non-wrack associated benthic intertidal macroinvertebrates (McLachlan 1996).

After wrack is deposited onto beaches, it begins desiccation and burial, goes back out to sea during a subsequent higher tide, or gets transported higher up the beach (Orr et al. 2005). Desiccation and decomposition of beach-cast wrack affect organism colonization and successional development of the wrack community (Olabarria et al. 2007). Succession of macroinvertebrate users of wrack is apparent throughout the stages of wrack decomposition (Colombini et al. 2000, Olabarria et al. 2007, Beeler et al. 2009), and rates of decomposition vary among macroalgal species (Mews et al. 2006). Aging wrack results in changes to the microclimate that it creates for consumers (Davis and Keppel 2021), and aged wrack is generally preferred over fresh wrack (Beeler 2009).

As wrack decomposes, it releases nutrients into the surrounding area, acting as a natural fertilizer for nearby vegetation (Dugan and Hubbard 2010, Dugan et al. 2011). Wrack contains nitrogen, phosphorus, potassium, and many trace elements that are desired for healthy plant growth. In addition to wrack being applied to the soil as a mulch, it can be added to compost heaps as an activator. This recognition has led to increased harvesting of wrack for use as garden fertilizer. Wrack is harvested for personal and commercial uses in the US (Alaska), Canada, Australia, and Ireland (Kirkman and Kendrick 1997, McLaughlin et al. 2006, Holden et al. 2018). Removal of wrack from beaches is also common practice in areas where recreation and tourism are high (Fairweather and Henry 2003, Noriega et al. 2012). Studies have shown considerable ecological consequences associated with wrack removal, including a reduction in species richness, abundance, and biomass of wrack-associated macrofauna (Dugan et al. 2000, Davenport and Davenport 2006, Defeo et al. 2009).

This study addresses four objectives to explore the importance of wrack as habitat and resource in a high-latitude estuary, with a particular focus on characterizing the organisms that utilize wrack. Results of this study can be used to inform the management of this resource.

Objectives

1. Characterize macroinvertebrate communities among beach-cast wrack, drifting wrack, and bare sediment habitats over time.
2. Determine if macroinvertebrate communities in beach-cast wrack, drifting wrack, and bare sediment habitats correlate with biotic and abiotic environmental variables.
3. Determine which birds associate with beach-cast wrack.
4. Determine if there are successional states in macroinvertebrate communities as beach-cast wrack ages.

Methods

Study Area

This study was conducted in Kachemak Bay, a large fjord-type estuary in Lower Cook Inlet, Alaska (Figure 1). Some incoming oceanic water diverging from the Alaskan Coastal Current mixes with local waters and enters Kachemak Bay joining the flow that generally circulates counterclockwise along the coastline to ultimately flow out of the north (Johnson 2021). Macroalgal reefs around the bay are exposed to dynamic high latitude conditions including wind-induced stress, extreme tidal forcing, and glacially influenced freshwater flux, contributing to the accumulation of subtidal drifting organic material that washes ashore as wrack. This beach-cast wrack is commonly harvested by the public for personal use as an additive to garden fertilizer (G. Hollowell, Alaska Department of Fish and Game, pers. comm.) though, in most places, it is highly regulated (Table 1).

Twelve beaches were chosen throughout the bay in areas easily accessible to the public along the Homer and Seldovia road systems or by small boat: Anchor Point, Bishop's Beach, Bluff Point, Camel Rock, Grewingk River, Halibut Cove, outer Jakolof Bay, inner Jakolof Bay, MacDonald Spit, Outside Beach, Tutka Bay, and Wosnesenski River (Figure 1). Beaches were sampled monthly from April to August in 2021 and parameters examined (i.e., beach-cast wrack, drifting wrack, and bare sediment) varied by beach. These months were selected given the results of a pilot study that demonstrated that macroinvertebrates were rare during winter months, likely due to life histories and icy conditions in which wrack was usually frozen and covered in snow.

All sites were characterized for wave exposure, beach slope, and substrate type to examine relationships between static environmental conditions and macroinvertebrate communities found in beach-cast wrack, drifting wrack, and bare sediment habitats (Table 1). Wave exposure and beach slope were determined from NOAA's Alaska ShoreZone website (https://alaskafisheries.noaa.gov/mapping/sz_js/), under "Derived ShoreZone Attributes." Wave exposure was determined by the "Biological Wave Exposure" data from where exposure ranks of exposed, protected, semi-exposed, or semi-protected are classified. Beach slope was identified under "Intertidal Zone Slope," where calculated slopes (in degrees) are provided. Substrate type was characterized one time for each site using a modified Wentworth scale within ten 1-m^2 quadrats haphazardly placed along the wrack line, from which percent cover of boulder, cobble, gravel, and sand was visually estimated (Wentworth 1922).

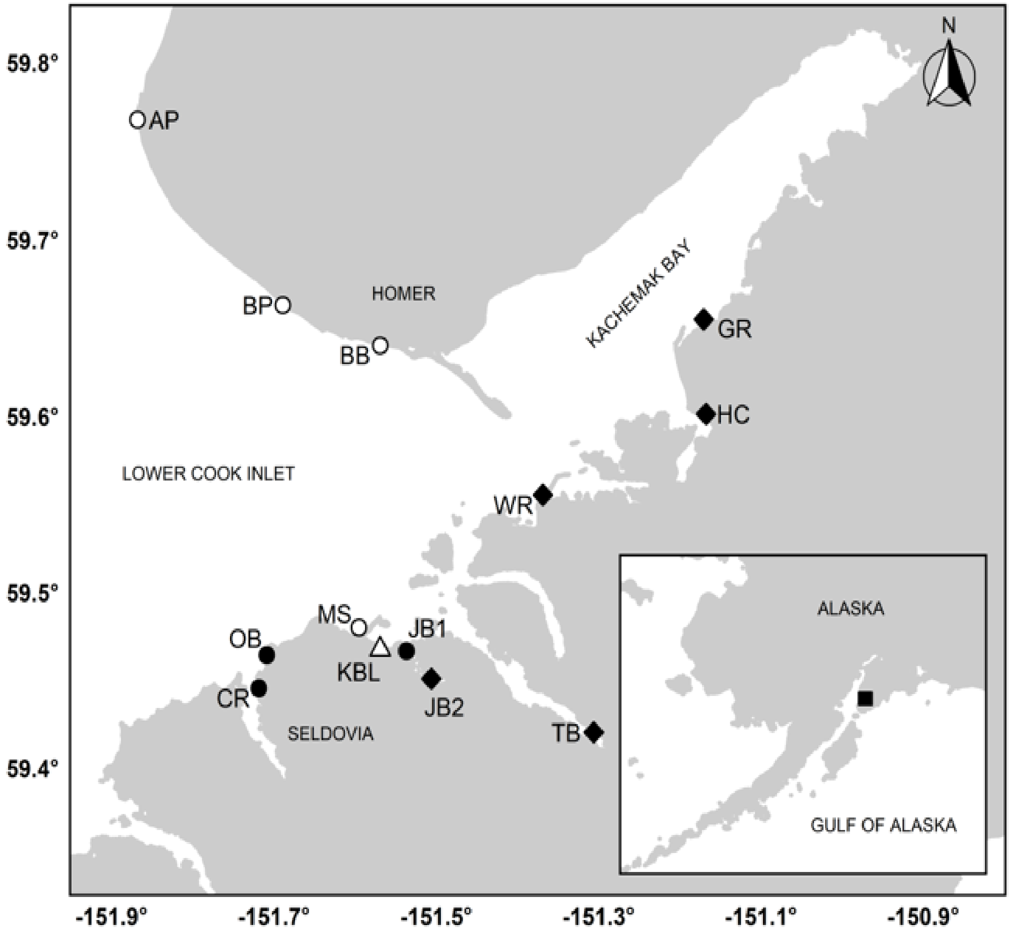

Figure 1. Map showing study beaches located in Kachemak Bay, Alaska (black rectangle of inset map). Circles denote study beaches from which beach-cast wrack and bare sediment samples were collected. Open circles denote where bird surveys were conducted. Black diamonds denote study beaches from which beach-cast wrack and drifting wrack samples were collected. The white triangle denotes the National Oceanic and Atmospheric Administration NOAA/University of Alaska Fairbanks Kasitsna Bay Laboratory where macroinvertebrate community succession in aging wrack experiments were conducted.

Table 1. Beach characteristics including regulations for personal-use harvests, wave exposure, beach slope, and percent cover of substrate types.

Location	Site	Personal-Use Harvest Limits	Wave Exposure	Slope (˚)	Boulder (%)	Cobble (%)	Gravel (%)	Sand (%)
Anchor Point	AP	Weight + Season	Semi-Exposed	1	0.0	11.2	16.8	72.0
Bishop's Beach	BB	Weight + Season	Semi-Protected	1	0.0	80.9	19.1	0.0
Bluff Point	BP	Weight + Season	Semi-Exposed	2	1.5	15.6	13.1	69.8
Camel Rock	CR	Weight	Semi-Exposed	9	0.0	3.5	94.5	2.0
Grewingk River	GR	Weight + Season	Semi-Exposed	8	0.0	17.0	39.5	43.5
Halibut Cove	HC	Weight + Season	Semi-Protected	10	0.0	0.0	95.0	5.0
outer Jakolof Bay	JB1	Weight	Protected	6	0.0	30.0	70.0	0.0
inner Jakolof Bay	JB2	Weight	Protected	19	90.0	10.0	0.0	0.0
MacDonald Spit	MS	Weight	Semi-Exposed	7	0.0	0.0	28.6	71.4
Outside Beach	OB	Weight	Semi-Exposed	7	0.0	0.4	99.6	0.0
Tutka Bay	TB	Weight + Season	Protected	2	0.0	25.2	74.8	0.0
Wosnesenski River	WR	Weight + Season	Semi-Exposed	5	0.0	0.0	34.0	66.0

Personal-use harvest limits: Weight = 10 gal/person/day
Personal-use season: wrack harvests allowed January 1 to April 30 and September 1 to December 31

Wrack and Macroinvertebrate Collections

Biomass and composition of macroalgal wrack along with biomass, composition, and abundance of macroinvertebrates that appeared in the beach-cast wrack and in the sand under the wrack were determined monthly at all twelve beaches. Along a 50-m horizontal (along-shore) transect, a vertical (cross-shore) transect was placed every five meters between the upper and lower boundaries of the wrack line, defined by trailing pieces of wrack that were separated by at least 1 m. Randomly along each vertical transect, one 11-cm diameter steel corer was pushed down through the wrack and into the underlying sediment to a depth of approximately 10 cm to collect macroalgae and macroinvertebrates in the beach-cast wrack (n = 10 beach-cast wrack cores/site/month; Deidun et al. 2009, MacMillan and Quijón 2012, Heerhartz et al. 2014). Bare sediment cores were also taken at seven of the beaches (Anchor Point, Bishop's Beach, Bluff Point, Camel Rock, outer Jakolof Bay, MacDonald Spit, and Outside Beach) to a depth of approximately 10 cm at least 1 m away from the wrack line (both landward and seaward) to qualitatively assess macroinvertebrate habitat association in bare substrate (n = 10 bare sediment cores/beach/month).

Drifting wrack was collected at five of the beaches (Grewingk River, Halibut Cove, inner Jakolof Bay, Tutka Bay, and Wosnesenski River) by beach seining and was sampled from the nets using the same 11-cm diameter corer used to collect beach-cast wrack and bare sediment samples. Three nearshore beach seines were pulled by two people walking parallel to the shoreline for 4-5 minutes, one in ankle-deep water and one in approximately waist-deep water (net length = 15 m; mesh size = 1.2 cm). Once the net was brought ashore, the cores were placed at three fixed points near the cod end, but not pushed into the sediment, to collect any retained drifting macroalgae and macroinvertebrates from the drifting wrack debris ($n = 9$ drifting wrack cores/beach/month).

All beach-cast wrack, drifting wrack, and bare sediment cores were immediately sieved separately through a 1-mm mesh bag in the swash zone (Dugan et al. 2003, McLachlan and Brown 2006, Schlacher et al. 2008b, Deidun et al. 2009, MacMillan and Quijón 2012). All retained macroalgae and macroinvertebrates were immediately bagged by replicate and transported to a -20˚C freezer at the NOAA/UAF Kasitsna Bay Laboratory until subsequent processing. Frozen samples were thawed in trays filled with a thin layer of seawater. Thawed samples were sorted, macroalgae were identified and weighed, and macroinvertebrates were identified to the lowest practical taxonomic level, counted, and weighed. Processed macroinvertebrate samples were sent to the Museum of the North at the University of Alaska Fairbanks for identification confirmation and long-term curation.

During each monthly sampling event, tidal elevation of the beach-cast wrack line was measured using a site level and stadia rod. Ten haphazardly chosen macroalgal samples of approximately 10 g each were collected from the wrack line for moisture content analysis using a loss-on-drying (LOD) technique (see Olabarria et al. 2007, MacMillan and Quijon 2012). Briefly, each macroalgal wrack sample was weighed separately, dried in a drying oven at a constant temperature of 60˚C (for at least 24 h) until a constant weight was achieved (± 0.01 g), and re-weighed to determine percent moisture content.

Statistical analyses were carried out in PRIMER v7 software with the PERMANOVA+ package and the opensource R software (R Core Team 2021) Multivariate data were fourth root transformed to increase normality following standardization so that measurements on relative community biomass and abundance were comparable given the slightly different methods of core collections among habitats (i.e., beach-cast wrack, drifting wrack, and bare sediment). Univariate data remained non-normal (Shapiro-Wilk test, biomass: $p < 0.001$; abundance: $p < 0.001$), but the robustness of analysis of variance (ANOVA) was considered appropriate for univariate analysis given the very large number of samples collected. Separate one-way ANOVA tests were used to determine variability in total macroinvertebrate biomass and abundance by site, month, and habitat (i.e., beach-cast wrack, drifting wrack, and bare sediment). When ANOVA tests suggested significance, Tukey honest significant difference (HSD) post-hoc tests were carried out to confirm pairwise differences. Separate resemblance matrixes were calculated using a Bray-Curtis similarity index for permutational analysis of multivariate macroinvertebrate community relative biomass and abundance data. A three-factor permutational multivariate analysis of variance (PERMANOVA) was used to test for responses of macroinvertebrate communities to grouping factors of site, month, and habitat. Non-metric multidimensional scaling (NMDS) ordinations were used to visually explore compositional dissimilarities among grouping factors. Similarity percentage (SIMPER) analyses were carried out to determine which macroinvertebrate taxa were most responsible for driving compositional differences among grouping factors. Pearson correlation coefficients were computed to assess relationships between beach-cast wrack, drifting wrack, and bare sediment macroinvertebrate communities and wrack line (tidal height, moisture content, and macroalgal biomass) and beach characteristics (wave exposure, beach slope, and substrate types). A cyclic resemblance model matrix was used in the RELATE routine to assess monthly shifts in macroinvertebrate communities.

Bird Survey

At four of the beaches (Anchor Point, Bishop's Beach, Bluff Point, and MacDonald Spit), a 1-km section of coastline was identified, georeferenced, and revisited every month from April to August in 2021 to conduct bird surveys. Survey sections were chosen based on their predominately sandy beach characteristics. Surveys were intentionally conducted between 2.4 and 4.6 m tidal height so that enough of the beach was exposed (Tarr and Tarr 1987, Dugan et al. 2003, Lafferty et al. 2013). A modified distance sampling approach was used (Tarr and Tarr 1987, Hubbard and Dugan 2003, Neuman et al. 2008, Byrne et al. 2009, Brown et al. 2012) that consisted of walking parallel to shore, centered between the bluffs and swash zone. There were three 200-m blocks within the 1-km section where the surveyor walked line transects for approximately 5 minutes (n = 3 line transects/beach/month). The location of the blocks within the 1-km section were randomized each month. In each block, the beach was divided into horizontal distance bins that were approximately 15-m wide. Habitat features within each bin were recorded, such as substrate type and presence or absence of wrack during each survey. The wrack line was expected to occupy different bins depending on the tidal activity prior to each survey event. Birds were counted, identified, and designated to a bin within the vertical boundaries of the outermost bins. Since birds were rare in our field surveys, no formal distance sampling analyses could be completed. As such, all transects were pooled and a single-factor PERMANOVA was used to test for the response of bird assemblages on and off the beach-cast wrack line. Field observations are discussed.

Succession Experiment

To determine if there was succession in the wrack-associated macroinvertebrate communities as wrack aged, 18 marked piles each with 1 to 2 kg wet weight of freshly harvested macroalgae (e.g., kelps, rockweed, *Ulva* spp., *Palmaria* spp., filamentous algae) and collected terrestrial debris were combined and mixed by hand to create artificial wrack piles and deposited just above the highest predicted tide line of the cycle on a beach near the NOAA/UAF Kasitsna Bay Laboratory (as in Olabarria et al. 2007 and MacMillan and Quijón 2012). Piles were placed approximately 1 to 2 m apart and other naturally present accumulations of wrack were removed before placing the experimental plots. Experiments were conducted monthly from April to August 2021 (n = 18 experimental wrack piles/month). A pilot study conducted in March of 2020 indicated the absence of macroinvertebrates in frozen wrack covered in snow. Survey flags were placed next to each pile to mark their positions. Starting on Day 0, three of the piles were randomly sampled every three days (every six days in August) to quantify temporal changes in the macroinvertebrate communities (n = 3 experimental cores/sampling day). Each pile of wrack was sampled using one 11-cm diameter steel sediment corer pushed down through the wrack and into the underlying sediment to a depth of approximately 10 cm (Deidun et al. 2009, MacMillan and Quijón 2012, Heerhartz et al. 2014). Control cores were taken from bare sediments to a depth of approximately 10 cm at least 1 m away from the experimental wrack piles during each sampling event (n = 3 control cores/sampling day). All experimental and control cores were immediately sieved separately through a 1-mm mesh bag (Dugan et al. 2003, McLachlan and Brown 2006, Schlacher et al. 2008b, Deidun et al. 2009, MacMillan and Quijón 2012). Retained macroalgae and macroinvertebrates from the sieved cores were immediately bagged by replicate and transported to a -20˚C freezer at the NOAA/UAF Kasitsna Bay Laboratory until subsequent processing. Frozen samples were thawed in trays filled with a thin layer of seawater. Thawed samples were sorted, macroalgae were weighed, and macroinvertebrates were identified to the lowest practical taxonomic level, counted, and weighed.

HOBO Pendant temperature loggers (Onset; Bourne, MA) were used to determine temperature microhabitats formed by the experimental wrack piles for the duration of each monthly experiment. Among the experimental wrack piles, loggers were attached to rebar and fixed above the sediment to record external ambient air temperatures over time (n = 2 external loggers). Loggers were also placed within wrack piles (n = 2 internal loggers) and buried in the sand underneath wrack piles (n = 2 buried loggers). Separate samples of macroalgae from each wrack pile were taken alongside each core for moisture content analysis using the LOD technique as described above (n = 3 moisture content samples/sampling day).

A Bray-Curtis similarity index was calculated to produce a resemblance matrix for permutational analysis of multivariate macroinvertebrate community data collected from the succession experiments. A three-factor PERMANOVA was used to determine macroinvertebrate community differences between experimental and control groups and to test for succession in wrack-associated macroinvertebrate communities over time (days and months). Separate one-way ANOVA tests were used to determine variability in total macroinvertebrate biomass and abundance and diversity (Shannon Index) by day of experiment and treatment (experimental and control). When ANOVA tests suggested significance, Tukey honest significant difference (HSD) post-hoc tests were carried out to confirm pairwise differences. SIMPER analyses were carried out to determine which taxa were most responsible for driving compositional differences over time. Pearson correlation coefficients were calculated to determine which environmental variables (moisture content and internal temperature of wrack) correlated with variability in macroinvertebrate community composition.

Results

Macroinvertebrate Communities

A total of 80 different taxa were identified from 37,653 individuals collected from beach-cast wrack, drifting wrack, and bare sediment habitats (Table 2). With all months and sites combined, total macroinvertebrate biomass and abundance differed among the three habitats (ANOVA, biomass: $F_{2,1145} = 19.1$, $p < 0.001$; abundance: $F_{2,1145} = 14.5$, $p < 0.001$; Figure 2). Total macroinvertebrate biomass and abundance in bare sediment were significantly lower than beach-cast wrack (Tukey, biomass: $p < 0.001$; abundance: $p < 0.001$) and drifting wrack (Tukey, biomass: $p < 0.001$; abundance: $p < 0.001$) habitats (Figure 2). Total macroinvertebrate biomass in beach-cast wrack was significantly lower than in drifting wrack; however, total macroinvertebrate abundance was similar between beach-cast and drifting wrack habitats (Tukey, biomass: $p < 0.01$; abundance: $p = 0.28$). Differences in total macroinvertebrate biomass and abundance in beach-cast wrack were significant over time and among beaches (Table 3; Figure 4). Differences in total macroinvertebrate abundance in drifting wrack were also significant over time (Table 3; Figure 3) but not significant among beaches (Table 3; Figure 4).

Table 2. Taxonomic list of all macroinvertebrates identified from beach-cast wrack (BW), drifting wrack (DW), and bare sediment (BS) habitats. The habitat column indicates the habitats from which the taxa were collected.

Class	**Order**	**Family**	**Subfamily**	**Genus**	**Species**	**Habitat**
Annelida						BW
Arachnida	Acari					BW/BS
	Araneae					BW/DW
		Gnaphosidae				DW
	Trombidiformes	Bdellidae		*Neomolgus*	*littoralis*	BW/BS
Asteroidea	Forcipulatida	Asteriidae				BW/DW
Bivalvia	Cardiida	Cardiidae		*Clinocardium*		BW/DW
		Tellinidae		*Macoma*		BW/DW
	Carditida	Astartidae		*Astarte*		BW/DW
	Myida	Myidae		*Mya*		BW/DW
	Mytilida	Mytilidae				BW/DW/BS
	Venerida	Veneridae		*Saxidomus*		BW
Chilopoda	Geophilomorpha					BW/DW/BS
	Lithobiomorpha					BW/DW
Echinoidea	Echinoida	Strongylocentrotidae		*Strongylocentrotus*		BW
Entognatha	Collembola					BW/DW/BS
Euchelicerata	Pseudoscorpiones	Neobisiidae	Microcreagrinae	*Halobisium*	*occidentale*	BW/DW/BS
Gastropoda						BW/DW/BS
	Cephalaspidea	Gastropteridae		*Gastropteran*	*pacificum*	DW
	Lottiidae					BW/DW
Gymnolaemata	Ctenostomata	Flustrellidridae		*Flustrellidra*	*corniculata*	BW
Holothuroidea						BW/DW
Insecta	Coleoptera	Hydrophilidae				BW
		Anthicidae				BW
		Carabidae				BW/DW
		Circulionidae	Molytinae	*Sthereus*		BW
		Coccinellidae				DW
		Elateridae	Dendrometrinae	*Hypolithus*	*littoralis*	BW
		Heteroceridae				BW/DW
		Hydraenidae				BW
		Lycidae		*Dictyoptera*	*simplicipes*	BW
		Scarabaeidae	Aphodiinae			DW
		Scraptiidae				BW
		Staphylinidae				BW/DW/BS
			Aleocharinae			BW/DW
			Aleocharinae	*Amblopusa*	*brevipes*	BW/BS
			Staphylininae			BW
				Eusphalerum		BW
				Hadrotes	*crassus*	BW
	Diptera					BW/DW/BS
		Empididae				BW

Class	**Order**	**Family**	**Subfamily**	**Genus**	**Species**	**Habitat**
		Chironomidae				BW/DW
		Bibionidae				BW/DW
		Culicidae				BW
		Sciaridae				BW
		Tipulidae				BW/DW
	Ephemeroptera					DW
	Hemiptera					BW/DW
		Aphididae				BW/DW
		Cicadellidae				BW/DW
		Psylloidea				BW
		Saldidae				BW
	Hymenoptera					DW
		Ichneumonidae				BW/DW
		Braconidae	Alysiinae			BW/DW/BS
		Figitidae	Eucoilinae			BW/DW
		Formicidae	Formicinae	*Camponotus*	*herculeanus*	BW
				Formica		BW
		Vespidae	Vespinae	*Vespula*		BW
	Lepidoptera					BW/DW
	Neuroptera	Hemerobiidae				DW
	Plecoptera					BW/DW
	Trichoptera					BW
Malacostraca	Amphipoda	Ampithoidae		*Peramphithoe*	*mea*	DW
		Caprellidae				BW
		Talitridae		*Traskorchestia*	*traskiana*	BW/BS
	Cumacea					BW/DW/BS
	Decapoda	Majidae		*Hyas*	*lyratus*	DW
		Brachyura				BS
		Caridae				DW
		Paguridae				BW/DW
	Isopoda					BW/DW/BS
Nematoda						BW/DW/BS
Ophiuroidea						DW
Polychaeta						BW/DW/BS
	Eunicida	Lumbrineridae		*Scoletoma*		BW/DW
	Terebellida	Flabelligeridae		*Brada*		BW
Polyplacophora	Chitonida	Ischnochitonidae	Lepidochitoninae	*Tonicella*		BW
Stenolaemata	Cyclostomata	Crisiidae		*Crisia*		BW/DW
Thecostraca	Cirripedia					BW/DW/BS

Table 3. ANOVA results for total macroinvertebrate biomass and abundance (bold numbers indicate significant difference).

Habitat	Variable	Data	*F*-value	*df*	Residuals	*p*-value
Beach-Cast Wrack	Month	Biomass	6.4	4	570	**<0.001**
Beach-Cast Wrack	Month	Abundance	12.4	4	570	**<0.001**
Beach-Cast Wrack	Site	Biomass	4.6	11	563	**<0.001**
Beach-Cast Wrack	Site	Abundance	6.2	11	563	**<0.001**
Drifting Wrack	Month	Biomass	0.5	4	218	0.7
Drifting Wrack	Month	Abundance	2.7	4	218	**0.03**
Drifting Wrack	Site	Biomass	0.6	11	218	0.9
Drifting Wrack	Site	Abundance	1.5	11	218	0.1
Bare Sediment	Month	Biomass	1.8	4	345	0.1
Bare Sediment	Month	Abundance	1.5	4	345	0.2
Bare Sediment	Site	Biomass	1.0	11	343	0.5
Bare Sediment	Site	Abundance	0.8	11	343	0.6

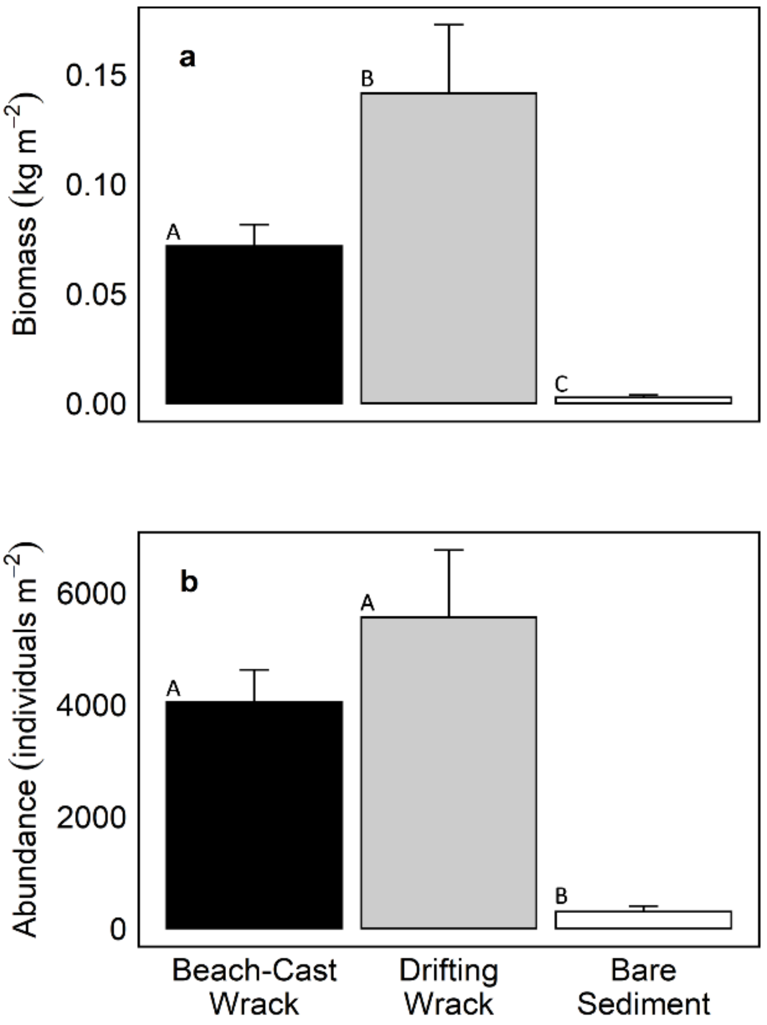

Figure 2. Bar plots of mean total macroinvertebrate (a) biomass (kg m^{-2}) and (b) abundance (individuals m^{-2}) for beach-cast wrack, drifting wrack, and bare sediment habitats (bars represent standard error). Significantly different means among habitats are denoted by the letters above each bar.

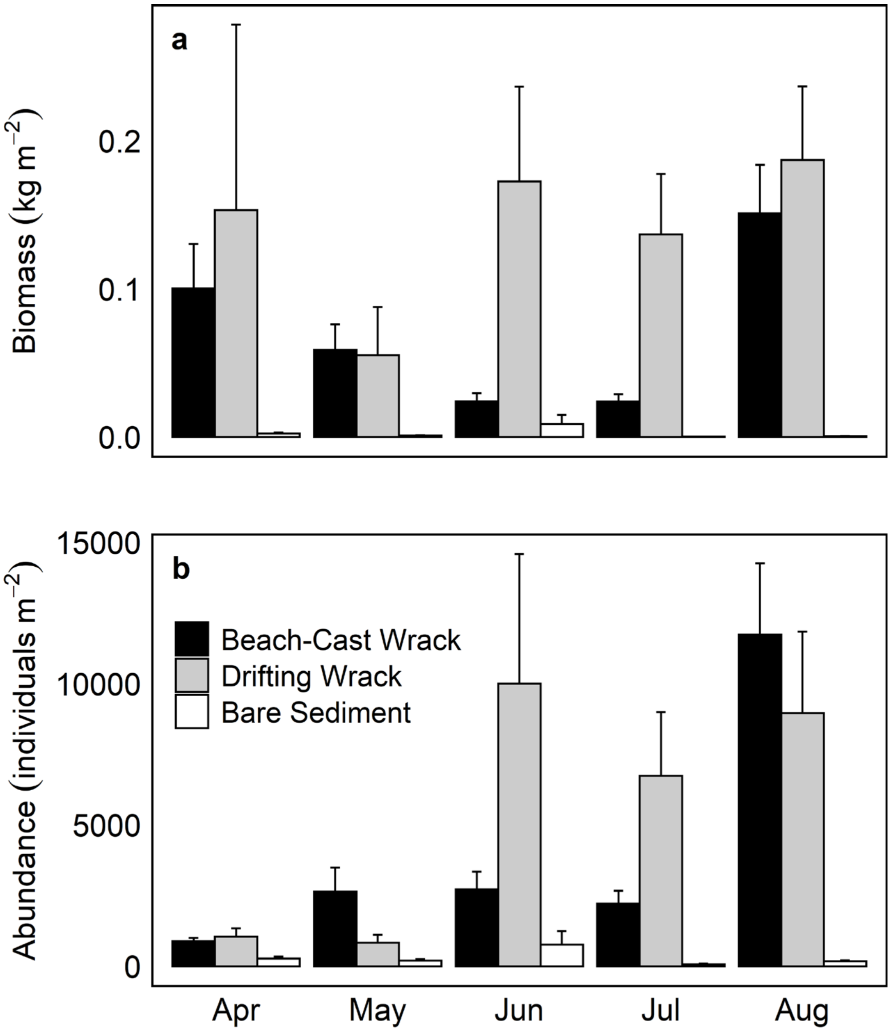

Figure 3. Bar plots of monthly mean total macroinvertebrate (a) biomass (kg m^{-2}) and (b) abundance (individuals m^{-2}) for beach-cast wrack, drifting wrack, and bare sediment habitats (bars represent standard error).

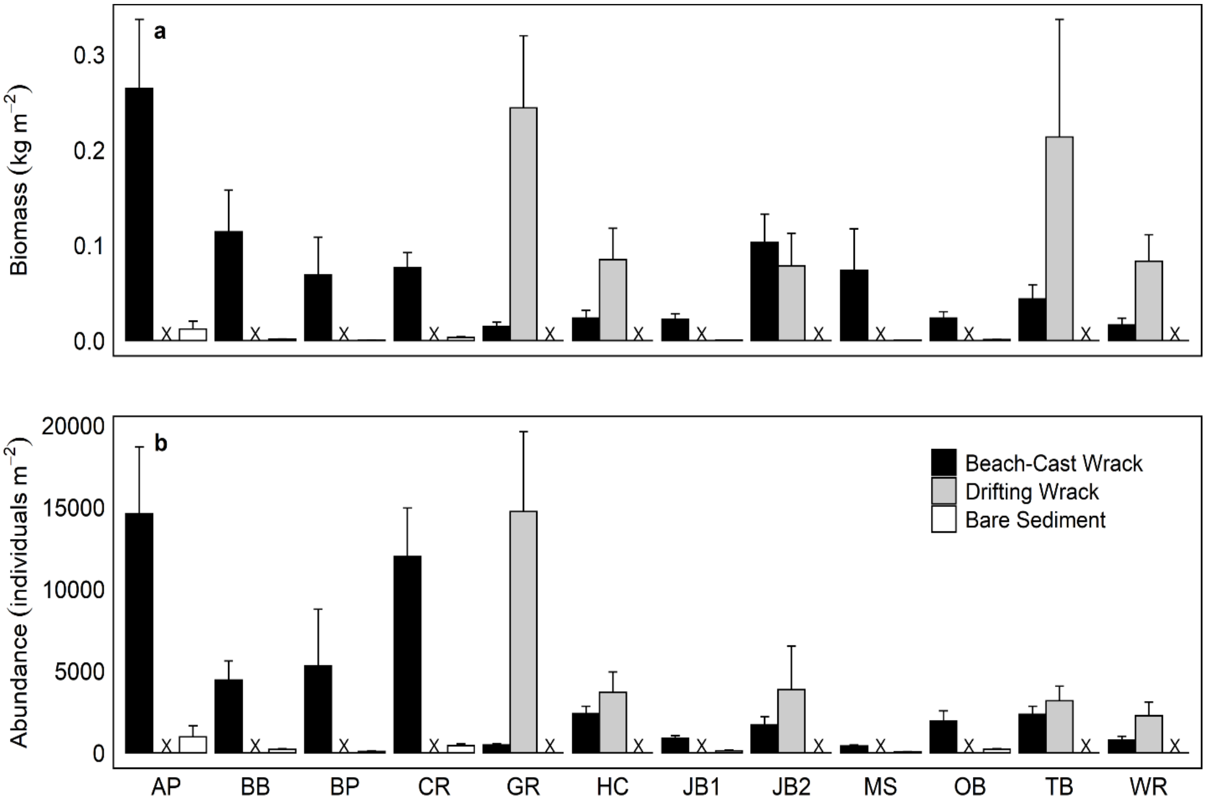

Figure 4. Bar plots of mean total macroinvertebrate (a) biomass (kg m^{-2}) and (b) abundance (individuals m^{-2}) for beach-cast wrack, drifting wrack, and bare sediment habitats (bars represent standard error) across study beaches. Habitats with no data for a given site are denoted by "X."

Macroinvertebrate community relative biomass and abundance were significantly different among beach-cast wrack, drifting wrack, and bare sediment habitats (PERMANOVA, biomass: $F_{12,718} = 4.9$, $p = 0.001$; abundance: $F_{12,704} = 5.8$, $p = 0.001$; Figure 5). SIMPER analyses revealed that differences in macroinvertebrate communities based on both relative biomass and abundance among habitats were mostly driven by the taxonomic orders of Amphipoda, Cirripedia, Coleoptera, Diptera, Gastropoda, Mytilida, Nematoda, Polychaeta (Figure 6). Beach-cast wrack generally had more Cirripedia (molts), Coleoptera, and Diptera. Drifting wrack generally had more Amphipoda, Gastropoda, Mytilida, and Polychaeta. Bare sediment was consistently composed mostly of Nematoda. Differences in macroinvertebrate community composition were also significant among beaches and over time (Table 4). Though there were monthly differences in macroinvertebrate community composition, there were no significant seasonal trends across habitats (Table 5; Figure 7). SIMPER analyses revealed that monthly differences in macroinvertebrate communities based on both relative biomass and abundance in all habitats were mostly driven by Amphipoda, Cirripedia, Coleoptera, Cyclostomata, Diptera, Gastropoda, Mytilida, Nematoda, Polychaeta (Figure 8).

Table 4. PERMANOVA results for macroinvertebrate community biomass and abundance. Data are standardized and fourth root transformed.

Variable	Data	*F*-value	*df*	Residuals	*p*-value
Habitat	Community Biomass	4.9	12	718	**0.001**
Habitat	Community Abundance	5.8	12	704	**0.001**
Month	Community Biomass	3.2	4	718	**0.001**
Month	Community Abundance	3.7	4	704	**0.001**
Site	Community Biomass	8.7	11	718	**0.001**
Site	Community Abundance	9.2	11	704	**0.001**

Table 5. RELATE results for macroinvertebrate community biomass and abundance. Data are standardized and fourth root transformed.

Data	Habitat	Pearson's *R*	*p*-value
Community Biomass	Beach-Cast Wrack	0.5	0.2
Community Biomass	Drifting Wrack	0.3	0.3
Community Biomass	Bare Sediment	0.1	0.3
Community Biomass	Global Test (Habitats Combined)	-0.1	0.8
Community Abundance	Beach-Cast Wrack	0.5	0.1
Community Abundance	Drifting Wrack	0.3	0.2
Community Abundance	Bare Sediment	0.1	0.5
Community Abundance	Global Test (Habitats Combined)	-0.1	0.8

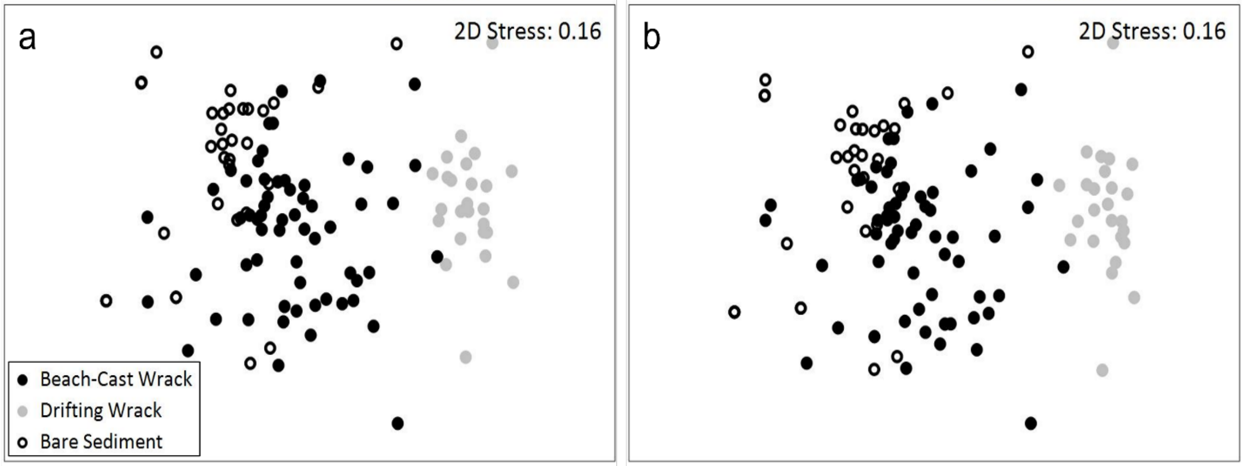

Figure 5. Non-metric multidimensional scaling (NMDS) ordination plots based on relative macroinvertebrate community (a) biomass and (b) abundance in beach-cast wrack, drifting wrack, and bare sediment habitats. Taxonomic resolution is at the level of order. Each point represents a monthly sampling event per site.

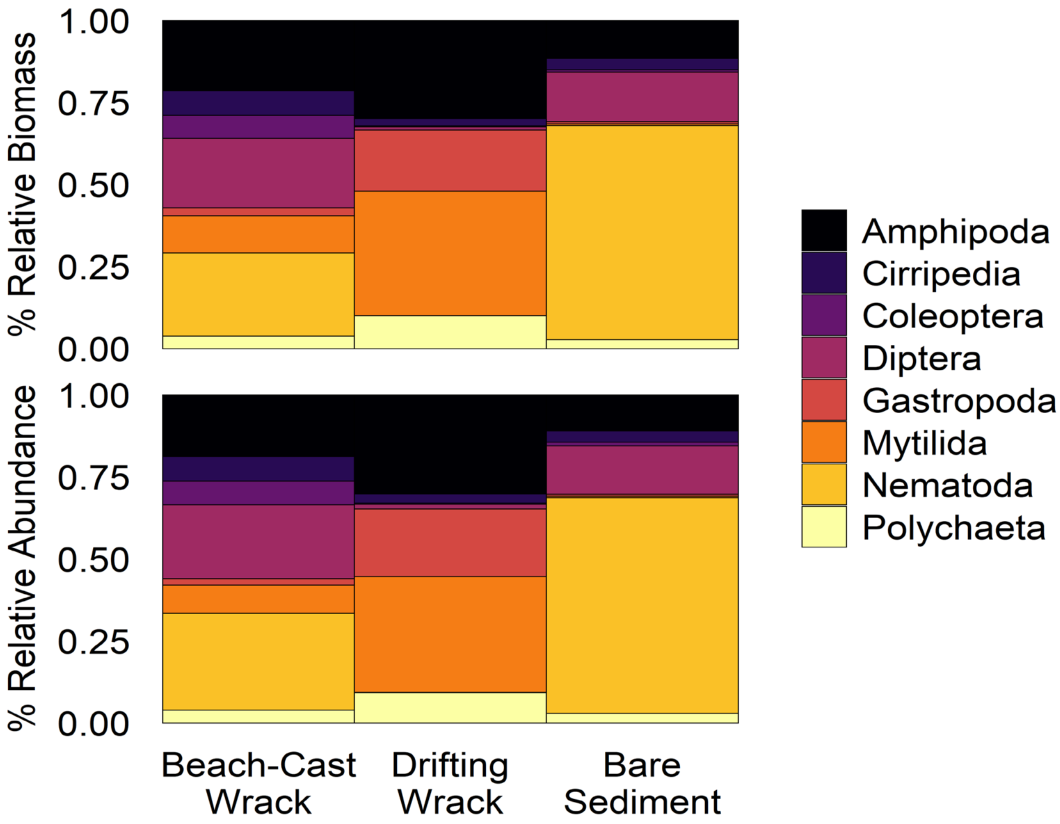

Figure 6. Stacked bar plots of macroinvertebrate taxa that were significant contributors to compositional differences of relative biomass (top panel) and abundance (bottom panel) among beach-cast wrack, drifting wrack, and bare sediment habitats.

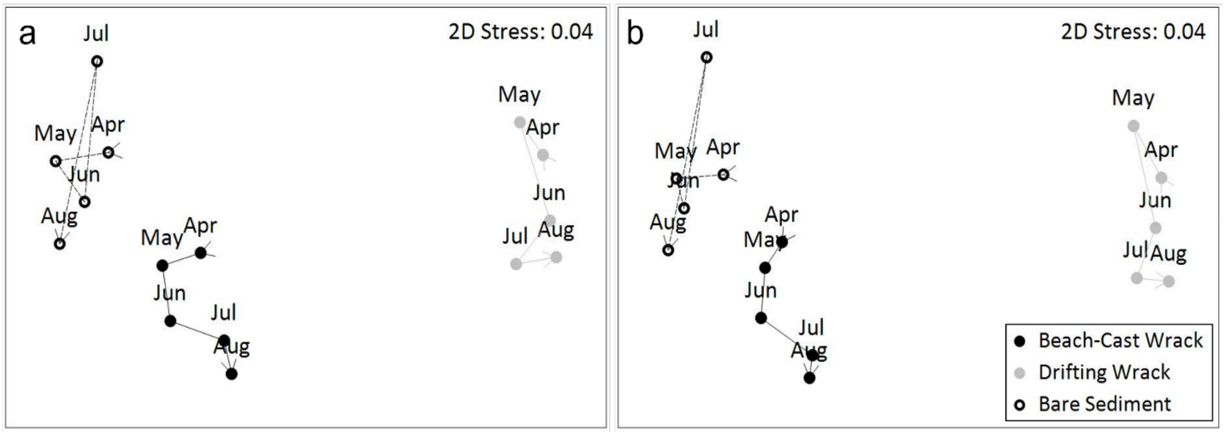

Figure 7. Non-metric multidimensional scaling (NMDS) ordination plots based on relative macroinvertebrate community (a) biomass and (b) abundance in beach-cast wrack, drifting wrack, and bare sediment habitats. Taxonomic resolution is at the level of order. Each point represents a monthly sampling event.

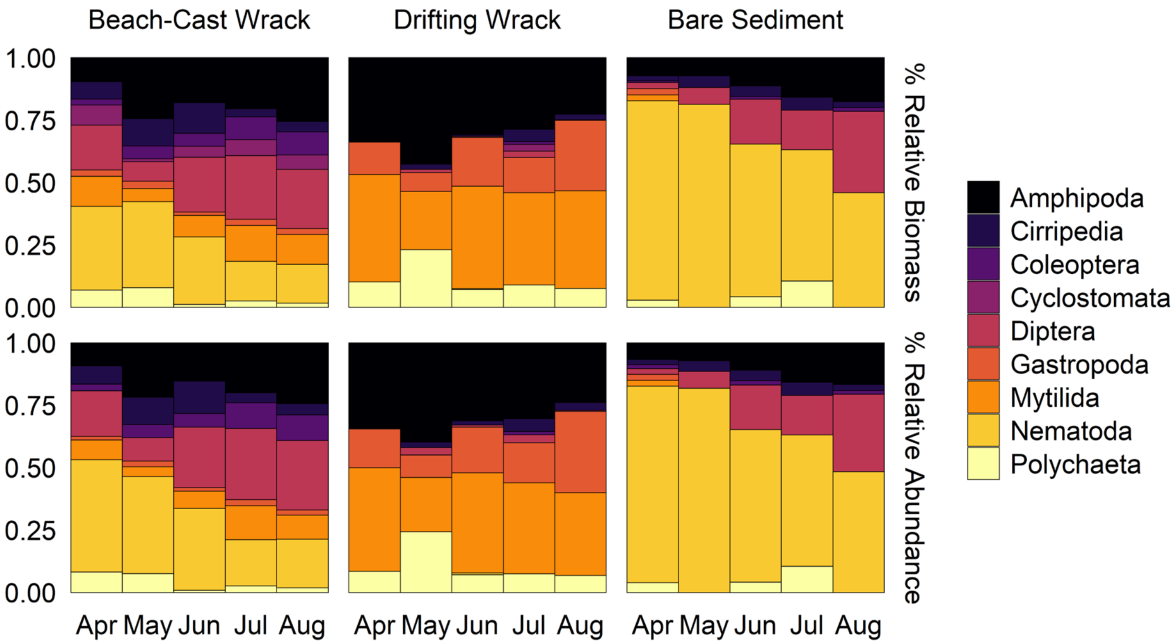

Figure 8. Stacked bar plots of macroinvertebrate taxa that were significant contributors to monthly compositional differences of relative biomass (top panels) and abundance (bottom panels) among beach-cast wrack, drifting wrack, and bare sediment habitats.

Response of Macroinvertebrate Communities to Environmental Characteristics

Draftsman plots indicated collinearity of percent boulder substrate with beach slope so these data were removed from the analysis (with a correlation cutoff of $|r| \geq 0.80$). Shannon Index calculated for macroinvertebrate communities based on biomass in beach-cast wrack was positively correlated with the tidal height of the wrack line and negatively correlated with percent sand substrate (Figure 9). Whereas Shannon Index for macroinvertebrate communities based on biomass in drifting wrack and bare sediment habitats did not correlate with any of the tested environmental variables (Figure 9). Shannon Index calculated for macroinvertebrate communities based on abundance in beach-cast wrack was positively correlated with the tidal height of the wrack line and wrack biomass, and negatively correlated with wave exposure (Figure 10). Whereas Shannon Index for macroinvertebrate communities based on abundance in drifting wrack and bare sediment habitats did not correlate with any of the tested environmental variables (Figure 10). Total macroinvertebrate biomass in both beach-cast and drifting wrack was positively correlated with wrack biomass (Figure 11). Whereas total macroinvertebrate biomass in bare sediment did not correlate with any of the tested environmental variables (Figure 11). Total macroinvertebrate abundance in both beach-cast and drifting wrack was positively correlated with wrack biomass (Figure 12). Whereas total macroinvertebrate abundance in bare sediment did not correlate with any of the tested environmental variables (Figure 12).

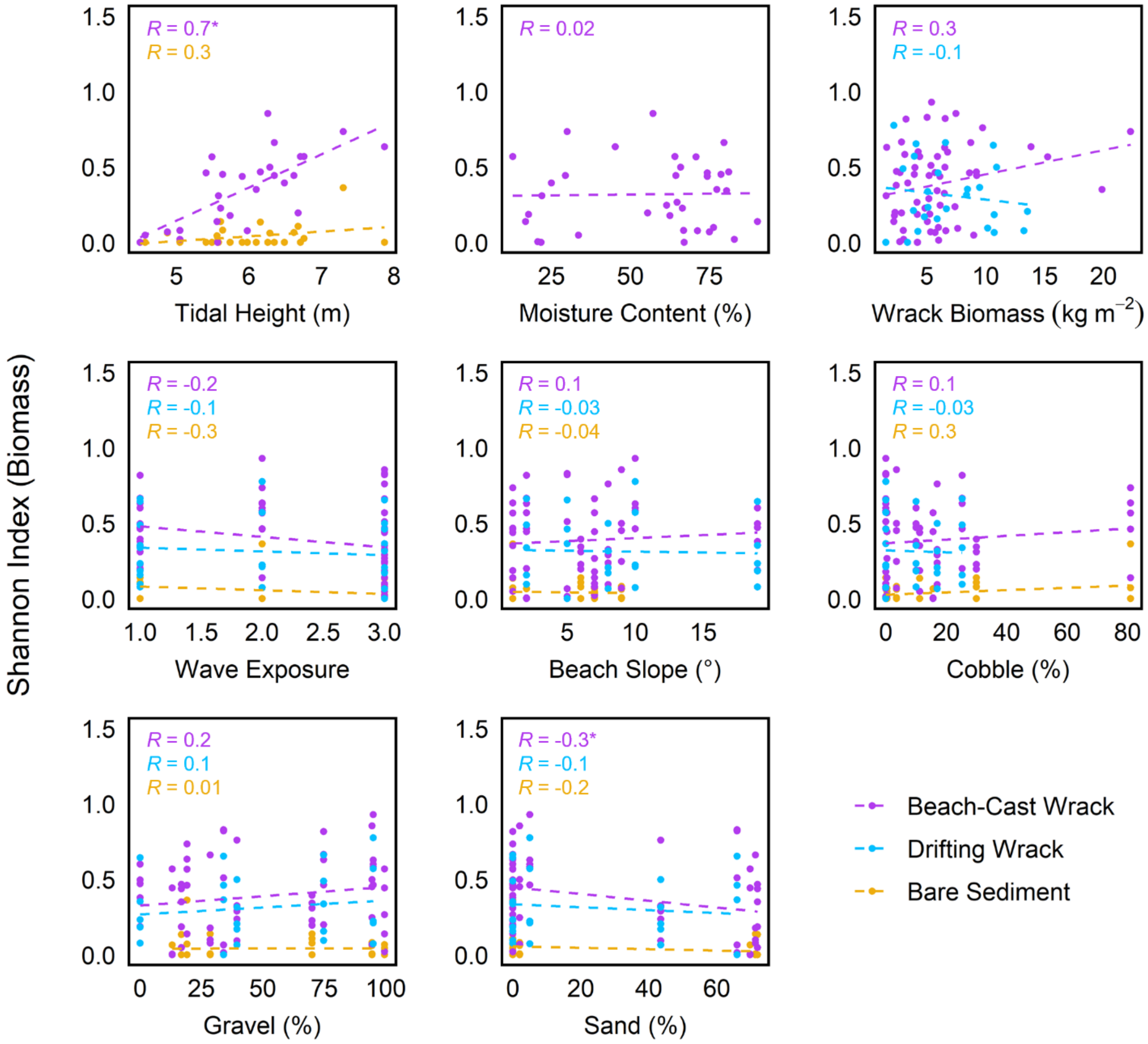

Figure 9. Scatterplot of Shannon Index values (based on macroinvertebrate biomass) and environmental variables for beach-cast wrack (purple), drifting wrack (blue), and bare sediment (orange) habitats with overlayed trendlines and Pearson correlation coefficients. An asterisk next to Pearson's *R* indicates significance.

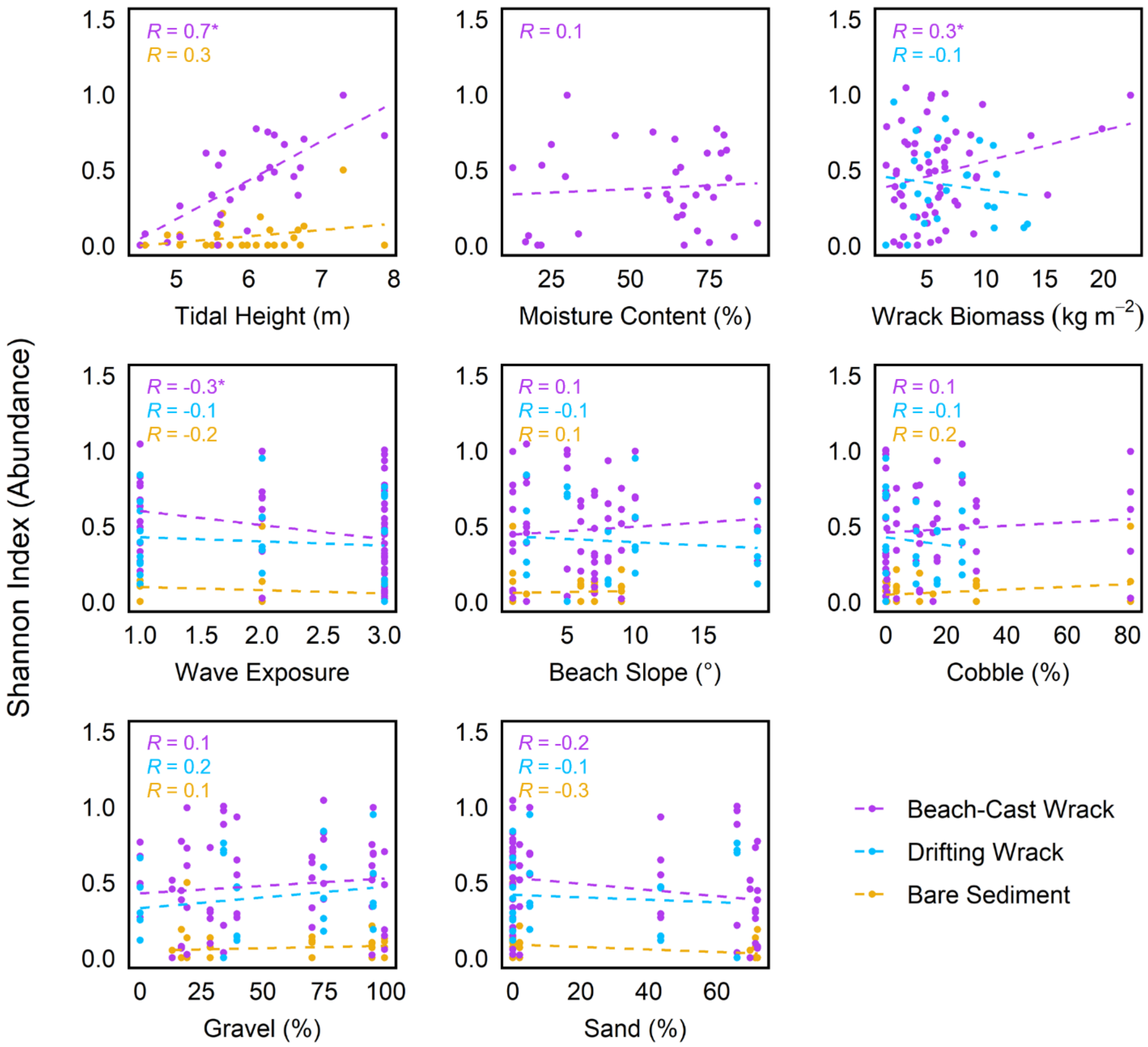

Figure 10. Scatterplot of Shannon Index values (based on macroinvertebrate abundance) and environmental variables for beach-cast wrack (purple), drifting wrack (blue), and bare sediment (orange) habitats with overlayed trendlines and Pearson correlation coefficients. An asterisk next to Pearson's *R* indicates significance.

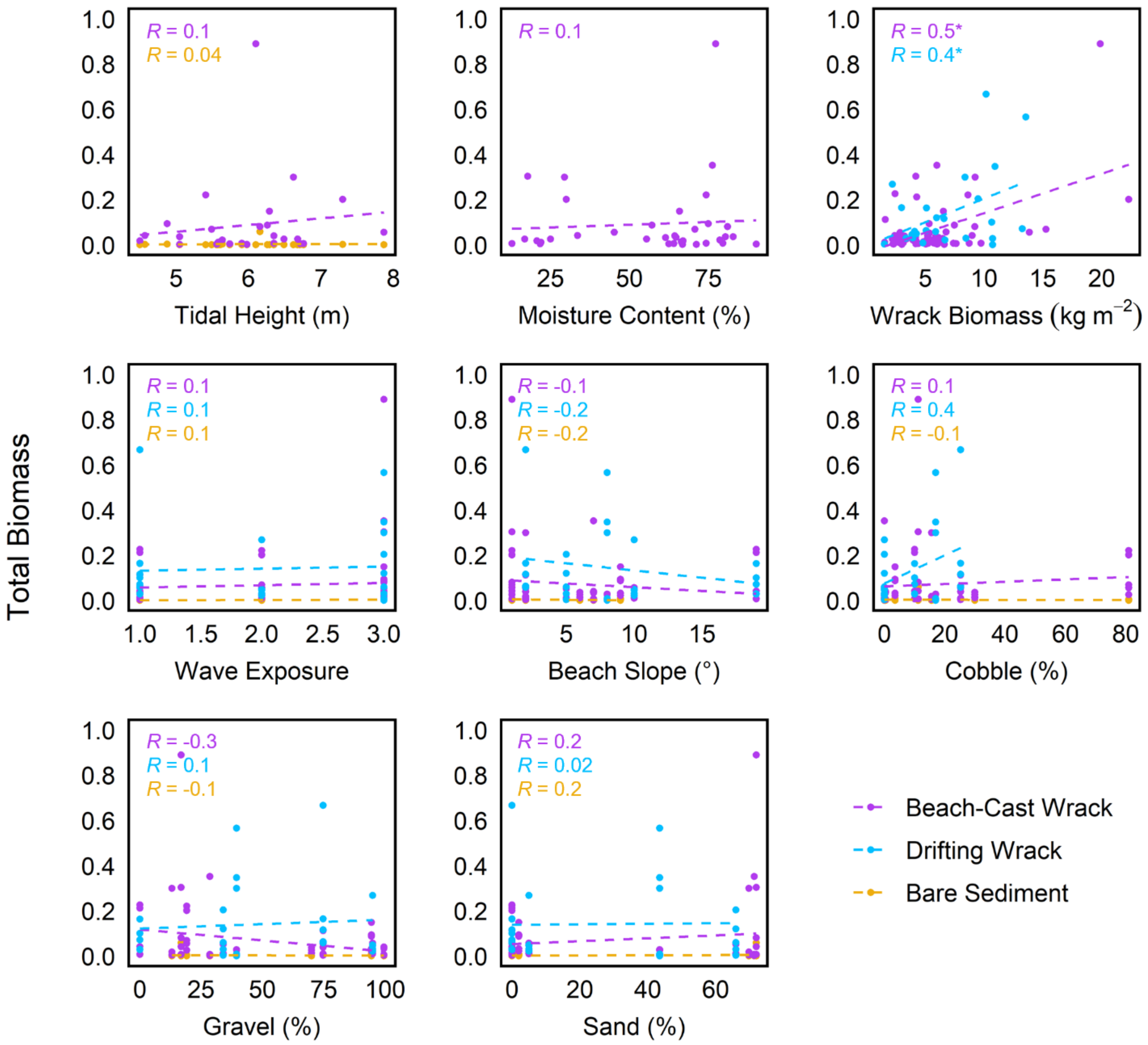

Figure 11. Scatterplot of total macroinvertebrate biomass and environmental variables for beach-cast wrack (purple), drifting wrack (blue), and bare sediment (orange) habitats with overlayed trendlines and Pearson correlation coefficients. An asterisk next to Pearson's *R* indicates significance.

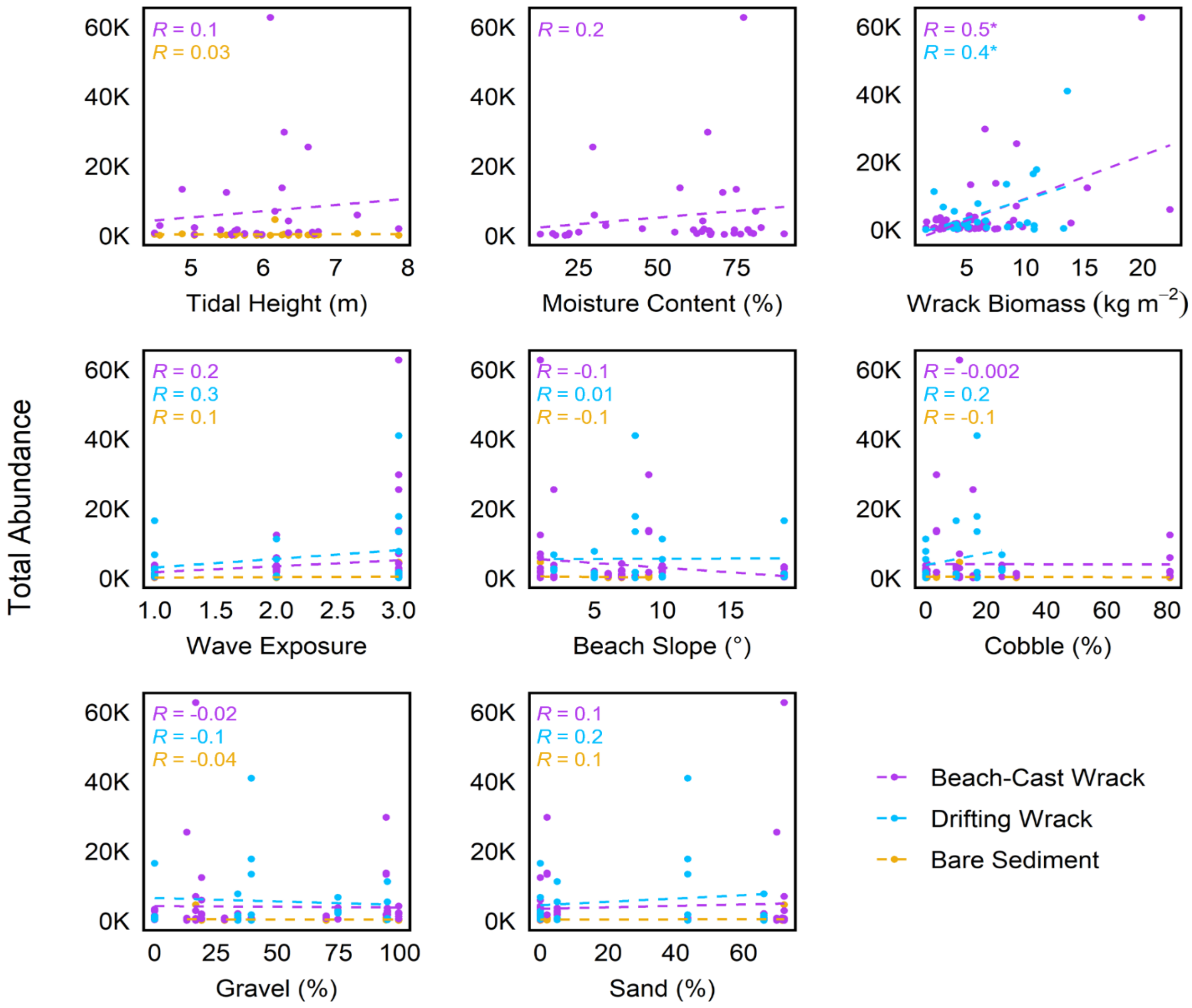

Figure 12. Scatterplot of total macroinvertebrate abundance and environmental variables for beach-cast wrack (purple), drifting wrack (blue), and bare sediment (orange) habitats with overlayed trendlines and Pearson correlation coefficients. An asterisk next to Pearson's *R* indicates significance.

Wrack as Foraging Grounds for Birds

Though birds were rare during the transect surveys, seven species were accounted for, including *Haliaeetus leucocephalus* (bald eagle), *Pica hudsonia* (black-billed magpie), *Arenaria melanocephala* (black turnstone), *Paridae* spp. (chickadee), *Corvus* spp. (crow/raven), *Larus glaucescens* (glaucous-winged gull), and *Numenius phaeopus* (whimbrel). With the data that were collected, bird assemblages were similar on and off the beach-cast wrack line (PERMANOVA, $F_{1,6} = 1.3$, $p = 0.3$; Figure 13). Crows and glaucous-winged gulls were the predominant species foraging in the wrack. Black turnstones and whimbrels were the only shorebirds observed during the surveys. Whimbrels, however, were observed to feed both on and off the beach-cast wrack line.

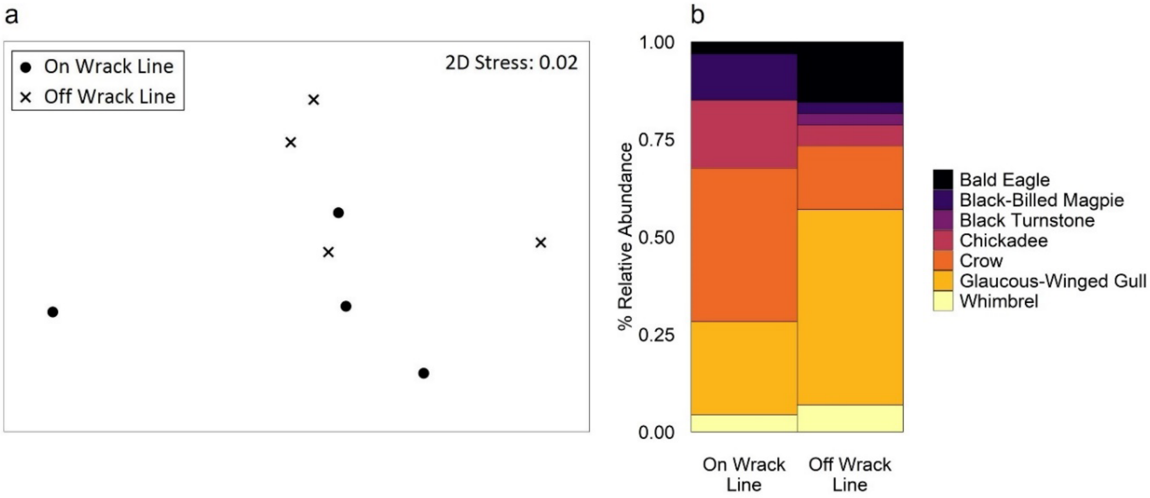

Figure 13. (a) Non-metric multidimensional scaling (NMDS) ordination plot of bird communities based on relative abundance on and off the beach-cast wrack line (each point represents a site) and (b) stacked bar plot of all bird taxa observed on and off beach-cast wrack surveys.

Succession in Aging Wrack

Wrack piles created microclimates by retaining moisture and decreasing the range in temperature fluctuation within the wrack and in the underlying sediments compared to the ambient air temperatures (Figure 14).

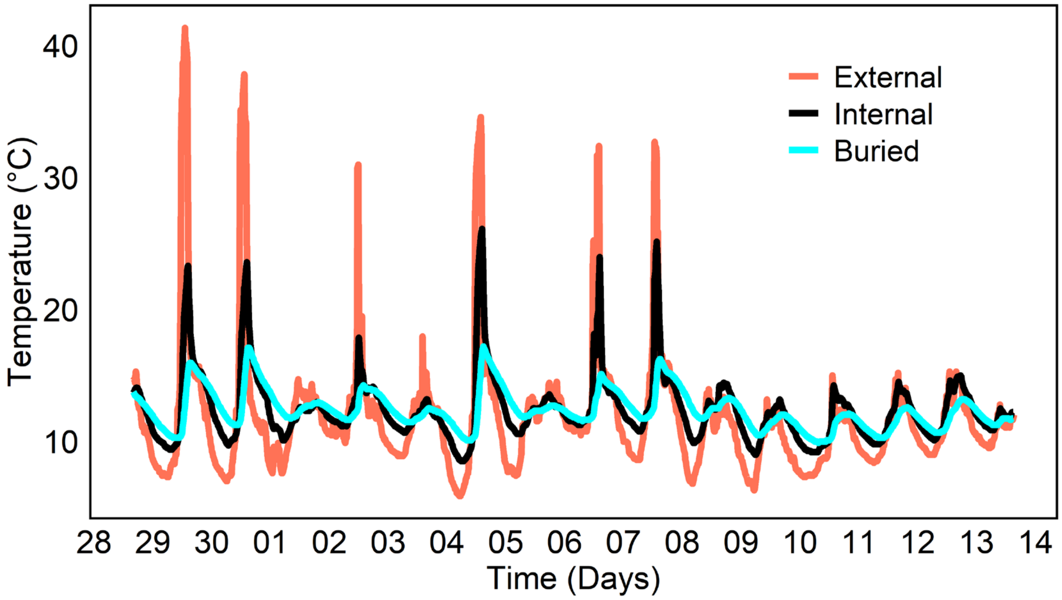

Figure 14. Temporal variability in measured temperatures during the July succession experiment in beach-cast wrack. External temperature (ambient air outside of wrack piles) = red; Internal temperature (inside of wrack piles) = black; Buried temperature (buried in sediment underneath wrack piles) = blue.

Macroinvertebrate communities generally increased in diversity over time (Shannon Index based on biomass and abundance; Figure 15). In April, diversity peaked on Day 12 (Figure 15). In May, diversity peaked earlier on Day 6. In June, diversity increased on Day 3 before fluctuating until Day 15. In July, diversity increased on Day 3 and remained relatively constant until Day 15. During the longer experiment in August, diversity peaked on Day 12 before decreasing on Day 18 and increasing again on Day 24.

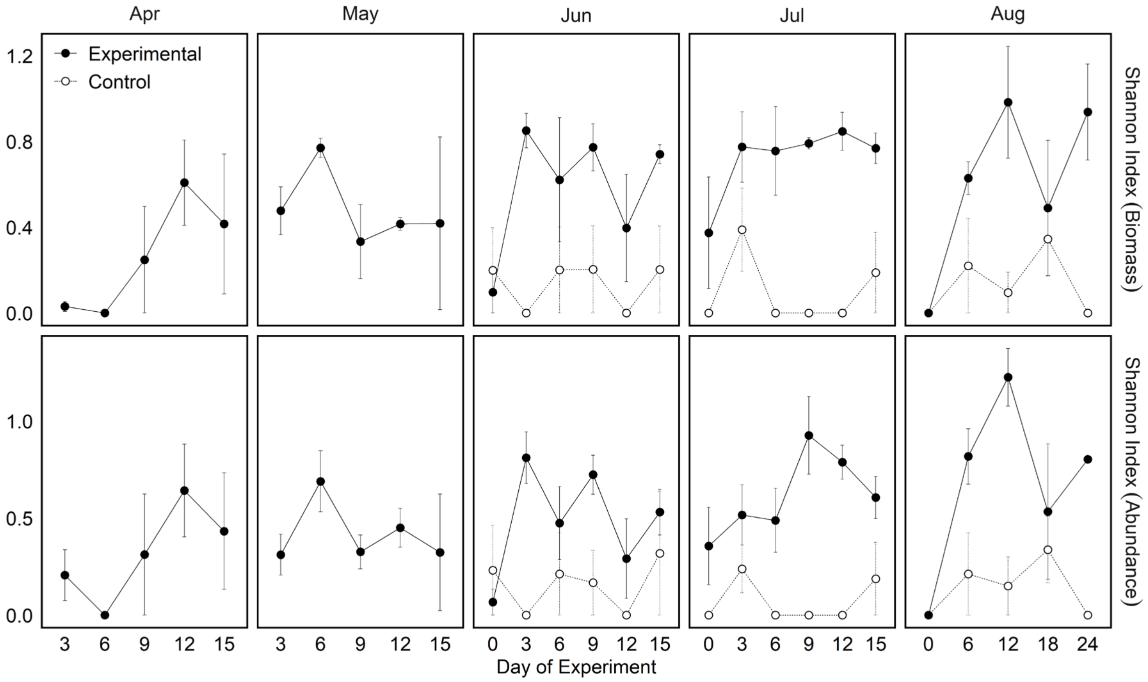

Figure 15. Daily macroinvertebrate community Shannon Index means based on biomass (top panels) and abundance (bottom panels) from monthly wrack succession experiments (bars represent standard error). There were no controls in April and May experiments.

Total biomass and abundance of macroinvertebrate communities were significantly higher in experimental wrack piles than in bare sediment controls (ANOVA, biomass: $F_{1,126}$ = 13.03, $p < 0.001$; abundance: $F_{1,126}$ = 18.4, $p < 0.001$; Figure 16). Macroinvertebrate communities also generally increased in total biomass and abundance over the course of the experiments, with marginal differences across months (ANOVA, biomass: $F_{4,74}$ = 2.6, $p = 0.05$; abundance: $F_{4,74}$ = 2.5, $p = 0.05$; Figure 16). Total biomass and abundance of macroinvertebrates peaked on Day 9 in June and July (Figure 16). In April, May, June, and July, changes in total macroinvertebrate biomass (ANOVA, April: $F_{4,10}$ = 1.1, $p = 0.41$; May: $F_{4,10}$ = 0.9, $p = 0.52$; June: $F_{5,12}$ = 1.9, $p = 0.17$; July: $F_{5,12}$ = 2.1, $p = 0.14$) and abundance (ANOVA, April: $F_{4,10}$ = 1.2, $p = 0.37$; May: $F_{4,9}$ = 3.4, $p = 0.06$; June: $F_{5,12}$ = 1.7, $p = 0.2$; July: $F_{5,12}$ = 1.9, $p = 0.16$) were not considered significant over days of the experiment in each month. In the longer August experiment, total biomass and abundance of macroinvertebrates peaked on Day 18 and were significantly higher than the other days of the experiment for that month (ANOVA, biomass: $F_{4,9}$ = 4.8, $p = 0.02$; abundance: $F_{4,9}$ = 17.8, $p < 0.001$; Figure 16).

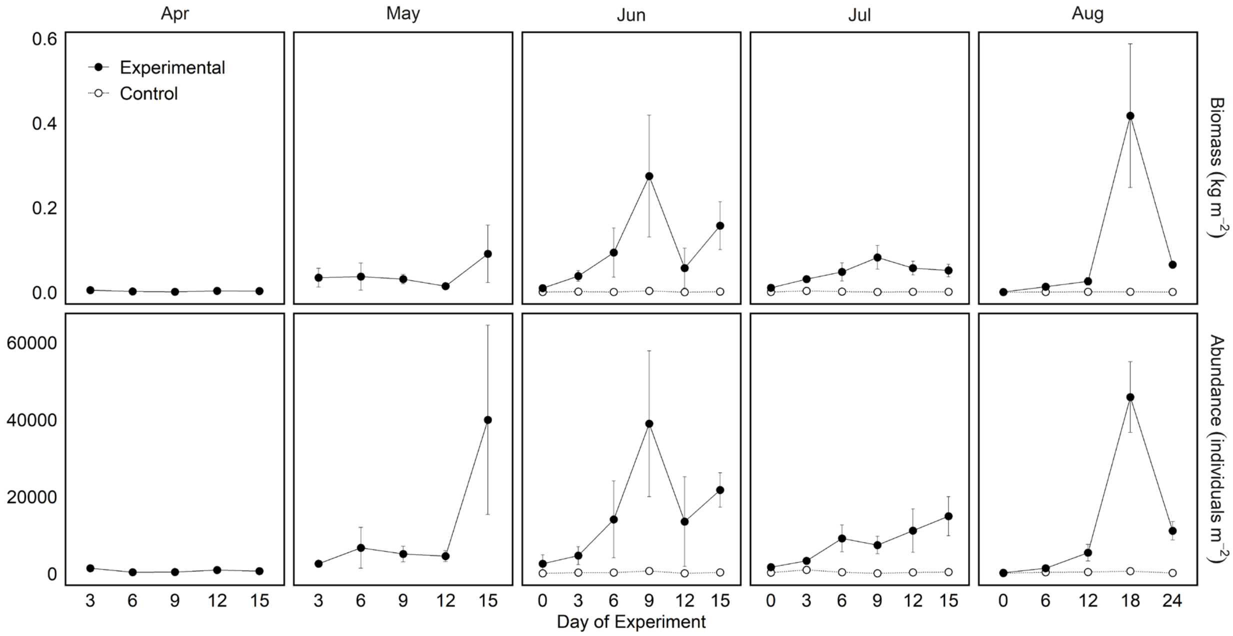

Figure 16. Daily macroinvertebrate community means of total biomass (top panels) and abundance (bottom panels) from monthly wrack succession experiments (bars represent standard error). There were no controls in April and May experiments.

Macroinvertebrate diversity (Shannon Index based on abundance) was negatively correlated with wrack moisture content in July (Figure 17). Total macroinvertebrate abundance was negatively correlated with moisture content of the wrack piles in May and August (Figure 17). Macroinvertebrate diversity (Shannon Index based on biomass and abundance) was positively correlated with internal wrack temperature in April but was negatively correlated with internal wrack temperature in August (Figure 18). Total macroinvertebrate biomass in June was positively correlated with internal wrack temperatures (Figure 18). Total macroinvertebrate abundance in May and June was also positively correlated with internal wrack temperatures (Figure 18); however, in August, total macroinvertebrate abundance was negatively correlated with internal wrack temperature (Figure 18).

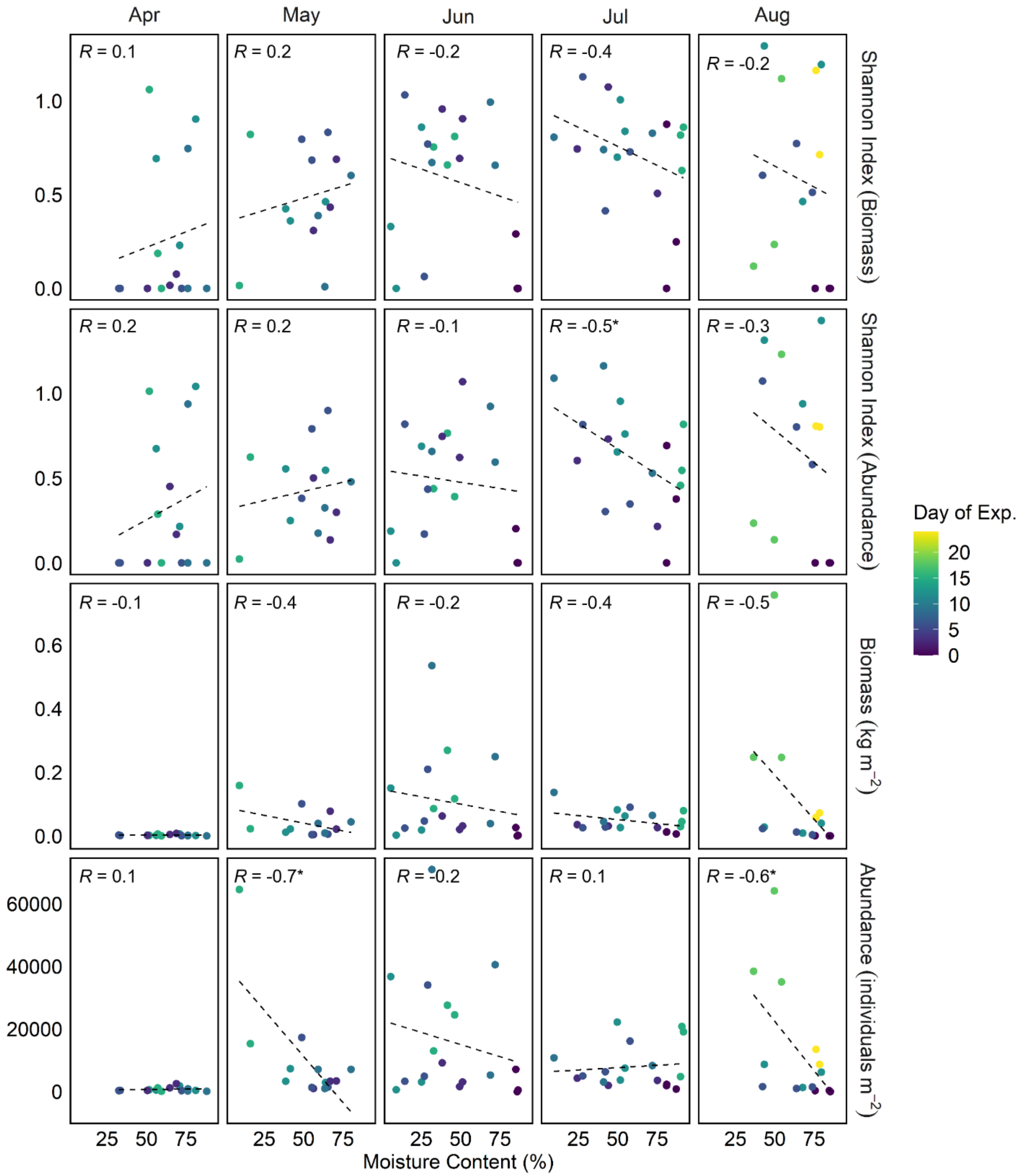

Figure 17. Scatterplot of macroinvertebrate Shannon Index based on biomass, Shannon Index based on abundance, total biomass, and total abundance with overlayed trendlines and Pearson correlation coefficients in relation to wrack moisture content from monthly succession experiments. Points are colored by day they were sampled during the experiment. An asterisk next to Pearson’s *R* indicates significance.

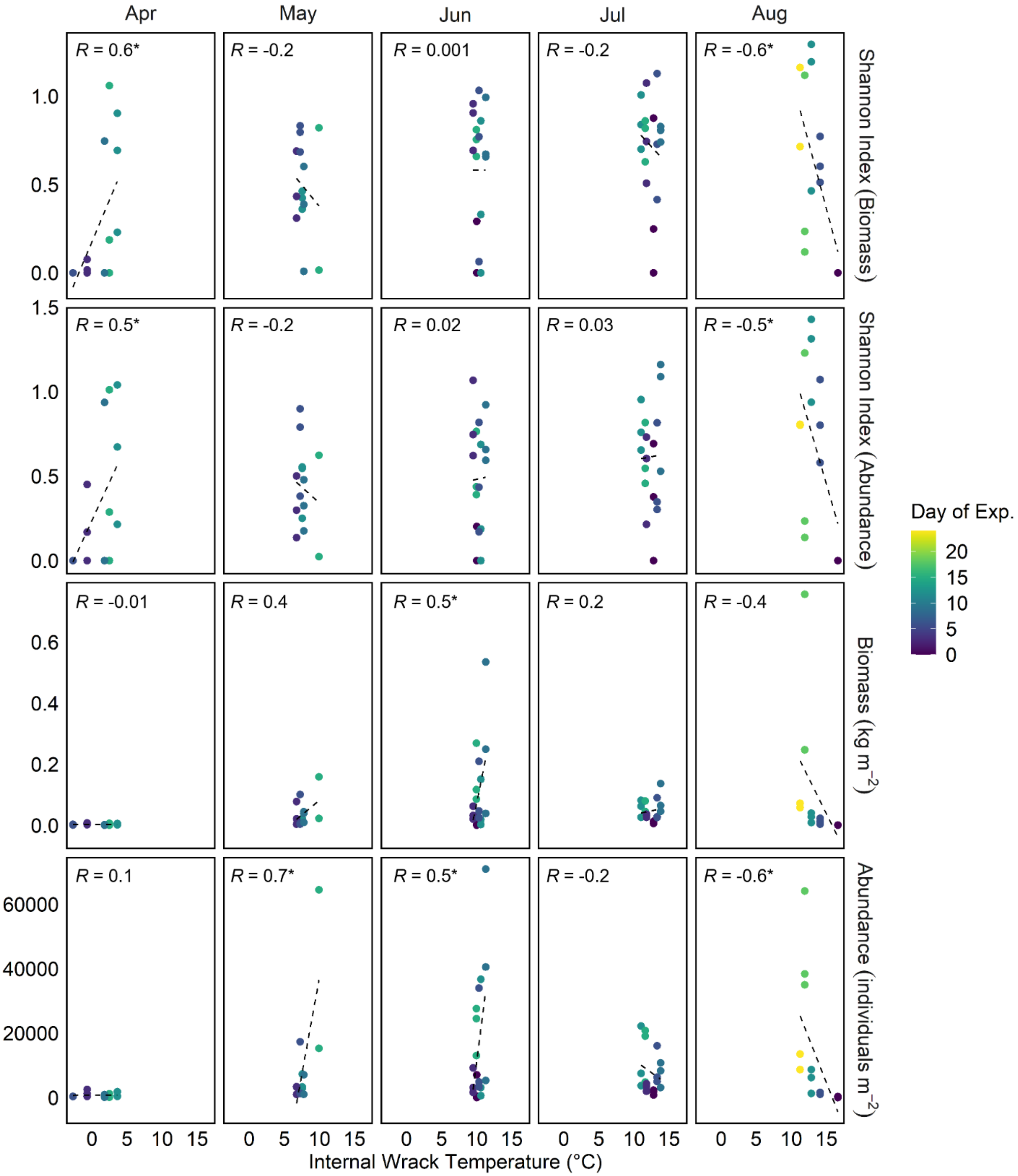

Figure 18. Scatterplot of macroinvertebrate Shannon Index based on biomass, Shannon Index based on abundance, total biomass, and total abundance with overlayed trendlines and Pearson correlation coefficients in relation to internal wrack temperature from monthly succession experiments. Points are colored by day they were sampled during the experiment. An asterisk next to Pearson’s *R* indicates significance.

Macroinvertebrate communities that developed and changed over time in the monthly wrack succession experiments were significantly different than controls (PERMANOVA, biomass: $F_{1,70} = 140.7$, $p = 0.001$; abundance: $F_{1,70} = 111.6$, $p = 0.002$) and among days in each month (PERMANOVA, biomass: $F_{22,70} = 1.7$, $p = 0.03$; abundance: $F_{22,70} = 1.8$, $p = 0.03$). Community composition based on biomass was significantly different among months (PERMANOVA, $F_{4,70} = 2.4$, $p = 0.03$); however, community composition based on abundance did not change significantly among months (PERMANOVA, $F_{4,70} = 1.8$, $p = 0.09$). Few taxa were present on Day 0 of each experiment, but these included Araneae, Diptera, Geophilomorpha, and Nematoda. These taxa were also common in control samples from bare sediment. After Day 0 in every month except for April, both Amphipoda and Diptera appeared and, along with Nematoda, remained predominant for the remainder of the experiment (Figure 19). Hydrophilids (Coleoptera) appeared on Days 6 and 9 in the June and July experiments but did not appear until Days 12 and 18 in August (Figure 19). Staphylinids (Coleoptera) consistently began appearing on Day 9 in May, June, and July. Day 9 was not sampled in August, but Staphylinidae appeared at least on Day 12 (Figure 19).

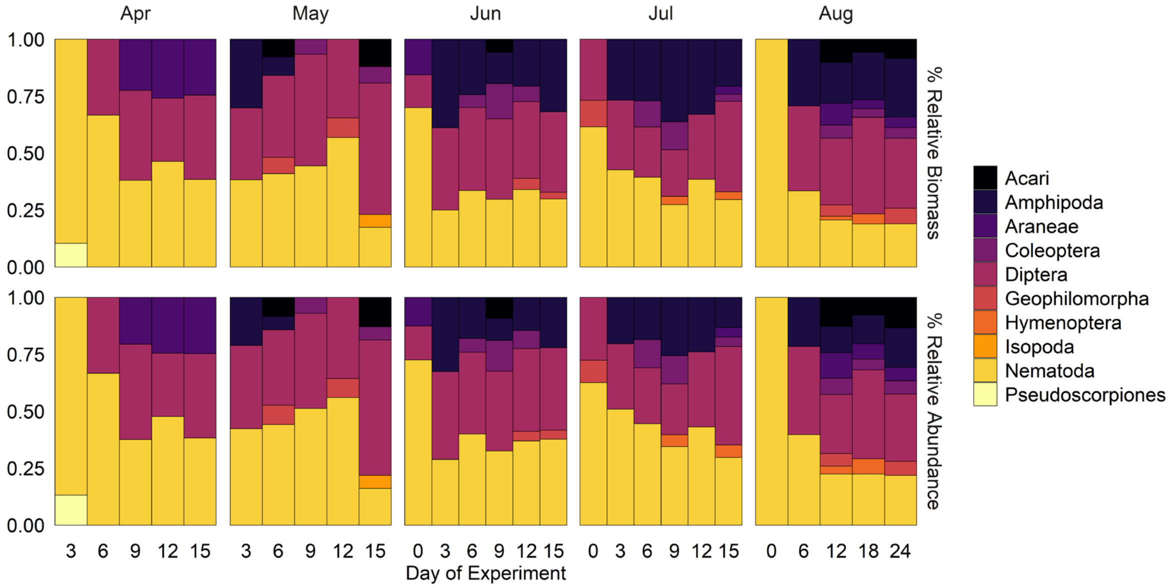

Figure 19. Stacked bar plots of macroinvertebrate taxa that were significant contributors to compositional differences of relative biomass (top panels) and abundance (bottom panels) over time (days and months) during succession experiments.

DISCUSSION

Macroinvertebrate Communities

The widely accepted autotrophs-first paradigm is contradicted by the well-observed phenomenon of the heterotrophs-first hypothesis on beaches (Sikes and Slowik 2010). For example, following a catastrophic volcanic eruption, wrack-associated dipteran flies persisted, presumably due to the presence of wrack subsidies (Sikes and Slowik 2010). Wrack subsidies provide habitat for intertidal consumers where productivity is otherwise low or non-existent.

The present study determined that both beach-cast and drifting wrack support more diverse and greater numbers of macroinvertebrates compared to bare soft-sediment habitats. Some taxa (Nematoda) were ubiquitous across beach habitats whether wrack was present or not, but the presence of wrack sometimes increased their abundance. Drifting wrack supported greater numbers of Amphipoda (primarily *Peramphithoe mea*), while beach-cast wrack supported fewer Amphipoda (primarily *Traskorchestia traskiana*). These beach-cast amphipods generally dwell beneath piles of wrack during the day to avoid warmer temperatures and predators, and they may be found actively feeding on and foraging in piles of seaweed at night (Dugan et al. 2003). Macroinvertebrates in beach-cast wrack (e.g., amphipods, isopods, and insects) can make up more than 37% of the species on beaches (Dugan et al. 2003). Similarly, the present study found that amphipods alone accounted for approximately 20-25% of biomass and abundance on beaches in wrack. Dipteran flies (adults, pupae, and larvae combined) contributed similar proportions of 20-25% to macroinvertebrate communities in wrack on the beach. Hydrophilidae (Coleoptera) and Staphylinidae (Coleoptera) beetles were also more common in wrack than in surrounding bare sediment and appeared occasionally in drifting wrack. Some staphylinid beetles are adapted to the marine environment by reducing metabolic rate and oxygen consumption when submerged in seawater (Topp and Ring 1988). Mytilida (mussels) and Gastropoda (snails) recruits were common in drifting wrack. Not only do more mobile taxa rely on floating wrack debris for assisted transport (Baring et al. 2018), sessile mussel recruits that attach to seaweeds that get dislodged also may benefit from assisted transport in wrack. Amphipods, flies, centipedes (Geophilomorpha), pseudoscorpions (*Halobisium occidentale*), and worms (Nematoda) were present in bare sediment, though bare sediment habitat supported substantially fewer animals than both wrack habitats,

Response of Macroinvertebrate Communities to Environmental Characteristics

Many studies that characterized macroinvertebrate communities associated with wrack were conducted on sandy beaches; however, some work has been done to characterize wrack degradation rates on pebble substrate (Gilson et al. 2021). The present study determined that macroinvertebrate community diversity (Shannon Index based on biomass) decreases significantly with percent sand substrate. The tidal height at which the beach-cast wrack line was deposited positively correlated with diversity, abundance, and biomass of macroinvertebrate communities. This may be explained by the accessibility of higher elevation wrack deposits to macroinvertebrates of terrestrial origin, such as beetles, ants, pseudoscorpions, spiders, and centipedes. Not only does higher elevation of wrack deposition attract more terrestrial insects, but the Talitrid amphipods that feed on the wrack often inhabit the upper intertidal and supralittoral zones (Dugan et al. 2003). Findings of Dugan et al. (2003) suggest that macroinvertebrate communities are more strongly influenced by wrack subsidies than beach morphodynamics. Like other studies that found beach-cast wrack increases macrofaunal biomass and species richness (e.g., Dugan et al. 2000, MacMillan and Quijón 2012, Ruiz-Delgado et al. 2015, Vieira et al. 2016), the present study also found that macroinvertebrate diversity, biomass, and abundance increased with biomass of seaweed wrack subsidies. Wrack biomass appears to play a more important role in wrack community development than the substrate on which wrack is deposited. The increased biomass of wrack creates more complex habitats on beaches for different animals to exploit and partition the subsidized resource, possibly decreasing competitive interactions. For example, amphipods may leave wrack to find other feeding grounds to decrease intraspecific competition (Colombini and Chelazzi 2003).

Macroinvertebrate community diversity decreased with exposure to wave action. Given that swash climate and associated factors (e.g., wave exposure) have little influence on wrack-associated macroinvertebrate communities (Dugan et al. 2003), there must be an alternative explanation for why diversity decreased with wave exposure. Wrack from the sites with the highest exposure to waves (Anchor Point, Bluff Point, Camel Rock, Grewingk River, MacDonald Spit, Outside Beach, and Wosnesenski River) was predominately inhabited by either Amphipoda, Diptera, or Nematoda, with other taxa appearing more rarely. These taxa may be less sensitive to frequent disturbances by waves and associated effects due to their highly developed orientation behavior (Amphipoda; Scapini et al. 1995), increased mobility (Diptera), and ubiquity (Nematoda).

Wrack as Foraging Grounds for Birds

Shorebirds have been observed to forage for invertebrates (e.g., beetles, amphipods, isopods) that are living in wrack (Dugan et al. 2003, Mellbrand et al. 2011, Fox et al. 2014). In regions outside of Alaska, studies investigating shorebird abundance and washed-up wrack suggest that shorebird abundance is positively correlated with wrack cover and biomass of wrack-associated prey (Hubbard and Dugan 2003, Dugan et al. 2003). Stopover areas (and the availability of food) are critical to the fitness of migrating shorebirds (Schnurr et al. 2020). More shorebirds were expected to be feeding in the wrack, especially in late April and early May during northern migrations along which Kachemak Bay is a stopover area where birds refuel before they reach the Arctic to breed. Turnstones are ground foragers with a feeding style that involves flipping over stones and debris on the beach, and they have been observed to forage in seaweed wrack in other regions of the world where turnstones stage (Burger et al. 2018). As such, black turnstones were expected to be seen foraging in the wrack, but they were only spotted lower in the intertidal foraging among courser rocky substrate. Turnstones may not primarily feed in the wrack as food is sufficiently available in the rocky intertidal where they were observed. Examples of shorebirds that might not be expected to be associated with wrack foraging include whimbrels and godwits. These sandpipers also respond to visual cues, but they look for signs of entrances into the sand from burrowing invertebrates (e.g., sand crabs and amphipods; Turpie and Hockey 1993). Their morphological adaptation of having a long bill allows them to probe the substrate for burrowing animals; however, the present study observed whimbrels opportunistically foraging and pecking in the wrack, though they were more often observed foraging in the sands of the swash zone.

Since wrack is potentially an important foraging ground for migrating shorebirds (Dugan et al. 2003; Burger et al. 2018), the management of this resource might play a critical role in maintaining stopover habitat quality. As there is a concern for global declines in shorebird abundance, including North American inhabitants (Bart et al. 2007), any impact that human activity may have on shorebirds is critical to their persistence. If the availability of food at stopover sites is reduced, due to wrack removal or contamination, then foraging behavior and increased length of time spent foraging may have carry-over effects for shorebird populations.

Though the present study observed very few birds, Kachemak Bay is an important stopover site for shorebirds during spring northern migration (Matz 2017). Thus, the management of coastal resources may be most important during times of migration. More research is needed to assess the use of wrack by shorebirds in Alaska. The sites sampled in this study were close to major road systems around Homer and Seldovia where recreational activity is high, which may have played a role in why so few birds were observed. There may be other shores throughout Kachemak Bay where birds can utilize wrack. Since northward migrating shorebirds are primarily income breeders (McGuire et al. 2020), meaning they need to sufficiently fuel after they arrive at their breeding grounds, the health of stopover sites is critical to help birds meet fueling demand during migration.

Succession in Aging Wrack

Early colonizers of beach-cast wrack are often detritivores, including amphipods and dipteran flies, followed by isopods and predatory coleopteran beetles (Olabarria et al. 2007). The present study observed a similar order of succession in aging wrack with decreased moisture content over time. Amphipods are direct consumers of the seaweed (Colombini and Chelazzi 2003). Flies deposit their eggs onto moist piles of seaweed wrack, in which the eggs eventually produce fly larvae that feed on the bacterial mats that are functioning to decompose the wrack (Jędrzejczak 2002). The adult flies are saprophagous and feed on the decaying seaweed. The richness and rapid reproduction of kelp flies and the developing larvae attract predators. Predatory beetles (Coleoptera) and spiders (Araneae) feed on insects, such as mites (Acari) and dipteran larvae, that might also be foraging in the wrack (Colombini and Chelazzi 2003). Occasionally, other marine invertebrates will be found feeding in the wrack (e.g., herbivorous snails and crabs; Colombini and Chelazzi 2003). The species richness within this coastal food web may be high, including members from the ocean and the land converging at this interface; however, Gilson et al. (2021) determined that macroinvertebrates may have a more limited role in the breakdown of wrack subsidies and suggested that meiofauna and microbes play a major role in wrack processing.

The facilitation model of succession (Connell and Slatyer 1977) is apparent throughout the process of wrack decomposition. Under this model, ecological succession of the ecosystem proceeds if the pioneer colonizers of the system modify the substrate to a point that is habitable for other organisms to settle and grow. This is apparent in wrack communities because of ecological function during each stage of decomposition and colonization. The bacteria and fly larvae decompose the wrack, and this aged wrack is generally preferred by herbivorous invertebrates (e.g., amphipods; Pelletier et al. 2011). The succession experiments corroborated likely biological interactions between taxa. For example, Hymenopterans (i.e., Family: Braconidae; Subfamily: Alysiinae) were found in aging wrack only after Dipteran flies colonized and larvae began permeating the heaps of wrack. This order of succession aligns with the common observation of braconids as parasitoids of Diptera by ovipositing into their larvae (Ranjith et al. 2022). Centipedes (Geophilomorpha) are of terrestrial origin but are tolerant to seawater and possibly use seaweed wrack as foraging grounds and possible means of passive dispersal (Barber 2011). Geophilomorpha may also seek refuge from predators in wrack (Barber 2011). This is likely, given that they disappeared early in the successional stages to avoid predatory pressure, but reappeared after biomass and abundance of wrack colonizers reached their peak. Coleopterans were more abundant in wrack following surges in colonization by amphipods, likely due to the increased availability of prey.

Conclusions

This study is the first investigation into wrack-associated macroinvertebrates found in Alaska and corroborates the general understanding that wrack is an important resource to ecological processes on beaches and in the near-subtidal zone. Attached macroalgal reefs are in decline globally due to multiple stressors (Filbee-Dexter and Wernberg 2018), with oil extraction disasters as an ongoing and increasing threat to these systems (Airame et al. 2003). In the case of contamination, wrack no longer serves as an ecological subsidy, but becomes an ecological hindrance. This research offers essential information on the importance of wrack in coastal systems and encourages focused management of this resource. Further research should focus efforts on increasing the spatial scale of bird surveys (i.e., more point counts or line transects) and frequency of site visits (i.e., more consecutive days of surveying) to better characterize the use of wrack by shorebirds during northward migrations through Lower Cook Inlet.

Acknowledgments

Thank you to the Coastal Marine Institute (CMI) and the Bureau of Ocean and Energy Management (BOEM) for supporting my graduate student research. With additional support from the National Science Foundation under award #OIA-1757348 and by the state of Alaska, I was able to hire an undergraduate research team to conduct fieldwork. A special thank you to Kyah Mingo and Jennifer Tusten for the many hours they dedicated to helping me sort through rocks, sand, and macroalgae for critters. Thank you to the many other student volunteers who helped with fieldwork and sample processing. I would like to thank my graduate student committee – Brenda Konar, Katrin Iken, Ted Otis, Kristen Gorman, and Derek Sikes – for their invaluable perspective and support throughout the entire process of my degree. Thank you to the National Oceanic and Atmospheric Administration (NOAA)/ University of Alaska Fairbanks (UAF) Kasitsna Bay Laboratory and Kachemak Bay National Estuarine Research Reserve (KBNERR) staff for field and laboratory support.

References

Airame, S., J.E. Dugan, K.D. Lafferty, H. Leslie, D.A. McArdle, and R.R. Warner. 2003. Applying ecological criteria to marine reserve design: a case study from the California Channel Islands. Ecological Applications. 13: 170-184.

Barber, A. 2011. Geophilomorph centipedes and the littoral habitat. Terrestrial Arthropod Reviews. 4: 17-39.

Baring, R.J., R.E. Lester, and P.G. Fairweather. 2018. Trophic relationships among animals associated with drifting wrack. Marine and Freshwater Research. 69: 1248-1258.

Barreiro, F., M. Gómez, M. Lastra, J. López, and R. de la Huz. 2011. Annual cycle of wrack supply to sandy beaches: Effect of the physical environment. Marine Ecology Progress Series. 433: 65-74.

Bart, J., S. Brown, B. Harrington, and R.I.G. Morrison. 2007. Survey trends of North American shorebirds: Population declines or shifting distributions? Journal of Avian Biology. 38: 73-82.

Beeler, H.E. 2009. Community succession in macroalgal wrack implications for prey resources of breeding western snowy plovers (*Charadrius alexandrines nivosus*) on northern California beaches. Humboldt State University. MSc Thesis.

Brown, S., S. Kendall, R. Churchwell, A. Taylor, and A.M. Benson. 2012. Relative shorebird densities at coastal sites in the Arctic National Wildlife Refuge. Waterbirds. 35: 546-554.

Burger, J., L. Niles, C. Jeitner, and M. Gochfeld. 2018. Habitat risk: Use of intertidal flats by foraging red knots (*Calidris canutus rufa*), ruddy turnstones, (*Arenaria interpres*), semipalmated sandpipers (*Calidris pusilla*), and sanderling (*Calidris alba*) on Delaware Bay beaches. Environmental Research. 165: 237-246.

Byrne, M., J. DeVivo, J. Maxfield, C. Wright, and E. Thompson. 2009. Methods for monitoring migratory and wintering shorebirds in southeast coast network parks. Natural Resource Report NPS/SECN/NRR—2009/107.

Colombini, I., A. Aloia, M. Fallaci, G. Pezzoli, and L. Chelazzi. 2000. Temporal and spatial use of stranded wrack by the macrofauna of a tropical sandy beach. Marine Biology. 136: 531-541.

Colombini, I., and L. Chelazzi. 2003. Influence of marine allochthonous input on sandy beach communities. Oceanography and Marine Biology: An Annual Review. 41: 115-159.

Connell, J.H., and R.O. Slatyer. 1977. Mechanisms of succession in natural communities and their role in community stability and organization. The American Naturalist. 111: 1119-1144.

Davenport, J., and J.L. Davenport. 2006. The impact of tourism and personal leisure transport on coastal environments: A review. Estuarine Coastal and Shelf Science. 67: 280-292.

Davis, T.J., and G. Keppel. 2021. Fine-scale environmental heterogeneity and conservation management: Beach-cast wrack creates microhabitats for thermoregulation in shorebirds. Journal of Applied Ecology. 58: 1291-1301.

de la Huz, R., M. Lastra, J. Junoy, C. Castellanos, and J.M. Vieitez. 2005. Biological impacts of oil pollution and cleaning in the intertidal zone of exposed sandy beaches: Preliminary study of the “Prestige” oil spill. Estuarine, Coastal and Shelf Science. 65:19-29.

Defeo, O., A. McLachlan, D.S. Schoeman, T.A. Schlacher, J. Dugan, A. Jones, M. Lastra, and F. Scapini. 2009. Threats to sandy beach ecosystems: A review. Estuarine, Coastal and Shelf Science. 81: 1-12.

Deidun, A.A., S. Saliba, and P.J. Schembri. 2009. Considerations on the ecological role of wrack accumulations on sandy beaches in the Maltese Islands and recommendations for their conservation management. Journal of Coastal Research. 1: 410-414.

Dugan, J.E., and D.M. Hubbard. 2010. Loss of coastal strand habitat in Southern California: The role of beach grooming. Estuaries and Coasts. 33: 67-77.

Dugan, J., D. Hubbard, D. Martin, J. Engle, D. Richards, G. Davis, K. Lafferty, and R. Ambrose. 2000. Macrofauna communities of exposed sandy beaches on the Southern California mainland and Channel Islands. Fifth Calif Islands Symp Miner Manag Serv 339-346.

Dugan, J.E., D.M. Hubbard, M.D. McCrary, and M.O. Pierson. 2003. The response of macrofauna communities and shorebirds to macrophyte wrack subsidies on exposed sandy beaches of southern California. Estuarine, Coastal and Shelf Science. 58: 25-40.

Dugan, J.E., D.M. Hubbard, H.M. Page, and J.P. Schimel. 2011. Marine macrophyte wrack inputs and dissolved nutrients in beach sands. Estuaries and Coasts. 34: 839-850.

Ely, C.R., B.J. McCaffery, and R.E. Gill Jr. 2018. Shorebirds adjust spring arrival schedules with variable environmental conditions: Four decades of assessment on the Yukon - Kuskokwim Delta, Alaska. In W.D. Shuford, R.E. Gill Jr., and C.M. Handel (Eds.), Trends and Traditions: Avifaunal Change in Western North America. Studies in Western Birds 3 (pp. 296–311). Camarillo, CA: Western Field Ornithologists.

Fairweather, P.G., and R.J. Henry. 2003. To clean or not to clean? Ecologically sensitive management of wrack deposits on sandy beaches. Ecological Management and Restoration. 4: 227-229.

Fanini, L., C.M. Cantarino, and F. Scapini. 2005. Relationships between the dynamics of two *Talitrus saltator* populations and the impacts of activities linked to tourism. Oceanologia. 47: 93-112.

Filbee-Dexter, K., and T. Wernberg. 2018. Rise of turfs: A new battlefront for globally declining kelp forests. BioScience. 68: 64-76.

Fox, C.H., R. El-Sabaawi, P.C. Paquet, and T.E. Reimchen. 2014. Pacific herring *Clupea pallasii* and wrack macrophytes subsidize semi-terrestrial detritivores. Marine Ecology Progress Series. 495: 49-64.

Gilson, A.R., D.A. Smale, M.T. Burrows, and N.E. O’Connor. 2021. Spatio-temporal variability in the deposition of beach-cast kelp (wrack) and inter-specific differences in degradation rates. Marine Ecology Progress Series. 674: 89-102.

Harris, C., D.L. Strayer, and S. Findlay. 2014. The ecology of freshwater wrack along natural and engineered Hudson River shorelines. Hydrobiologia. 722: 233-245.

Heerhartz, S.M., M.N. Dethier, J.D. Toft, J.R. Cordell, and A.S. Ogston. 2014. Effects of shoreline armoring on beach wrack subsidies to the nearshore ecotone in an estuarine fjord. Estuaries and Coasts. 37: 1256-1268.

Holden, J.J., B.C. Kingzett, S. MacNeill, W. Smith, F. Juanes, and S.E. Dudas. 2018. Beach-cast biomass and commercial harvesting of a non-indigenous seaweed, *Mazzaella japonica*, on the east coast of Vancouver Island, British Columbia. Journal of Applied Phycology. 30: 1175-1184.

Hubbard, D.M., and J.E. Dugan. 2003. Shorebird use of an exposed sandy beach in southern California. Estuarine Coastal and Shelf Science. 58: 41-54.

Jaramillo, E., R. de la Huz, C. Duarte, and H. Contreras. 2006. Algal wrack deposits and macroinfaunal arthropods on sandy beaches of the Chilean coast. Revista Chilena de Historia Natural. 79: 337-351.

Jędrzejczak, M.F. 2002. Stranded *Zostera marina* L. vs wrack fauna community interactions on a Baltic sandy beach (Hel, Poland): a short-term pilot study Part II. Driftline effects of succession changes and colonization of beach fauna. Oceanologia. 44: 367-387.

Johnson, M.A. 2021. Subtidal surface circulation in lower Cook Inlet and Kachemak Bay, Alaska. Regional Studies in Marine Science. 41: 101609.

Kirkman, H., and G.A. Kendrick. 1997. Ecological significance and commercial harvesting of drifting and beach-cast macro-algae and seagrasses in Australia: a review. Journal of Applied Phycology. 9: 311-326.

Krumhansl, K., and R.E. Scheibling. 2012. Production and fate of kelp detritus. Marine Ecology Progress Series. 467: 281-302.

Lafferty, K.D., D.A. Rodriguez, and A. Chapman. 2013. Temporal and spatial variation in bird and human use of beaches in southern California. Springer Plus. 2: 1-38.

MacMillan, M.R., and P.A. Quijón. 2012. Wrack patches and their influence on upper-shore macrofaunal abundance in an Atlantic Canada sandy beach system. Journal of Sea Research. 72: 28-37.

Matz, G. 2017. Kachemak Bay Shorebird Monitoring Project Report 1–47 https://www.pacificbirds.org/wp-content/uploads/2017/10/2017-Kachemak-Bay-Shorebird-Monitoring-Project-1.pdf.

McGuire, R.L., R.B. Lanctot, S.T. Saalfeld, D.R. Ruthrauff, and J.R. Liebezeit. 2020. Shorebird reproductive response to exceptionally early and late springs varies across sites in Arctic Alaska. Frontiers in Ecology and Evolution. 8: 577652.

McLachlan, A. 1996. Physical factors in benthic ecology: effects of changing sand particle size on beach fauna. Marine Ecology Progress Series. 131: 205-217.

McLachlan, A., and A.C. Brown. 2006. 14-Human impacts. The ecology of sandy shores, 2nd Edition. Academic Press, Burlington, pp. 273-301.

McLaughlin, E., J. Kelly, D. Birkett, C. Maggs, and M. Dring. 2006. Assessment of the effects of commercial seaweed harvesting on intertidal and subtidal ecology in Northern Ireland. Environment and Heritage Service Research and Development Series. No. 06/26; ISSN 2043-7722. https://www.gov.scot/publications.

Mellbrand, K., P.S. Lavery, G. Hyndes, and P.A. Hambäck. 2011. Linking land and sea: Different pathways for marine subsidies. Ecosystems. 14: 732-744.

Mews, M., M. Zimmer, and D.E. Jelinski. 2006. Species-specific decomposition rates of beach-cast wrack in Barkley Sound, British Columbia, Canada. Marine Ecology Progress Series. 328: 155-160.

Michaud, K., K.A. Emery, J.E. Dugan, D.M. Hubbard, and R. Miller. 2019. Wrack resource use by intertidal consumers on sandy beaches. Estuarine, Coastal and Shelf Science. 221: 66-71.

Neuman, K.K., L.A. Henkel, and G.W. Page. 2008. Shorebird use of sandy beaches in Central California. Waterbird Society Publisher 31: 115–121.

Noriega, R., T.A. Schlacher, and B. Smeuninx. 2012. Reductions in ghost crab populations reflect urbanization of beaches and dunes. Journal of Coastal Research. 279: 123-131.

Olabarria, C., M. Lastra, and J. Garrido. 2007. Succession of macrofauna on macroalgal wrack of an exposed sandy beach: Effects of patch size and site. Marine Environmental Research. 63: 19-40.

Orr, M., M. Zimmer, D.E. Jelinski, and M. Mews. 2005. Wrack deposition on different beach types: spatial and temporal variation in the pattern of subsidy. Ecology. 86: 1496-1507.

Peckol, P., S.C. Levings, and S.D. Garrity. 1990. Kelp response following the World Prodigy oil spill. Marine Pollution Bulletin. 21: 473-476.

Pelletier, A.J.D., D.E. Jelinski, M. Treplin, and M. Zimmer. 2011. Colonisation of beach-cast macrophyte wrack patches by Talitrid amphipods: a primer. Estuaries and Coasts. 34: 863.

Polis, G.A., W.B. Anderson, and R.D. Holt. 1997. Toward an integration of landscape and food web ecology: the dynamics of spatially subsidized food webs. Annual Review of Ecology and Systematics. 28: 289-316.

R Core Team. 2021. R: A language and environment for statistical computing. R Foundation for Statistical Computing, Vienna, Austria. https:www.R-project.org

Ranjith, A.P., D.L.J. Quicke, K. Manjusha, B.A. Butcher, and M. Nasser. 2022. Completely predatory development is described in a braconid wasp. Scientific Reports. 12: 1747.

Ruiz-Delgado, M.C., M.J. Reyes-Martínez, J.E. Sánchez-Moyano, J. López-Pérez, and F.J. García-García. 2015. Distribution patterns of supralittoral arthropods: wrack deposits as a source of food and refuge on exposed sandy beaches (SW Spain). Hydrobiologia. 742: 205-219.

Scapini, F., Buiatti, M., De Matthaeis, E., and Mattoccia, M. 1995. Orientation behaviour and heterozygosity of sandhopper populations in relation to stability of beach environments. Journal of Evolutionary Biology. 8: 43-52.

Schlacher, T.A., D.S. Schoeman, J. Dugan, M. Lastra, A. Jones, F. Scapini, and A. McLachlan. 2008b. Sandy beach ecosystems: key features, management challenges, climate change impacts, and sampling issues. Marine Ecology. 29: 70-90.

Schnurr, P.J., M.C. Drever, R.W. Elner, J. Harper, and M.T. Arts. 2020. Peak abundance of fatty acids from intertidal biofilm in relation to the breeding migration of shorebirds. Frontiers in Marine Science. 7: 63.

Sikes, D.S., and J. Slowik. 2010. Terrestrial Arthropods of pre- and post-eruption Kasatochi Island, Alaska, 2008-2009: a shift from a plant-based to a necromass-based food web. Arctic, Antarctic, and Alpine Research. 42: 297-305.

Tarr, J.G., and P.W. Tarr. 1987. Seasonal abundance and the distribution of coastal birds on the northern Skeleton Coast, Southwest Africa/Namibia. Madoqua. 15: 63-72.

Topp, W., and R.A. Ring. 1988. Adaptations of Coleoptera to the marine environment. I. Observations on rove beetles (Staphylinidae) from sandy beaches. Canadian Journal of Zoology. 66: 2464-2468.

Turpie, J.K., and P.A.R. Hockey. 1993. Comparative diurnal and nocturnal foraging behaviour and energy intake rate of premigratory Grey Plovers *Pluvialis squatarola* and Whimbrels *Numenius phaeopus* in South Africa. Ibis. 135: 156-165.

Ulaski, B.P., E.O. Otis, and B. Konar. in prep. How landscape variables influence the relative abundance, composition, and reproductive viability of macroalgal wrack in a high-latitude glacially-influenced estuary.

Vieira, J.V., M.C. Ruiz-Delgado, M.J. Reyes-Martínez, C.A. Borzone, A. Asenjo, J.E. Sánchez-Moyano, and F.J. García-García. 2016. Assessment the short-term effects of wrack removal on supralittoral arthropods using the M-BACI design on Atlantic sandy beaches of Brazil and Spain. Marine Environmental Research. 119: 222-237.

Wickham, S.B., N. Shackelford, C.T. Darimont, W. Nijland, L.Y. Reshitnyk, J.D. Reynolds, and B.M. Starzomski. 2020. Sea wrack delivery and accumulation on islands: factors that mediate marine nutrient permeability. Marine Ecology Progress Series. 635: 37-54.

Wentworth, C.K. 1922. A scale of grade and class terms for clastic sediments. The Journal of Geology. 30: 377-392.

Elizabeth Hasan

Subtidal Habitat Mapping in Lower Cook Inlet for Current and Predictive Sea Otter Habitat Associations

Contents

List of Figures

List of Tables

Abstract

Sea otters (*Enhydra lutris*) are a federally protected species that have been recovering and reoccupying north Pacific coasts since they were nearly extirpated by commercial fur harvesting that ended in 1911. Sea otter populations were also adversely impacted by the 1989 *Exxon Valdez* Oil Spill in the northern Gulf of Alaska. Understanding sea otter habitat requirements can inform management practices to support their recovery. The goals of this project were to (1) develop benthic habitat maps in current and potential areas of sea otter occupancy in lower Cook Inlet, Alaska, (2) quantify biological and physical habitat attributes across a gradient of sea otter density, and (3) develop predictive maps for areas of likely sea otter occupation due to expansion.

This study utilized remotely operated vehicle (ROV) technology as a novel approach to examine the links between benthic habitat and sea otter occurrence. In 2021, ROV video surveys were conducted in six coastal regions of lower Cook Inlet, Alaska: Lake Clark National Park and Preserve, Katmai National Park and Preserve, western Cook Inlet, Chinitina Bay, eastern Cook Inlet, and Kachemak Bay. ROV data were analyzed for physical and biological habitat composition. Sea otter distribution data previously collected by U.S. Fish and Wildlife Service, U.S. Geological Survey, and the National Park Service (NPS) were overlaid with habitat maps to create suitability models for sea otter habitat. Subtidal habitat in uncolonized waters of Lake Clark National Park and Preserve and Chinitina Bay was significantly ($p < 0.05$) different from that in colonized areas of lower Cook Inlet. Sea otter presence in lower Cook Inlet was most associated with shell, boulder, pebble, and macroalgae. Based on modeled relationships, sea otter colonization of currently uncolonized areas of lower Cook Inlet has a likelihood of <50%. This study aids resource management around oil and gas and fisheries operations by providing comprehensive maps of current and potential sea otter habitats in lower Cook Inlet. Additionally, this study expands the coastal habitat maps in Alaska and contributes to the growing field of geospatial survey technology.

Introduction

Sea otters are an important keystone species (Estes and Palmisano 1974) that are federally protected by the Marine Mammal Protection Act of 1972. Sea otters were historically abundant across much of Alaska, but their stocks were significantly depleted due to commercial hunting from the 1700s to the early 1900s (Kenyon 1969). Sea otters were protected in 1911 by the International Fur Seal Treaty, which allowed for some recovery (Kenyon 1969); however, in 1989, the *Exxon Valdez* Oil Spill severely impacted sea otters in Prince William Sound and surrounding waters. Sea otters retained spilled oil in their fur, leading to hypothermia, and consumed oil through their oil-impacted prey (Bodkin et al. 2012). After the oil spill, accurate mortality estimates could not be made due to a lack of pre-spill population estimates (Ballachey et al. 1994, Bodkin et al. 2002), but sea otters did experience high mortality rates, and long-term spill effects persisted for more than 25 years. In 2014, sea otters in southcentral Alaska were declared "recovered" (Ballachey et al. 2014, Esler et al. 2018); however, the western Cook Inlet stock remains listed as "threatened" under the 2005 Endangered Species Act https://www.mmc.gov/priority-topics/species-of-concern/northern-sea-otters/. The most recent population survey estimates (from 2017) are approximately 10,000 sea otters in western Cook Inlet and approximately 6,000 sea otters in Kachemak Bay, with this latter stock expanding north to Clam Gulch (Figure 1; Garlich-Miller et al. 2018).

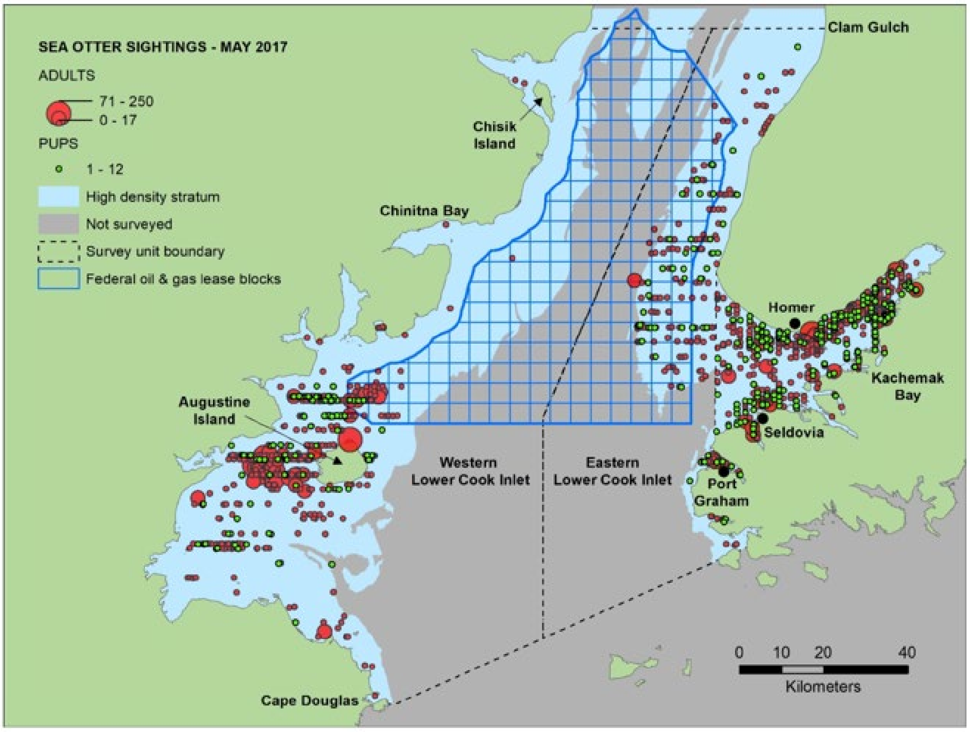

Figure 1: Number of adult (red points) and pup (green points) sea otter sightings encountered during replicate aerial surveys in May 2017. Point size indicates the relative number of sea otters at each location. Blue grid lines identify federal oil and gas lease blocks and blue shading represents the surveyed extent of lower Cook Inlet (from Garlich-Miller et al. 2018).

As sea otter populations grow in lower Cook Inlet, they are recolonizing areas where they have been absent since the fur trade. In 2019, sea otters began to expand up western Cook Inlet towards Lake Clark National Park and Preserve (NPS observations). This recent expansion raises concern for the potential interactions of sea otters with oil and gas leasing and exploration activities as well as interactions with existing commercial and personal use clam and crab fisheries. Being able to predict sea otter expansion into uncolonized areas will assist with understanding potential interactions; however, this can only be accomplished with a thorough understanding of sea otter habitat associations. Sea otters generally use nearshore waters that are associated with kelp or preferred prey (e.g., clams, crabs; Rotterman and Simon-Jackson 1988), and hard substrates are thought to be a higher quality habitat than soft substrates due to kelp forest occurrence (Nicholson et al. 2018, Tinker et al. 2019). While these general habitat associations are known, finer scale subtidal habitat associations (i.e., vegetative cover, invertebrate composition, and substrate complexity) are unclear. In addition, many sea otter habitat studies have occurred in hard-bottom or mixed, heterogeneous habitats (Kvitek et al. 1992, Jolly 1997, Maldini et al. 2008, Gilkinson et al. 2011, Wolt et al. 2012), so there is a dearth of information about sea otters in predominantly soft-bottom and tidally-driven systems, such as lower Cook Inlet. Previous sea otter habitat studies in soft or mixed-sediments have focused on the top-down effects of sea otters on invertebrate prey communities (Kvitek et al. 1992, Weitzman 2013, Stewart et al. 2014, Traiger et al. 2016), but there is a limited understanding of how habitat influences sea otters from the bottom-up-habitat perspective in Alaska (except see Coletti et al. 2016 and Williams et al. 2019).

Previous studies have used shore-based (Bodkin et al. 2007, Bodkin et al. 2012, Weitzman 2013), SCUBA-based (Stewart et al. 2014, Traiger et al. 2016), and Geographical Information System (GIS) (Coletti 2006, Gilkinson et al. 2011) methods to study sea otter habitat. Shore-based studies have primarily investigated sea otter behavior and foraging ecology to understand prey selection, metabolic rates, and ecosystem change (Bodkin et al. 2007, Bodkin et al. 2012, Weitzman 2013). SCUBA-based studies can provide a fine-scale assessment of habitat, although the ability to sample larger areas is constrained by the intensity of fieldwork (Stewart et al. 2014). Studies using GIS-derived information, such as depth and distance from shore, extend the area of inference beyond what can be observed from shore (Coletti 2006, Gilkinson et al. 2011). The present study is the first to leverage remotely operated vehicle (ROV) technology for *in situ* sampling of subtidal sea otter habitats. Here, we map habitat types within the current sea otter range and correlate these data with population distribution. Specifically, this study investigates the benthic habitat characteristics (i.e., vegetative cover, invertebrate composition, and substrate) that support a gradient of sea otter abundance (uncolonized, low, mid, and high density) in lower Cook Inlet, Alaska. This study rigorously extends the information we have gleaned from previous intertidal zone studies, such as ShoreZone and Gulf Watch Alaska, into the subtidal zone.

Objectives

1. Develop benthic habitat maps in areas where sea otters are present (Katmai National Park and Preserve, eastern Cook Inlet, western Cook Inlet, and Kachemak Bay) and areas currently absent of sea otters (Lake Clark National Park and Preserve and Chinitina Bay).
2. Quantify biological and physical habitat attributes across a gradient of sea otter density to understand the correlation of sea otter density to benthic habitat.
3. Develop predictive maps for areas of likely sea otter utilization due to expansion in the lower Cook Inlet area, specifically Lake Clark National Park and Preserve and Chinitina Bay.

Methods

Study Area

Lower Cook Inlet is a tidally-driven sub-Arctic system located in southcentral Alaska. Sea otters inhabiting lower Cook Inlet are divided into two separately managed populations: the southwest Alaska stock, which extends from western Cook Inlet through the Aleutians Islands, and the southcentral Alaska stock, which includes eastern Cook Inlet, Kachemak Bay, and Prince William Sound. Benthic habitat surveys using an ROV were conducted in eastern Cook Inlet (ECI), Kachemak Bay (KBAY), Lake Clark National Park and Preserve (LACL), western Cook Inlet (WCI), Chinitina Bay (CBAY), and Katmai National Park and Preserve (KATM) through the support of multiple funding sources and agencies (Table 1, Figure 2). In Lake Clark National Park and Preserve, western Cook Inlet, and Katmai National Park and Preserve surveys were conducted from cruises of opportunity. Surveys were completed across a gradient of sea otter population density and occupation (i.e., uncolonized, low density, mid density, and high density; Table 1, Figure 3; see Data Analysis, Objective 2).

Table 1. Surveys conducted in lower Cook Inlet.

Survey region	Sea otter density categories surveyed	Funding source/supporting agency
Eastern Cook Inlet	Low, mid, high	Coastal Marine Institute
Kachemak Bay	High	Coastal Marine Institute
Lake Clark National Park and Preserve	Uncolonized	National Park Service
Western Cook Inlet	Low, high	U.S. Geological Survey, Bureau of Ocean Energy Management
Chinitina Bay	Uncolonized	U.S. Geological Survey, Bureau of Ocean Energy Management
Katmai National Park and Preserve	Low, mid	National Park Service, Gulf Watch Alaska

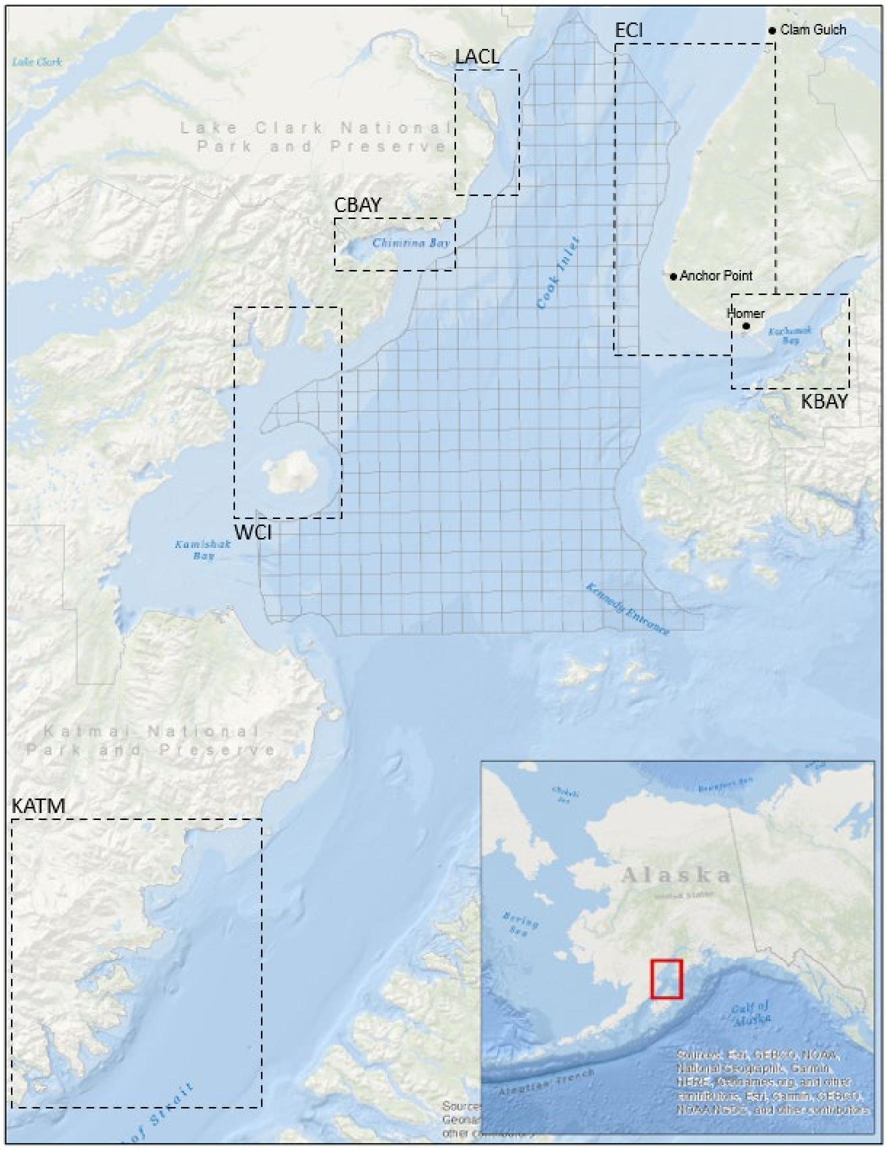

Figure 2. Map of study region showing six survey areas: western Cook Inlet (WCI), Chinitina Bay (CBAY), Lake Clark National Park and Preserve (LACL), eastern Cook Inlet (ECI), Katmai National Park and Preserve (KATM), and Kachemak Bay (KBAY). Grid lines show the Bureau of Ocean Energy Management lease blocks.

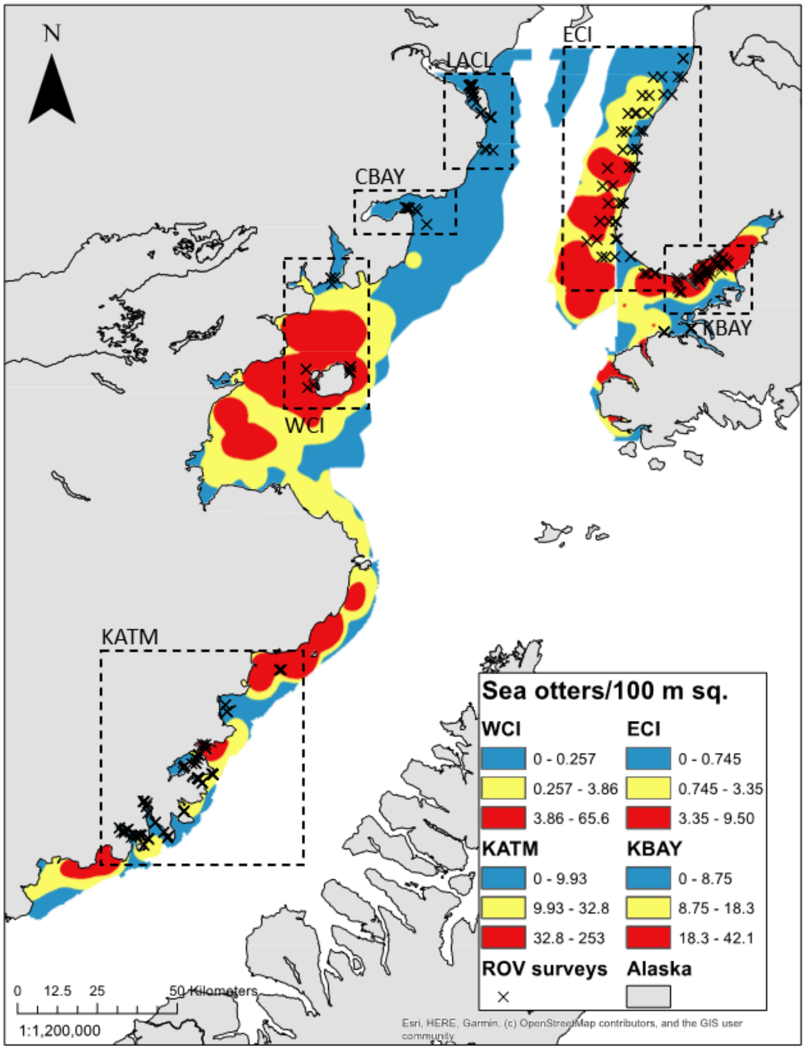

Figure 3. Sea otter density estimates and ROV survey sites in lower Cook Inlet, Alaska; blue, yellow, and red represent low, mid, and high density, respectively, and survey sites are marked by X. Chinitina Bay (CBAY) and Lake Clark National Park and Preserve (LACL) had densities of zero.

Data Collection

ROV (VideoRay Mission Pro 5) benthic habitat video surveys were conducted between May and October 2021 in six areas of lower Cook Inlet with varying sea otter population densities (Figure 3). The ROV is a submersible unit with a high-definition camera, LED lights, location tracking, and a 100-m data relay tether. The ROV is deployed and guided from a vessel and has survey mobility at depths up to ~30 m. At each survey area, sites were located at 5 m (when feasible based on vessel limitations), 10 m, 20 m, and 30 m depths. These depths were selected because sea otters typically forage in waters 40 m or shallower (Kenyon 1975, Bodkin et al. 2004). Site selection in Lake Clark National Park and Preserve, Katmai National Park and Preserve, western Cook Inlet, and Chinitina Bay was influenced by vessel limitations, weather, and locations of other relevant data streams (e.g., Gulf Watch Alaska nearshore monitoring sites), but were otherwise haphazard. Sites in eastern Cook Inlet and Kachemak Bay were spaced every 3 km from Clam Gulch to Anchor Point and into the north side of Kachemak Bay (Figures 2 and 3). Surveys were typically oriented perpendicular to the shoreline. If the current was strong (e.g., 1.5 NM/h), surveys were driven into the current (i.e., against the direction of the flow). Surveys were operated in a maximum current of 2 NM/h due to a reduction in visibility in currents greater than 2 NM/h. The length of each survey transect was determined by available tether, resulting in surveys averaging ~70 m in length.

Lower Cook Inlet sea otter abundance data were collected by the United States Geological Survey and the United States Fish and Wildlife Service (USFWS) in 2017 using aerial surveys (Garlich-Miller et al. 2018, Esslinger et al. 2021). Aerial transects were flown in lower Cook Inlet following the Bodkin and Udevitz (1999) method, as described in Garlich-Miller et al. (2018). Katmai National Park and Preserve sea otter abundance data were collected as part of the Gulf Watch Alaska monitoring program in 2018 using the same methods (Esslinger 2018).

Data Analysis

Objective 1: Develop Benthic Habitat Maps

All ROV surveys were manually processed through 2D visual image analysis. Videos were assigned to survey locations by matching time stamps of imagery and tracking data. Each video transect was first cut into frames (24 fps) in Adobe Photoshop. 150 images were then randomly selected for quality assessment. The images were manually assessed and any images that were not suitable for analysis were removed. The remaining images were randomly ordered to eliminate bias toward the beginning of the transect survey, and the first 30 images were then selected for analysis (Molloy et al. 2013, Perkins et al. 2016). This process was repeated for all surveys.

Images were analyzed in PhotoQuad software for habitat characterization using a random point count method (Trygonis and Sini 2012). Images were analyzed for percent cover of substrate using a modified Wentworth scale (Wentworth 1922), algal cover, and mobile and sessile epibenthic invertebrates. Substrate included boulder, cobble, pebble, gravel, shell, sand, and mud. Algae included understory kelp (hereafter referred to as kelp), macroalgae (all macroalgae excluding kelp and filamentous algae), filamentous microalgae, and coralline algae. Any invertebrates that were observed were recorded; however, this was limited to mobile and sessile epibenthic invertebrates seen on the substrate or above the algae. Cryptic invertebrates and infaunal invertebrates were not able to be observed. A trapezoidal frame was overlaid on top of each image as this was the extent of clear imagery and translated to a rectangle on the seafloor. Substrate attributes, algal cover, and invertebrate observations were assigned at 50 randomly selected points within the frame for each image. This translates to a percent cover estimate for each observed habitat attribute. Some surveys were excluded from the analysis due to file corruption or low visibility. Limited survey data from Katmai National Park and Preserve is presented as analysis of these surveys is still in progress. Habitat maps were produced in

ArcGIS (ArcGIS version 10.3, ESRI) to show the distribution of substrate and algal habitat attributes. Percent cover values were averaged by transect before mapping. Invertebrate distribution was not mapped as image-level invertebrate observations were sparse and all transect averages resulted in zeroes for all observed invertebrates.

Objective 2: Quantify Biological and Physical Habitat Attributes

To compare habitat attributes across a gradient of sea otter density, sea otter aerial survey data first had to be analyzed to estimate density across space. Kernel density estimation was conducted in R software (R Core Team 2021) using the kde function from the SpatialKDE package. Kernel density estimates were calculated for Kachemak Bay, eastern Cook Inlet, western Cook Inlet, and Katmai National Park and Preserve. Only adult sea otters were used to estimate population density (i.e., no pups) because pup locations are dependent on mothers. If multiple sea otters were observed at one set of coordinates, location entries were repeated (one entry per otter) to accurately reflect density. A bandwidth of 7.5 km was used to smooth across replicate aerial transects (Bodkin and Udevitz 1999) and account for the home range of sea otters (Tarjan and Tinker 2016). An output cell size of 100 m was used, and all other function parameters were set to defaults. Prediction grids were produced for each region before calculating kernel density using the extents of all aerial transects. All four regions were smoothed independently. Each replicate survey (three each for ECI, WCI, and KATM and four for KBAY) was smoothed independently. The resulting kernel density estimates for each of the replicate surveys were averaged using the calc function in base R (R Core Team 2021) to produce the final kernel density estimates for each region. Boundaries of aerial transects for each region were used to mask the resulting kernel density raster layers.

Sea otter density estimates were extracted at each ROV survey location. Survey locations were then categorized into four sea otter density categories: uncolonized, low density, mid density, and high density. Low, mid, and high density were categorized based on 33% quantiles. Quantile breaks vary between regions as density categories were defined based on local density ranges to capture artifacts of unique habitat regimes. Uncolonized areas that were surveyed with the ROV include Chinitina Bay and Lake Clark National Park and Preserve. Density category was appended to ROV habitat data for comparative analysis.

Habitat data were compared across density categories by region using PRIMER software (Clarke and Gorley 2006). Habitat data were separated into biotic and abiotic datasets, with algae and invertebrates in the biotic dataset and substrate in the abiotic dataset. Data were square root transformed before analyses. Habitat composition was visualized using non-metric multidimensional scaling (nMDS). Data were averaged by transect before conducting the nMDS analyses. Invertebrate contribution to biological communities in the nMDS analyses was negligible as all transect averages resulted in zeroes for all observed invertebrates. Communities were statistically compared using PERMANOVA to test for differences between sea otter density categories by region. Invertebrate contribution to biological communities was included in PERMANOVA analyses because data inputs were at the image-level instead of averaged by transect. Pairwise comparisons were evaluated. Model design consisted of ROV images, nested in transects, nested in density by region.

Objective 3: Develop Predictive Maps

A MaxEnt model (Elith et al. 2011, Phillips and Dudík 2008, Phillips et al. 2006) was produced to determine subtidal habitat associations of sea otters and to predict the suitability of habitat in Lake Clark National Park and Preserve and Chinitina Bay in the face of sea otter population expansion. Data from Chinitina Bay and Lake Clark National Park were withheld from model calibration and were only used for prediction. Model calibration utilized habitat data from Kachemak Bay, eastern Cook Inlet, and western Cook Inlet. Habitat data from Katmai National Park and Preserve was not included in the MaxEnt model as analysis of these data is still in progress. Continuous habitat maps were produced using the kriging function in ArcGIS (ArcGIS version 10.3, ESRI) constrained to three points for interpolation to minimize smoothing over long distances. Sea otter habitat associations were modeled based on substrate and algal community composition. Invertebrate data were not included in the MaxEnt model because observations were too sparse to produce smooth maps. Species distribution was modeled using the MaxEnt algorithm (Elith et al. 2011, Phillips and Dudík 2008, Phillips et al. 2006) through the ENMeval package (Kass et al. 2021) in R (R Core Team 2021). Sea otters observed during the 2017 USFWS sea otter aerial abundance survey (Garlich-Miller et al. 2018) were used as presence locations in the model with only one observation retained per grid cell. A total of 711 sea otter presence locations and 9,314 background points were used. Background points were randomly selected from strip transect polygons as this was considered the available space of the surveyed area. Strip transect polygons were produced by creating transect lines from start and end coordinates and then buffering the line 200 m on either side to represent the 400 m band. Training and testing data were partitioned using random k-fold partitioning with five folds. Multicollinearity between habitat data was assessed using a stepwise variance inflation factor method using the vif function (Naimi et al. 2014) in R (R Core Team 2021).

Model settings were determined through model tuning in the ENMeval (Kass et al. 2021) package in R (R Core Team 2021). Default MaxEnt 3.4.3 settings were used, except for permissible types of feature classes and the regularization multiplier. Twenty-five models were created with varying types of feature classes (i.e., linear, quadratic, hinge, and combinations of linear/quadratic and linear/quadratic/hinge) and regularization multipliers from 1-5. Feature class type dictates the shape of the relationship of covariates to response (Bohl et al. 2019). The regularization multiplier dictates the penalty for model complexity with a high regularization multiplier corresponding to a large penalty (Elith et al. 2011, Merow et al. 2013, Phillips and Dudík 2008). Together, these settings influence model complexity. Model selection was conducted using the sample-size adjusted Akaike information criterion formula (AICc, Warren and Seifert 2011) to determine optimal model settings.

Once the best model was selected, model performance was evaluated by comparing results to a null model distribution. Some applications of MaxEnt models report model estimates, but there is no way to evaluate performance within the algorithm. Bohl et al. (2019) developed a framework for evaluating model performance by comparing the empirical model to a null model distribution. The novelty of this approach is a null model simulation that is validated with randomly selected occurrence points against the same testing dataset and background points used in the empirical model. This allows for a more direct comparison of model performance than in previous evaluation frameworks. As a non-parametric method, it is critical to employ an evaluation method to properly estimate effect size and model significance.

Null models were constructed over 1,000 iterations by calibrating with a random sample of points within the strip transect polygons and the same background points from the empirical model. Null models were validated with the same testing dataset as the empirical model so that performance measures were directly comparable (Bohl et al. 2019). Model performance of the empirical and null models was evaluated with the area under the receiver operating characteristic curve (AUC) for the training (AUC_{train}) and testing (AUC_{val}) datasets, the difference between AUC_{val} and AUC_{train} (AUC_{diff}), and omission error rate (OR) with a threshold that leads to 10% omission of calibration records (Liu et al. 2005). AUC_{val} and AUC_{train} are measures of discriminatory ability and AUC_{diff} and OR are measures of overfitting (Bohl et al. 2019). Standardized effect sizes (Ulrich and Gotelli 2010) and p-values were calculated to test whether the empirical model performed better than the null model distribution (Bohl et al. 2019). Covariate percent contribution was gathered from the MaxEnt model output to determine the importance of habitat attributes in predicting sea otter presence. The empirical model was then applied to all grid cells in the study area (i.e., the full extent of habitat raster layers), including Chinitina Bay and Lake Clark National Park and Preserve, to predict the probability of sea otter presence based on relationships with habitat covariates.

Results

Objective 1: Develop Benthic Habitat Maps

In total, ~180 ROV surveys were conducted, and 3,210 images have been analyzed thus far from 107 surveys. Maps of substrate and algal habitat were produced to demonstrate the distribution of habitat across ROV survey sites (Figures 4 and 5). Invertebrate cover was low across all regions so no map was produced for this habitat type. Invertebrates that were occasionally observed at the image-level include anemones, barnacles, bryozoans, crabs, hydroids, jellyfish, rock jingles, scallops, sea pens, sea stars, sea urchins, shrimp, snails, sponges, and tunicates. Substrate was primarily composed of mud, shell, and pebble (Figure 4). KBAY was dominated by mud with substantial shell cover. The southern half of ECI was dominated by shell cover with pebble intermixed. The northern half of ECI was nearly all mud. There is a mirrored transition of shell and pebble to mud only in LACL, directly west of northern ECI. CBAY was also predominantly mud-covered. WCI, around Augustine Island, as well as KATM, had mixed shell and mud cover. The majority of survey sites did not have algal cover and can be seen as bare ground (Figure 5). When algae were present, non-kelp macroalgae were most commonly observed. Algal cover was observed in KBAY, the southern sections of ECI and WCI, and KATM. Algae were most commonly observed in areas consistent with shell cover. The northern sections of eastern Cook Inlet, CBAY, and LACL were devoid of any type of algae.

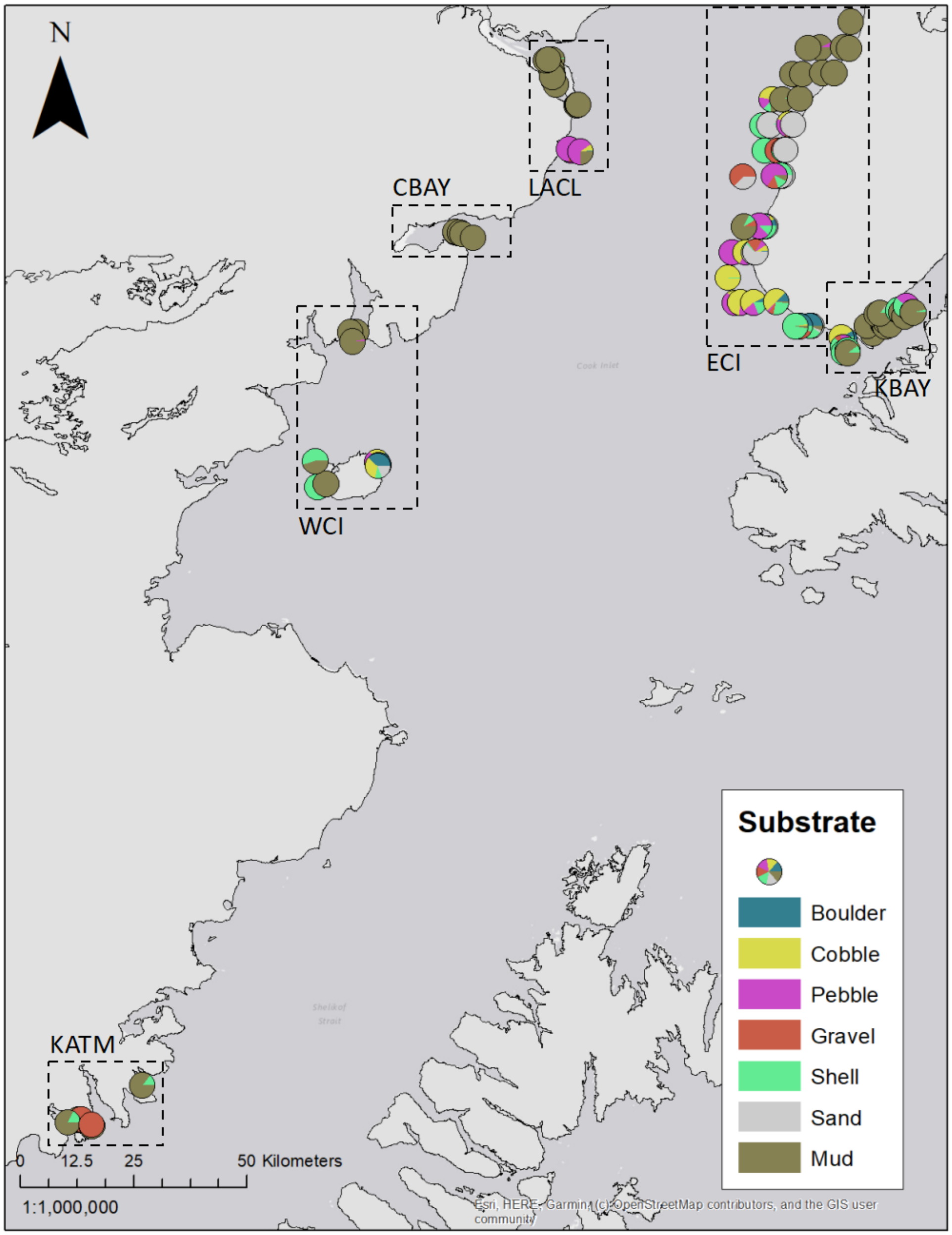

Figure 4. Map of substrate composition at ROV survey sites across the study region. Substrate composition is represented by pie charts where each pie is a survey and pie slivers equal the relative percent cover of substrate habitat attributes. Percent cover values are averages for each transect survey.

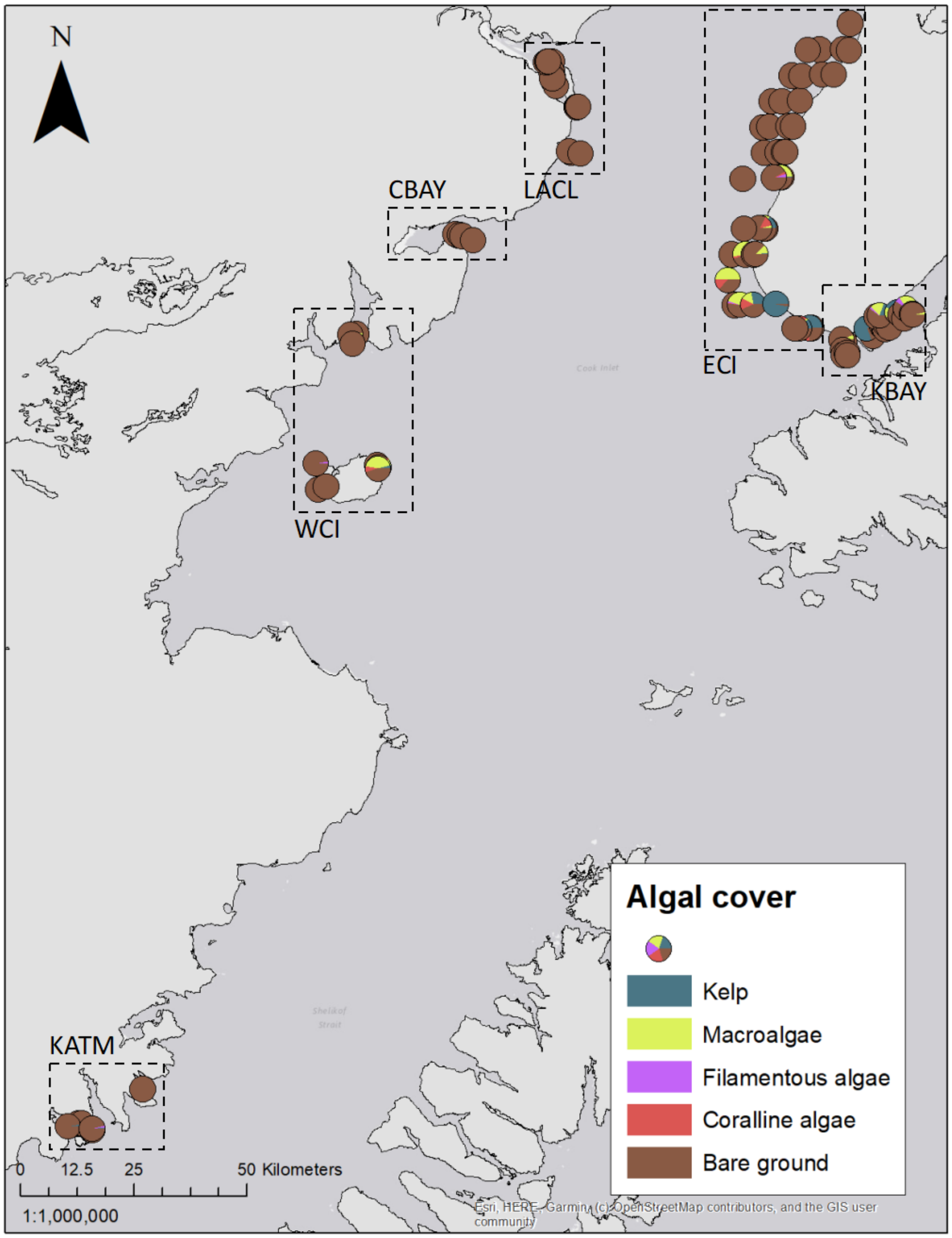

Figure 5. Map of algal cover at ROV survey sites across the study region. Algal composition is represented by pie charts where each pie is a survey and pie slivers equal the relative percent cover of algal habitat attributes. Percent cover values are averages for each transect survey.

Objective 2: Quantify Biological and Physical Habitat Attributes

Substrate Composition

Substrate composition in ECI is the most heterogeneous of all five regions, indicated by the spread of points throughout space (Figure 6). The substrate in ECI was composed of all attributes (i.e., boulder, cobble, pebble gravel, shell, sand, and mud), while all other regions were composed of fewer substrate attributes (Figure 4). The distribution of points across density categories appears to be randomly spread, indicating that there may not be a distinct trend between sea otter density and habitat composition. However, there is clustering of points from multiple regions on the right side of the plot, indicating a similarity in substrate composition at those locations. The 2D stress value for the substrate composition (2D stress = 0.15) is low and justifies interpretation of these results.

The PERMANOVA analysis of substrate composition and biological community between sea otter density categories by region revealed differences in habitat composition (Table 2, Table 3). Uncolonized waters of LACL had significantly different composition from ECI- mid, ECI- high, KBAY- high, and WCI- high. These differences were driven by the dominance of mud in LACL. Substrate composition in LACL was not significantly different from low density habitat in ECI, WCI, and low and mid density habitat in KATM. These similarities were driven by high mud cover. Uncolonized waters of CBAY had significantly different substrate composition from ECI- mid, ECI- high, KBAY- high, WCI- high, and KATM- mid. Substrate composition in CBAY was not significantly different from ECI- low or WCI- low. Similar to the results for LACL, these similarities and differences are driven by mud cover. Uncolonized habitats of LACL and CBAY were not significantly different from each other due to the dominance of mud in both habitats. Significant differences and similarities in substrate composition span density categories and regions, indicating that there is not a strict trend (Table 2, Figure 6).

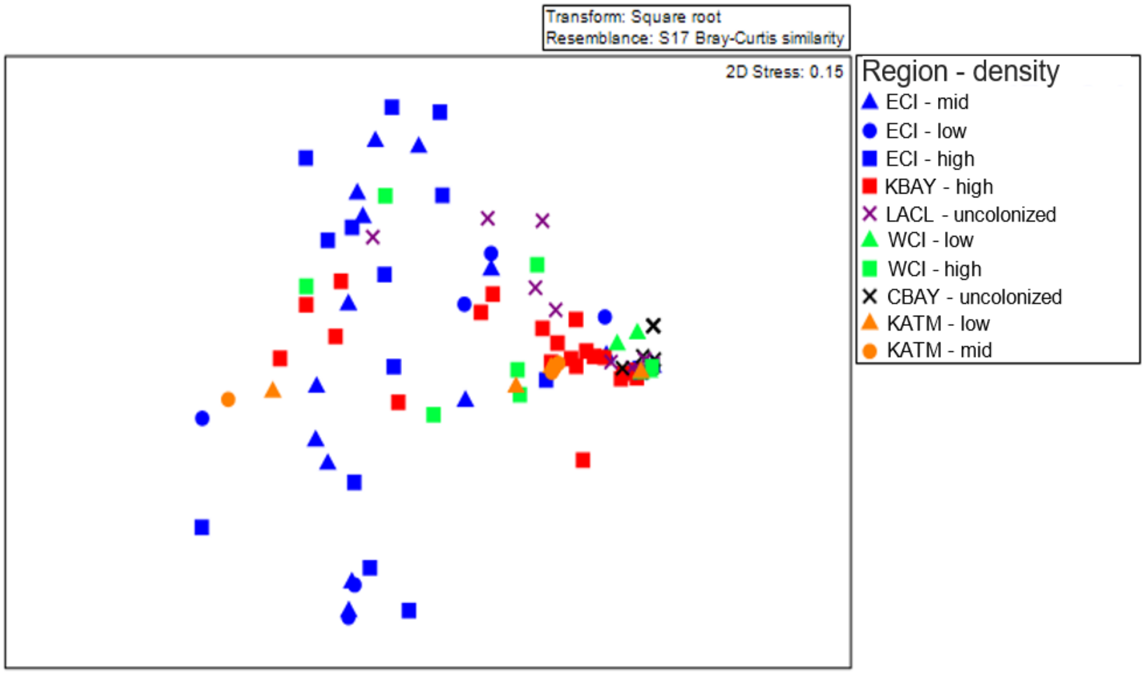

Figure 6. Non-metric multidimensional scaling plots of substrate composition between sea otter density categories across regions of lower Cook Inlet. Distance between points represents the relative similarity between communities. Symbol shape indicates sea otter density category and color indicates region.

Table 2. PERMANOVA results for comparison of substrate composition between sea otter population density categories by region: eastern Cook Inlet (ECI), western Cook Inlet (WCI), Chinitina Bay (CBAY), Kachemak Bay (KBAY), and Lake Clark National Park and Preserve (LACL). Population density categories include uncolonized, low, mid, and high density. Asterisks indicate a significant difference between categories (α=0.05).

Category 1	**Category 2**	**t value**	**p-value**
ECI- low	ECI- mid	1.75	0.035*
ECI- low	ECI- high	2.36	0.002*
ECI- low	KBAY- high	1.50	0.081
ECI- low	LACL- uncolonized	1.40	0.145
ECI- low	WCI- low	1.04	0.359
ECI- low	WCI- high	1.53	0.079
ECI- low	CBAY- uncolonized	1.29	0.192
ECI- low	KATM- low	0.83	0.563
ECI- low	KATM- mid	0.80	0.576
ECI- mid	ECI- high	0.77	0.684
ECI- mid	KBAY- high	1.92	0.015*
ECI- mid	LACL- uncolonized	3.18	0.001*
ECI- mid	WCI- low	2.03	0.017*
ECI- mid	WCI- high	1.06	0.361
ECI- mid	CBAY- uncolonized	2.52	0.002*
ECI- mid	KATM- low	1.15	0.269
ECI- mid	KATM- mid	1.03	0.391
ECI- high	KBAY- high	2.81	0.003*
ECI- high	LACL- uncolonized	4.14	0.001*
ECI- high	WCI- low	2.58	0.001*
ECI- high	WCI- high	1.51	0.069
ECI- high	CBAY- uncolonized	3.21	0.001*
ECI- high	KATM- low	1.57	0.059
ECI- high	KATM- mid	1.53	0.070
KBAY- high	LACL- uncolonized	2.15	0.007*
KBAY- high	WCI- low	1.59	0.079
KBAY- high	WCI- high	1.10	0.338
KBAY- high	CBAY- uncolonized	1.97	0.019*
KBAY- high	KATM- low	0.91	0.527
KBAY- high	KATM- mid	0.41	0.840
LACL- uncolonized	WCI- low	0.89	0.517
LACL- uncolonized	WCI- high	2.58	0.003*
LACL- uncolonized	CBAY- uncolonized	1.15	0.355
LACL- uncolonized	KATM- low	1.71	0.070
LACL- uncolonized	KATM- mid	1.46	0.099
WCI- low	WCI- high	2.03	0.030*
WCI- low	CBAY- uncolonized	0.30	0.784
WCI- low	KATM- low	1.68	0.113
WCI- low	KATM- mid	1.38	0.032*
WCI- high	CBAY- uncolonized	2.52	0.005*
WCI- high	KATM- low	1.19	0.259
WCI- high	KATM- mid	0.97	0.460
CBAY- uncolonized	KATM- low	2.12	0.056
CBAY- uncolonized	KATM- mid	1.75	0.008*
KATM- low	KATM- mid	Negative	NA

Biological Community Composition

The biological community of ECI is the most heterogeneous, indicated by the spread of points throughout space (Figure 7). KBAY and WCI also demonstrate some heterogeneity. KATM, CBAY, and LACL all demonstrate clustering, indicating homogeneity. The spread of points is driven by the presence or absence of one or more algal categories and the percent cover of bare ground. All points from LACL are overlapping demonstrating functionally complete homogeneity. Homogeneous (clustered) habitats are dominated by bare ground without algal cover. The 2D stress value for the biological community (2D stress = 0.09) is low and justifies interpretation of these results.

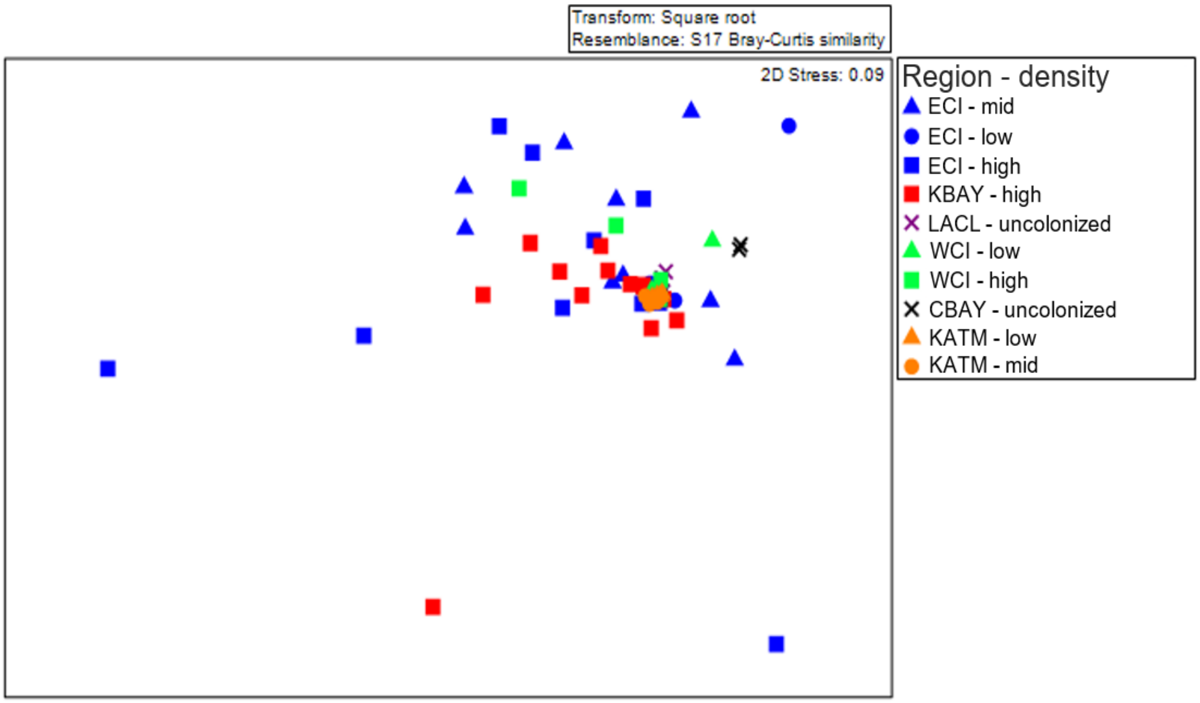

Figure 7. Non-metric multidimensional scaling plots of biological community composition between sea otter density categories across regions of lower Cook Inlet. Distance between points represents the relative similarity between communities. Symbol shape indicates sea otter density category and color indicates region.

Uncolonized waters of LACL had significantly different biological communities from those of ECI- mid, ECI- high, KBAY- high, WCI- low, WCI- high, and CBAY. Uncolonized waters of CBAY did not have significantly different biological communities from those of colonized areas. Similarities in biological communities also span density categories and regions (Table 3). There were few significantly different habitats between colonized areas with different density categories. ECI- low was significantly different from ECI- mid and ECI- high due to lack of algal cover. ECI- high was significantly different from KBAY- high, likely driven by higher coverage of coralline algae in ECI- high.

Table 3. PERMANOVA results for comparison of biological community composition, including algae and invertebrates, between sea otter population density categories by region: eastern Cook Inlet (ECI), western Cook Inlet (WCI), Chinitina Bay (CBAY), Kachemak Bay (KBAY), and Lake Clark National Park and Preserve (LACL). Density categories include uncolonized, low, mid, and high density. Asterisks indicate a significant difference between categories (α=0.05).

Category 1	Category 2	t value	p-value
ECI- low	ECI- mid	1.62	0.030*
ECI- low	ECI- high	1.93	0.028*
ECI- low	KBAY- high	1.54	0.053
ECI- low	LACL- uncolonized	1.25	0.188
ECI- low	WCI- low	0.29	0.929
ECI- low	WCI- high	1.24	0.179
ECI- low	CBAY- uncolonized	0.88	0.469
ECI- low	KATM- low	0.49	0.908
ECI- low	KATM- mid	0.57	0.871
ECI- mid	ECI- high	1.06	0.337
ECI- mid	KBAY- high	1.09	0.276
ECI- mid	LACL- uncolonized	2.42	0.001*
ECI- mid	WCI- low	0.99	0.391
ECI- mid	WCI- high	0.52	0.927
ECI- mid	CBAY- uncolonized	1.26	0.177
ECI- mid	KATM- low	1.11	0.311
ECI- mid	KATM- mid	1.08	0.321
ECI- high	KBAY- high	1.56	0.038*
ECI- high	LACL- uncolonized	2.72	0.001*
ECI- high	WCI- low	1.11	0.193
ECI- high	WCI- high	1.11	0.269
ECI- high	CBAY- uncolonized	1.40	0.108
ECI- high	KATM- low	1.21	0.262
ECI- high	KATM- mid	1.15	0.154
KBAY- high	LACL- uncolonized	2.34	0.001*
KBAY- high	WCI- low	0.97	0.345
KBAY- high	WCI- high	0.72	0.650
KBAY- high	CBAY- uncolonized	1.33	0.139
KBAY- high	KATM- low	1.01	0.360
KBAY- high	KATM- mid	0.96	0.349
LACL- uncolonized	WCI- low	2.24	0.006*
LACL- uncolonized	WCI- high	2.27	0.008*
LACL- uncolonized	CBAY- uncolonized	2.77	0.031*
LACL- uncolonized	KATM- low	1.02	0.372
LACL- uncolonized	KATM- mid	1.59	0.047*
WCI- low	WCI- high	0.90	0.598
WCI- low	CBAY- uncolonized	0.92	0.338
WCI- low	KATM- low	0.98	0.402
WCI- low	KATM- mid	1.05	0.175
WCI- high	CBAY- uncolonized	1.29	0.177
WCI- high	KATM- low	1.03	0.386
WCI- high	KATM- mid	0.98	0.460
CBAY- uncolonized	KATM- low	1.23	0.247
CBAY- uncolonized	KATM- mid	1.36	0.154
KATM- low	KATM- mid	0.88	0.533

Objective 3: Develop Predictive Maps

The evaluation of model settings using AICc resulted in the selection of features set to hinge and the regularization multiplier set to one as optimal settings (Figure 8). Allowing more feature types, as with hinge features, leads to a more complex model due to an increased number of parameters. Features are transformations of the covariates that the model is fit on (Elith et al. 2011). A lower regularization multiplier corresponds to a lower penalty on the model for complexity, resulting in a more complex framework and an increase in overfitting (Merow et al. 2013). The optimal model resulted in an omission rate of 0.134 and an AUC_{val} of 0.715. An omission rate higher than the given threshold (10%) indicates overfitting (Radosavljevic and Anderson 2013). Given the model omission rate of 0.134, the model demonstrates overfitting. The model AUC_{val} score of 0.715 indicates a prediction that deviates from random (AUC = 0.5) and is between "fair" and "good" performance (Swets 1988).

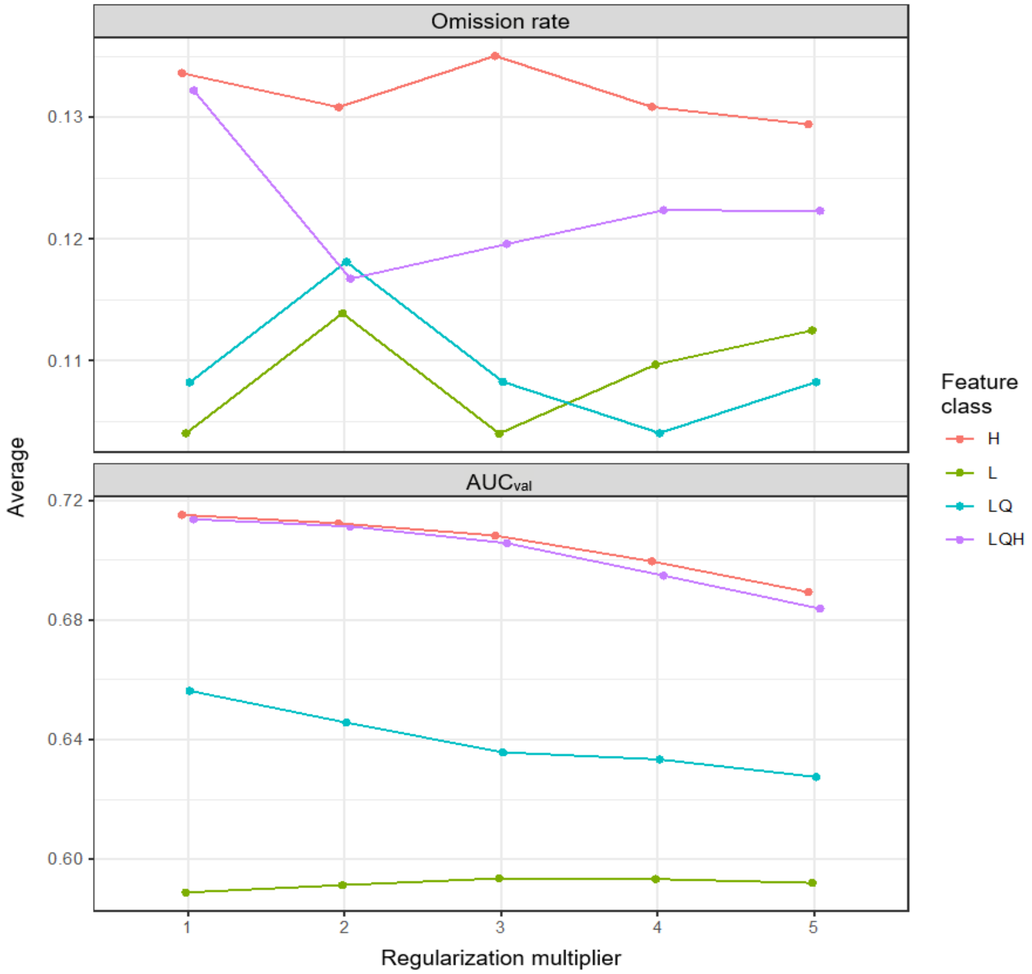

Figure 8. Line graphs of candidate model settings for model tuning. Lines are colored by feature settings (H: hinge, L: linear, LQ: linear and quadratic, LQH: linear, quadratic, and hinge). The x-axis indicates the regularization multiplier (1-5), and the y-axis indicates the evaluation metric value with omission rate on the top panel and AUC_{val} on the bottom panel.

The MaxEnt model with these parameter settings evaluated substrate, including pebble, shell, boulder, and macroalgae (excluding kelp) to be the four highest contributing habitat attributes to predicting sea otter occurrence (Table 4). Boulder percent cover had a positive relationship with likelihood of sea otter occurrence. Macroalgae had a quadratic relationship with likelihood of sea otter occurrence. Pebble and shell initially had negative and positive relationships, respectively, at low percent cover, and then plateaued to linear trends with likelihood of sea otter occurrence. All substrate and algal habitat attributes were found to contribute to predicting sea otter occurrence. Cobble had a positive relationship with likelihood of sea otter occurrence, while kelp, filamentous microalgae, gravel, and sand had negative relationships with likelihood of sea otter occurrence. Coralline algae had a relatively linear relationship with likelihood of sea otter occurrence. Mud was excluded from the analysis, determined through a stepwise variance inflation factor method (Naimi et al. 2014), as it was highly collinear with other covariates. The model was used to produce a map (Figure 9) of probability of sea otter occurrence in lower Cook Inlet based on the described habitat associations. The primary region of predictive interest is Lake Clark National Park and Preserve and Chinitina Bay as these areas are currently uncolonized by sea otters. The model predicted a <50% likelihood of sea otter occurrence in Lake Clark National Park and Preserve and Chinitina Bay with an accuracy of 71.5% (Figure 9).

Table 4. Variable contribution and permutational importance of substrate and algal habitat attributes in predicting sea otter presence from the MaxEnt model.

Variable	Percent contribution	Permutation importance
Shell	33.7	25.1
Boulder	19.9	23.9
Macroalgae	15.8	15
Pebble	12.7	10.9
Filamentous algae	5.9	6.7
Sand	3.6	2.6
Gravel	2.8	1.6
Understory kelp	2.8	3.3
Coralline algae	2.5	7.9
Cobble	0.4	2.8

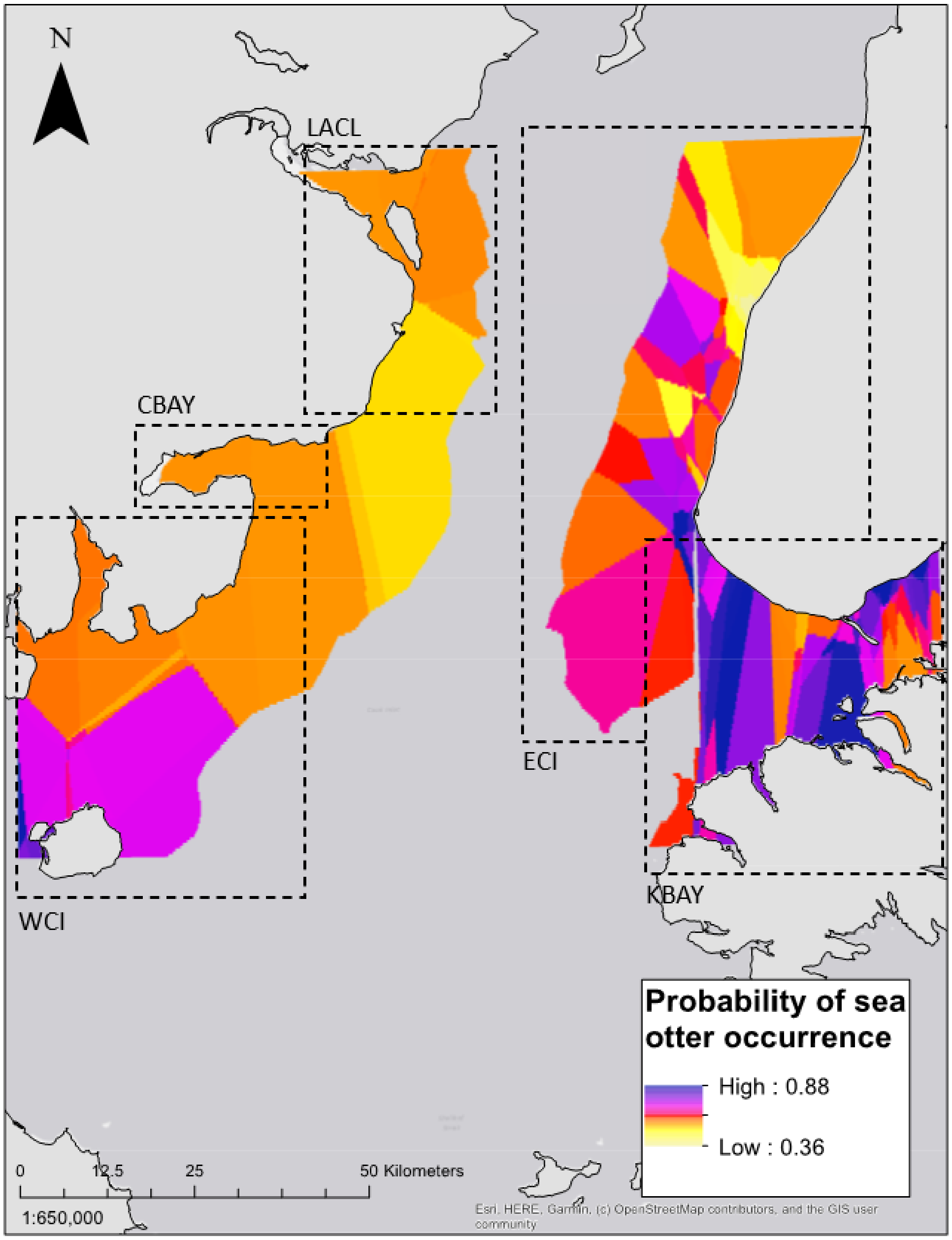

Figure 9. Map of predicted probability of sea otter occurrence in lower Cook Inlet based on subtidal habitat associations derived from the MaxEnt model.

The null model distribution was used to evaluate multiple model metrics against the empirical model. Discriminatory metrics, AUC_{train} and AUC_{val}, for the empirical model were 0.736 and 0.715, respectively, and 0.561 and 0.567 for the null model distribution, respectively. The p-values from a one-sided test comparing the empirical model to the null model distribution were $1.60x10^{-91}$ and $3.49x10^{-36}$ for AUC_{train} and AUC_{val}, respectively (Table 5). Empirical AUC_{train} and AUC_{val} fall outside of the 99th quantile of the null model distribution, showing significantly better ($\alpha = 0.05$) model performance than models with presence locations generated from random in the survey area (Figure 10). Metrics of overfitting, AUC_{diff} and OR, for the empirical model were 0.023 and 0.134, respectively, and 0.00844 and 0.0259 for the null model distribution respectively. The p-values from a one-sided test comparing the empirical model to the null model distribution were 0.0590 and 0.980 for AUC_{diff} and OR, respectively (Table 5). Empirical AUC_{diff} and OR do not demonstrate significantly different degrees of overfitting from models with presence locations generated from random in the survey area (Figure 10). The out-of-sample prediction for lower Cook Inlet has 71.5% (AUC_{val}) predictive accuracy with a standard deviation of 0.844% (Table 5).

Table 5. Model evaluation metrics for the empirical model and null model distribution. Z scores and p-values compare the empirical model to the null model distribution with a one-sided test.

Statistic	$\text{AUC}_{\text{train}}$	AUC_{val}	AUC_{diff}	OR
Empirical mean	0.736	0.715	0.023	0.134
Empirical standard deviation	NA	0.00844	0.0112	0.0259
Null mean	0.561	0.567	0.0383	0.104
Null standard deviation	0.00861	0.0119	0.00978	0.0142
z score	20.3	12.5	-1.56	2.06
p value	$1.60\text{x}10^{-91}$	$3.49\text{x}10^{-36}$	0.0590	0.980

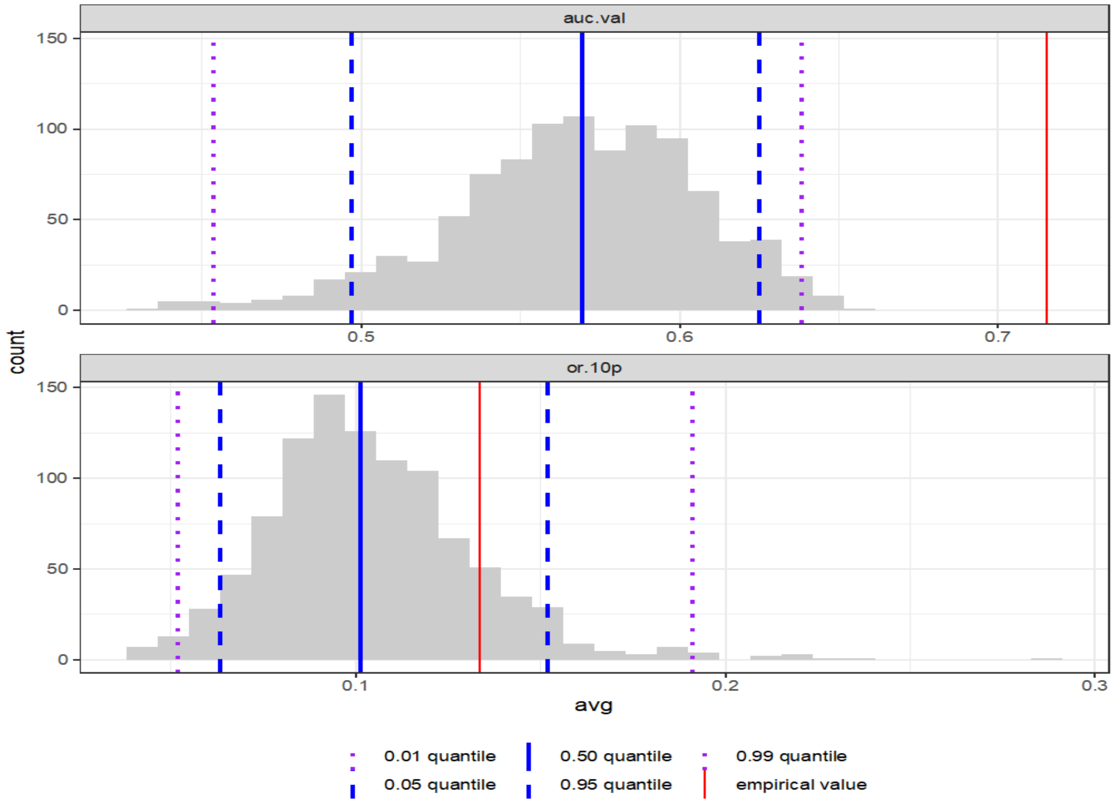

Figure 10. Histograms of the null model distribution. The red line indicates evaluation metric values for the empirical model. Dashed blue lines indicate the 0.05 and 0.95 quantiles, purple indicates the 0.01 and 0.99 quantiles, and the solid blue line indicates the median of the null model distribution. The x-axis of each panel corresponds to the AUC_{val} (top) and omission rate (bottom) values. The y-axis indicates frequency.

Discussion

The results of this study revealed statistically significant differences ($p < 0.05$) in habitat composition between sea otter colonized and uncolonized areas of lower Cook Inlet. Substrates of uncolonized areas (Lake Clark National Park and Preserve and Chinitina Bay) tended to be homogenous mud, while colonized areas (western Cook Inlet, eastern Cook Inlet, Kachemak Bay, and Katmai National Park and Preserve) varied in degree of habitat complexity. Biological communities of algae and invertebrates were nearly absent in Lake Clark National Park and Preserve, which differed from Chinitina Bay and colonized areas. However, the epibenthic invertebrate communities observed in this study were limited overall. This study demonstrates lower Cook Inlet habitat heterogeneity and what the subtidal environment can tell us about species distributions. While we did not find distinct trends in habitat composition across colonized areas, model predictions for the likelihood of sea otter occurrence were consistent with known low, mid, and high density areas. Throughout lower Cook Inlet, varying habitat composition supports low, mid, and high densities of sea otters, while Lake Clark National Park and Chinitina Bay are unlikely to support sea otters based on habitat composition alone.

The dominant substrate composition of lower Cook Inlet is soft sediment, specifically mud. Smaller grain sizes, including gravel and pebble, were also present, but transect averages resulted in a dominance of mud. Shell was also prominent throughout eastern and western Cook Inlet. It is likely that shell cover in areas colonized by sea otters is a result of sea otter foraging. Sea otters feed on infaunal bivalves and drop the shells, where they lay on the surface of the benthos (Kvitek et al. 1992). Many of the shells observed along the coastline of eastern Cook Inlet appeared to be razor clams (pers. obs.). Eastern Cook Inlet previously supported a razor clam fishery but has remained closed to personal use since 2015 due to population decline. This current study was not able to access clam populations in lower Cook Inlet because clams are infaunal bivalves, and grab samples were not included in the proposed work. Boulders and other larger grain sizes were patchy throughout survey sites. This is reflected in the patchy cover of macroalgae and kelp, as they require larger grain sizes to settle and persist (Steneck 2002). Bare ground was the dominant cover, meaning that all algal (kelp, other macroalgae, coralline algae, and filamentous microalgae) communities are limited.

The addition of eastern Cook Inlet to the study was intended to ensure a soft-sediment system similar to that of Lake Clark National Park and Preserve would be represented in the model. It was thought that the subtidal habitat of eastern Cook Inlet would also be muddy and homogeneous. However, we found that eastern Cook Inlet and Kachemak Bay contained the most heterogeneous substrate composition and biological communities. Substrate cover in eastern Cook Inlet and Kachemak Bay ranged from the finest sediment, mud, to the most course sediment, boulder. Biological communities contained all algal types (kelp, other macroalgae, coralline algae, and filamentous microalgae) and numerous mobile and sessile epibenthic invertebrates.

A comparison of sea otter population density categories by region revealed significant ($p < 0.05$) differences in substrate composition and biological communities of colonized and uncolonized areas. Specifically, Lake Clark National Park and Preserve, which is uncolonized by sea otters, has significantly different ($p < 0.05$) substrate composition and biological community structure than that of all mid and high density habitats. Lake Clark National Park and Preserve looked similar to low density habitats. In general, mid and high-density sea otter habitats had heterogeneous substrates, including small and large grain size, and biological community composition, including all algal categories (kelp, non-kelp macroalgae, coralline algae, and filamentous microalgae), while low-density and uncolonized habitats were homogeneous mud with occasional small grain sizes and limited biological habitat attributes. Chinitina Bay displayed similar trends in habitat homogeneity to that of Lake Clark National Park and Preserve demonstrating that subtidal habitat composition may play a role in the lack of sea otter presence in these areas. Colonized habitats in eastern Cook Inlet, Kachemak Bay, western Cook Inlet, and Katmai National Park and Preserve did not display an obvious trend in sea otter density categories between regions. This may indicate that prey availability, or other covariates not included in this study, are stronger drivers of sea otter density. For example, depth (Coletti 2006, Gilkinson et al. 2011) and distance from shore (Coletti 2006) have been shown to be important predictors of sea otter presence in Alaska. Image analysis of habitat data for Katmai National Park and Preserve is ongoing; thus, results for Katmai National Park and Preserve are considered preliminary. Further analyses with varying partitions in sea otter density category breaks may help determine whether there is a trend between sea otter density and specific habitat types.

Sea otters are a keystone species that can serve as ecosystem engineers; sea otters present in rocky and soft sediment ecosystems have led to higher diversity by promoting habitat for other species (Estes and Palmisano 1974, Kvitek et al. 1992). Kamishak Bay, where some of the western Cook Inlet ROV surveys were located, is thought to have had a remnant sea otter population after the end of the fur trading era (Lensink 1960). Sea otters did not colonize Kachemak Bay and eastern Cook Inlet until the 1960s and 1970s (Schneider 1976). Based on the expected impacts of sea otters on subtidal communities, we expected that western Cook Inlet would be equally, if not more, heterogeneous than Kachemak Bay and eastern Cook Inlet, which is contrary to what we found. However, these results have not considered infaunal diversity, which could be very important in this soft-sediment environment. As sea otters impact the productivity of clams (Weitzman 2013), it would be beneficial to consider infaunal species in future studies to fill in this knowledge gap. When modeling species distributions with a seascape approach, as done in this study, it is important to include many aspects of the physical habitat, environmental conditions, and prey availability to understand species presence in relation to the ecosystem (Pittman 2017).

Boulder, pebble, shell, and non-kelp macroalgae were found to be the most influential in predicting sea otter presence. As previously discussed, the association of sea otters with shell cover is likely due to sea otters foraging on infaunal bivalves (Kvitek et al. 1992). While the presence of shell litter may be an indicator that bivalve prey is available, it may not be the best predictor of likelihood of sea otter colonization. We likely would not see the same shell litter in an area uncolonized by sea otters, either because there are not many bivalves or they have not been turned over by sea otters. The relationships of boulder and macroalgae with sea otter presence are consistent with previous research (Tinker et al. 2021). Boulders are a stable substrate for macroalgal spores to settle on and grow because they are not as subject to disturbance as finer substrate grains (Steneck 2002). Pebble has not previously been identified directly as an important predictor of sea otter presence; however, it is consistent with sea otter foraging studies in mix-sediment systems (Gilkinson et al. 2011). The negative relationship of kelp with likelihood of sea otter occurrence contradicts the findings of other studies, where kelp was documented as an important component of sea otter habitat because it serves as a habitat for sea otter prey species (Foster and Schiel 1988, Estes and Duggins 1995). Interestingly, boulder and macroalgae had a strong influence on MaxEnt model predictions of sea otter presence, despite ample study sites with high densities of sea otters and soft substrate. The MaxEnt approach is a distribution-based method, not abundance-based, due to the restriction of one observation per grid cell (Phillips et al. 2006). Because groups of sea otters are recorded as counts at one coordinate (Garlich-Miller et al. 2018), only the coordinate is retained without the count value in the MaxEnt model. It is possible that habitat use by groups of sea otters is different than that of dispersed sea otters, leading to discrepancies between positively associated habitat attributes with sea otter occurrence and the composition of known high density sea otter habitats. Based on these habitat associations, Chinitina Bay and Lake Clark National Park and preserve were predicted to have a <50% likelihood of sea otter colonization. These results indicate that the habitat in these currently uncolonized areas is not suitable for sea otters. Future modeling efforts based on this study will utilize a density-based method to allow the prediction of density in addition to the likelihood of presence.

During model selection, there was a tradeoff in selecting model parameters to prioritize model performance or reduction in overfitting. In this case, model performance was prioritized as the goal was to predict the habitat suitability of uncolonized areas of lower Cook Inlet. Additional environmental covariates that explain sea otter habitat use, such as depth and distance from shore, may reduce overfitting and further increase model predictive performance. The results of the empirical to null model distribution comparison demonstrate that the discriminatory ability of the empirical model is significantly better than the null model distribution at $\alpha=0.05$, but the degree of overfitting is not significantly different. This result demonstrates that the model can predict the probability of sea otter presence based on the observed locations better than a randomly selected sample. This means that the model's performance is not due to chance and sea otter presence is influenced by the subtidal habitat.

Though we can predict the likelihood of sea otter colonization with 71.5% accuracy, it is challenging to know whether the habitat in Chinitina Bay and Lake Clark National Park and Preserve is truly unsuitable for sea otters or if the population has not had time to expand that far north. There is a strong caveat to this work that infaunal invertebrate communities were not part of the analysis, and the prey availability in Lake Clark National Park and Preserve and Chinitina Bay is unknown. Further analyses of prey availability would ecologically strengthen the predictability of suitability models. In addition, data on infaunal prey availability would allow for analyses linking infaunal communities to subtidal habitat types. Sea otter diet is expected to be composed of filter-feeding infaunal invertebrates if they are available (Estes et al. 1981, Kvitek et al. 1989, Bodkin et al. 2007). Clams, which were not surveyed in this study, may be present and shell cover may increase if sea otters colonize the area. If sea otters were to move into the area, the substrate composition and biological community may shift to look more like colonized habitat through habitat modification by sea otter foraging. This demonstrates a need for future infaunal sampling to fully understand the habitat of colonized and uncolonized areas. If suitable prey does occur in these areas, sea otters may colonize. However, it is hypothesized that currents in the area may be too strong (Johnson 2021) to allow for the persistence of substrate modification. Sea otter pits and deposited shells may be quickly washed away and covered again with finer sediment (Traiger et al. 2016). It would be possible to address this question through sediment core analysis and sediment flow dynamic experiments.

Cook Inlet is an area of concern due to oil and gas leasing and fisheries operations. As sea otters are a federally protected keystone species, preserving the health of their habitat is critical. In addition, sea otter colonization of a new area can change the present dynamics of the system and how humans interact with it (e.g., personal use clam fisheries). The results presented here are the preliminary stage of model development and provide the groundwork for future research. Predictive modeling of sea otter distributions in lower Cook Inlet is planned to continue, with the incorporation of additional model covariates and multibeam sonar data. Beyond this study, this subtidal habitat data can be used in environmental assessment studies of other species of interest (e.g., clams and crabs) and provide a benchmark for monitoring future change or disturbance to these systems.

Acknowledgments

I would like to thank the Coastal Marine Institute and the Bureau of Ocean and Energy Management for supporting this project, which allowed me to plan and lead field research as a student. The substantial field efforts in eastern Cook Inlet and Kachemak Bay would have otherwise not been possible. I would also like to thank the National Park Service, the U.S. Geological Survey, Gulf Watch Alaska, and the National Oceanic and Atmospheric Administration for supporting remotely operated vehicle surveys throughout the summer of 2021. Thank you to the College of Fisheries and Ocean Sciences at the University of Alaska Fairbanks for providing excellence in education and support of graduate research. I would like to extend my sincere gratitude to my graduate advisor, Dr. Brenda Konar, for her extensive support and guidance and for fostering my curiosity in marine research. Additional thanks to Dr. Tahzay Jones for his support of field research, education on research techniques, and mentorship, to my committee members Heather Coletti and Dr. Kristen Gorman for always providing feedback and guidance, and to the many other individuals who have been a part of this effort, including Dr. Dan Monson, Dr. Ben Weitzman, George Esslinger, Nicole LaRoche, and Ruby Scanlon. Thank you to the captains and crew of the *R/V Edgecumbe*, *R/V Alaskan Gyre, M/V Dreamcatcher, R/V Island C,* and Bottom Line Charters for accommodating my research needs and providing a commitment to safety.

References

Ballachey BE, Bodkin JL, DeGange AR. 1994. An overview of sea otter studies. In: Loughlin TR, editor. Marine Mammals and the *Exxon Valdez.* San Diego (CA): Academic Press. pp. 47-59.

Ballachey BE, Monson DH, Esslinger GG, Kloecker K, Bodkin J, Bowen L, Miles AK. 2014. 2013 Update on sea otter studies to assess recovery from the 1989 *Exxon Valdez* oil spill, Prince William Sound, Alaska. U.S. Geological Survey Open-File Report 2014-1030. 40 pp.

Bodkin JL, Udevitz MS. 1999. An aerial survey method to estimate sea otter abundance. In: Garner GW, Amstrup SC, Laake JL, Manly BJF, McDonald LL, Robertson DG, editors. Marine Mammal Survey and Assessment Methods. Rotterdam (Netherlands): A Balkema. pp. 13-26.

Bodkin J, Ballachey B, Dean T, Fukuyama A, Jewett S, McDonald L, Monson D, O'Clair C, VanBlaricom G. 2002. Sea otter population status and the process of recovery from the 1989 *Exxon Valdez* oil spill. Mar Ecol Prog Ser. 241:237-253.

Bodkin JL, Esslinger GG, Monson DH. 2004. Foraging depths of sea otters and implications to coastal marine communities. Mar Mamm Sci. 20:305-321.

Bodkin JL, Ballachey BE, Esslinger GG, Kloecker KA, Monson DH, Coletti HA. 2007. Perspectives on an invading predator- Sea otters in Glacier Bay. In: Piatt JF, Gende SM, editors. Proceedings of the Fourth Glacier Bay Science Symposium, October 26–28, 2004: U.S. Geological Survey Scientific Investigations Report 2007-5047. pp. 133-136.

Bodkin JL, Ballachey BE, Coletti HA, Esslinger GG, and others. 2012. Long-term effects of the *Exxon Valdez* oil spill: sea otter foraging in the intertidal as a pathway of exposure to lingering oil. Mar Ecol Prog Ser. 447:273-287.

Bohl CL, Kass JM, Anderson RP. 2019. A new null model approach to quantify performance and significance for ecological niche models of species distributions. J Biogeogr. 46(6):1101-1111.

Clarke KR, Gorley RN. 2006. PRIMER v6: User Manual/Tutorial. PRIMER-E, Plymouth.

Coletti HA. 2006. Correlating sea otter density and behavior to habitat attributes in Prince William Sound, Alaska: A model for prediction [Master's thesis]. University of New Hampshire. 86 pp.

Coletti HA, Bodkin JL, Monson DH, Ballachey BE, Dean TA. 2016. Detecting and inferring cause of change in an Alaska nearshore marine ecosystem. Ecosphere. 7(10):e01489.

Elith J, Phillips SJ, Hastie T, Dudík M, Chee YE, Yates CJ. 2011. A statistical explanation of MaxEnt for ecologists. Divers Distrib. 17:43-57.

Environmental Systems Research Institute (ESRI). 2012. ArcGIS Release 10.3. Redlands (CA).

Esler D, Ballachey BE, Matkin C, Cushing D, Kaler R, Bodkin J, Monson D, Esslinger G, Kloecker K. 2018. Timelines and mechanisms of wildlife population recovery following the *Exxon Valdez* oil spill. Deep Sea Res Part II: Top Stud Oceanogr. 147:36-42.

Esslinger GG. 2018. Gulf Watch Alaska Nearshore Component: sea otter aerial survey data from Katmai National Park and Preserve, 2008-2018 (ver. 2.0, March 2020): U.S. Geological Survey data release, doi.org/10.5066/F7930SG7.

Esslinger GG, Weitzman BP, Robinson BH. 2021. Sea otter aerial survey data from lower Cook Inlet, Alaska, 2017: U.S. Geological Survey data release, doi.org/10.5066/P9Q4DA3T

Estes JA, Palmisano JF. 1974. Sea otters: their role in structuring nearshore communities. Science. 185(4156):1058-1060.

Estes JA, Jameson RJ, Johnson AM. 1981. Food selection and some foraging tactics of sea otters. In: Chapman JA, Pursley D, editors. Worldwide Furbearer Conference Proceedings, Vol 1. Baltimore (MD): University of Maryland Press. pp. 606-641.

Estes JA, Duggins DO. 1995. Sea otters and kelp forests in Alaska: generality and variation in a community ecological paradigm. Ecol Monogr. 65(1):75-100.

Foster MS, Schiel DR. 1988. Kelp communities and sea otters: keystone species or just another brick in the wall? In: VanBlaricom GR, Estes JA, editors. The community ecology of sea otters. Heidelberg (Germany): Springer-Verlag Berlin Heidelberg. pp. 92-115.

Garlich-Miller JL, Esslinger GG, Weitzman BP. 2018. Aerial surveys of sea otters (*Enhydra lutris)* in Lower Cook Inlet, Alaska, May 2017. U.S. Fish and Wildlife Service, Marine Mammals Management Technical Report: MMM 2018-01. 22 pp.

Gilkinson AK, Finerty SE, Weltz F, Dellapenna TM, Davis RW. 2011. Habitat associations of sea otters (*Enhydra lutris*) in a soft- and mixed-sediment benthos in Alaska. J Mammal. 92(6):1278-1286.

Johnson M. 2021. Subtidal surface circulation in lower Cook Inlet and Kachemak Bay, Alaska. Reg Stud Mar Sci. 41:101609.

Jolly JM. 1997. Foraging ecology of the sea otter, *Enhydra lutris*, in a soft-sediment community [Master’s thesis]. University of California Santa Cruz. 62 pp.

Kass JM, Muscarella R, Galante PJ, Bohl C, Pinilla-Buitrago GE, Boria RA, Soley-Guardia M, Anderson RP. 2021. ENMeval 2.0: redesigned for customizable and reproducible modeling of species’ niches and distributions. Methods Ecol Evol. 12:1602-1608.

Kenyon KW. 1969. Sea otters in the eastern North Pacific Ocean. N Am Fauna. 68:1-352.

Kenyon KW. 1975. The Sea Otter in the Eastern Pacific Ocean. New York (NY): Dover Publications.

Kvitek RG, Oliver JS, DeGange AR, Anderson BS. 1992. Changes in Alaskan soft-bottom prey communities along a gradient in sea otter predation. Ecology. 73(2):413-428.

Lensink CJ. 1960. Status and distribution of sea otters in Alaska. J Mamm. 41:172-182.

Maldini D, Ward C, Cecchetti A, Riggin J. 2008. Southern sea otter diet in a soft sediment community. JMATE. 3(1):27-35.

Merow C, Smith MJ, Silander JA Jr. 2013. A practical guide to Maxent for modeling species’ distributions: what it does, and why inputs and settings matter. Ecography. 36:1058-1096.

Molloy PP, Evanson M, Nellas AC, Rist JL, Marcus JE, Koldewey HJ, Vincent ACJ. 2013. How much sampling does it take to detect trends in coral-reef habitat using photoquadrat surveys? Aquat Conserv. 23(6):820-837.

Monson DH, Doak DF, Ballachey BE, Johnson A, Bodkin JL. 2000. Long-term impacts of the *Exxon Valdez* oil spill on sea otters, assessed through age-dependent mortality patterns. Proc Natl Acad Sci. 97(12):6562-6567.

Naimi B, Hamm NAS, Groen TA, Skidmore AK, Toxopeus AG. 2014. Where is positional uncertainty a problem for species distribution modeling? Ecography. 37(2):191-203.

Perkins N, Foster S, Hill N, Barrett N. 2016. Image subsampling and point scoring approaches for large-scale marine benthic monitoring programs. Estuar Coast Shelf Sci. 176:36-46.

Phillips SJ, Anderson RP, Schapire RE. 2006. Maximum entropy modeling of species geographic distributions. Ecol Modell. 190:231-259.

Phillips SJ, Dudík M. 2008. Modeling of species distributions with MaxEnt: new extensions and a comprehensive evaluation. Ecography. 31:161-175.

Pittman SJ. 2017. Seascape Ecology. Hoboken (NJ): Wiley Blackwell.

Nicholson, TE, Mayer KA, Staedler MM, Fujii JA, Murray MJ, Johnson AB, Tinker MT, Van Houtan KS. 2018. Gaps in kelp cover may threaten the recovery of California sea otters. Ecography. 41(11):1751-1762.

R Core Team. 2021. R: A language and environment for statistical computing. R Foundation for Statistical Computing, Vienna, Austria. https:www.R-project.org

Rotterman LM, Simon-Jackson T. 1988. Sea otter. In: Lentfer JW, editor. Selected Marine Mammals of Alaska: species accounts with research and management recommendations Marine Mammal Commission. Washington (DC). pp. 237-271.

Schneider KB. 1976. Assessment of the distribution and abundance of sea otters along the Kenai Peninsula, Kamishak Bay, and the Kodiak Peninsula. Final Report for the Alaska Department of Fish and Game. Anchorage (AK). 72 pp.

Steneck RS, Graham MH, Bourque BJ, Corbett D, Erlandson JM, Estes JA, Tegner MJ. 2002. Kelp forest ecosystems: biodiversity, stability, resilience, and future. Environ Conserve. 29(4):436-459.

Stewart N, Konar B, Doroff A. 2014. Sea otter (*Enhydra lutris*) foraging habitat use in a heterogeneous environment in Kachemak Bay off Alaska. Bull Mar Sci. 90(4):921-939.

Swets JA. 1988. Measuring the accuracy of diagnostic systems. Science. 240(4857):1285-1293.

Tarjan LM, Tinker MT. 2016. Permissible home range estimation (PHRE) in restricted habitats: a new algorithm and an evaluation for sea otters. PLoS ONE. 11(3):0150547.

Tinker MT, Gill VA, Esslinger GG, Bodkin J, Monk M, Mangel M, Monson DH, Raymond WW, Kissling ML. 2019. Trends and carrying capacity of sea otters in southeast Alaska. J Wildl Manag. 83(5):1073-1089.

Tinker MT, Yee JL, Laidre KL, Hatfield BB, Harris MD, Tomoleoni JA, Bell TW, Saarman E, Carswell LP, Miles AK. 2021. Habitat features predict carrying capacity of a recovering marine carnivore. J Wildl Manag. 85:303-323.

Traiger SB, Konar B, Doroff A, McCaslin L. 2016. Sea otters versus sea stars as major clam predators: evidence from foraging pits and shell litter. Mar Ecol Prog Ser. 560:73-86.

Trygonis V, Sini M. 2012. PhotoQuad: a dedicated seabed image processing software, and a comparative error analysis of four photoquadrat methods. J Exp Mar Biol Ecol. 424-425:99-108.

Ulrich W, Gotelli NJ. 2010. Null model analysis of species associations using abundance data. Ecology. 91(11):3384-3397.

Warren DL, Seifert SN. 2011. Ecological niche modeling in Maxent: the importance of model complexity and the performance of model selection criteria. Ecol Appl. 21(2):335-342.

Weitzman BP. 2013. Effects of sea otter colonization on soft-sediment intertidal prey assemblages in Glacier Bay, Alaska [Master's thesis]. University of California Santa Cruz. 68 pp.

Wentworth CK. 1922. A scale of grade and class terms for clastic sediments. J Geol. 30(5):377-392.

Williams PJ, Hooten MB, Esslinger GG, Womble JN, Bodkin JL, Bower MR. 2019. The rise of an apex predator following deglaciation. Divers Distrib. 25(6):895-908.

Wolt RC, Gelwick FP, Weltz F, Davis RW. 2012. Foraging behavior and prey of sea otters in a soft- and mixed-sediment benthos in Alaska. Mamm Biol. 77:271-280.

Sonia Kumar

Acoustics of Cook Inlet Beluga Whales and Anthropogenic Noise in the Kenai River, Alaska

Contents

List of Figures

List of Tables

Abstract

Anthropogenic noise is creating an increasingly louder environment for marine life globally and Cook Inlet, Alaska, is no exception. Research into potential impacts is important for understanding and mitigating the negative implications of noise for marine ecosystems. Cook Inlet supports endangered Cook Inlet beluga (CIB) whales (*Delphinapterus leucas*), which use vocalizations and echolocation to communicate, hunt, and navigate. From spring to fall, CIB have been documented feeding on anadromous fishes in and around rivers that flow into Cook Inlet. This study used acoustic detections of CIB to determine riverine habitat use patterns in the Kenai and Kasilof rivers, both heavily used by commercial, personal use, and sport fisheries. Passive acoustic monitors (PAM) were deployed at the rivers to record beluga echolocation and anthropogenic noise to assess if there is a correlation between beluga acoustic presence and anthropogenic and environmental noise. Two types of instruments were used, F-PODs and SoundTrap 500s (ST-500s). F-PODs were programmed to log beluga echolocation in frequencies between 20 kHz and 160 kHz. ST-500s were programmed to record frequencies between 10 kHz and 24 kHz, aiming to capture anthropogenic and environmental noise. Two F-PODs and one ST-500 were deployed in the Kasilof River in mid-June 2021 and were recovered in late September 2021. Three F-PODs and one ST-500 were deployed in the Kenai River in mid-June 2021 and were recovered in early November 2021. Shore-based visual surveys were conducted in conjunction with acoustic monitoring to compare with PAM detections. Data from the Kenai River showed that belugas were acoustically detected 6 days earlier than observed visually. No belugas were detected in the Kasilof River. Knowing the timing of river use by belugas will strengthen our understanding of the year-round distribution of CIB whales and how their acoustic presence relates to anthropogenic noise and activity.

Introduction

Anthropogenic noise in the Cook Inlet region in southcentral Alaska has been steadily growing due to several factors, including oil and gas development, an increase in shipping traffic, and active world-renowned fisheries. These waters also provide habitat for endangered Cook Inlet beluga (CIB) whales (*Delphinapterus leucas*), which use a variety of vocalizations to communicate, hunt, and navigate (Castellote et al. 2020). Anthropogenic noise and activity are creating a new and louder environment for marine life. Understanding the impacts of noise is critical for mitigating any negative implications for marine organisms. Passive acoustic monitoring (PAM) is a non-invasive way to monitor anthropogenic underwater acoustic sources and marine organisms. My research used PAM devices to document CIB presence and anthropogenic and environmental noise in two rivers that feed into Cook Inlet, the Kenai River and the Kasilof River (Figure 1). Documenting detailed seasonal movements of CIB could help inform regulatory agencies, such as NOAA Fisheries and the Alaska Department of Fish and Game, to implement management plans that can account for beluga seasonal distribution.

Cook Inlet beluga whales are geographically isolated and genetically distinct from the other four stocks of belugas inhabiting waters off the coast of Alaska (O'Corry-Crowe et al. 1997). Apart from the St. Lawrence Estuary belugas in Canada, this is the only population in the world to reside near an urban area (O'Corry-Crowe et al. 1997, Lesage et al. 1999). These charismatic whales, which can be easily seen from shore, are ecologically and culturally important to Alaskans (Huntington 2000). Alaska Native subsistence hunters have traditionally harvested beluga whales in Cook Inlet. However, overharvesting resulted in dwindling numbers, and it was believed that the population would return to historical numbers once harvesting pressure decreased (Mahoney and Sheldon 2000). Native hunters voluntarily ceased beluga hunting in 1999, but this hiatus, along with various regulatory measures have yet to produce signs of recovery (Shelden et al. 2019).

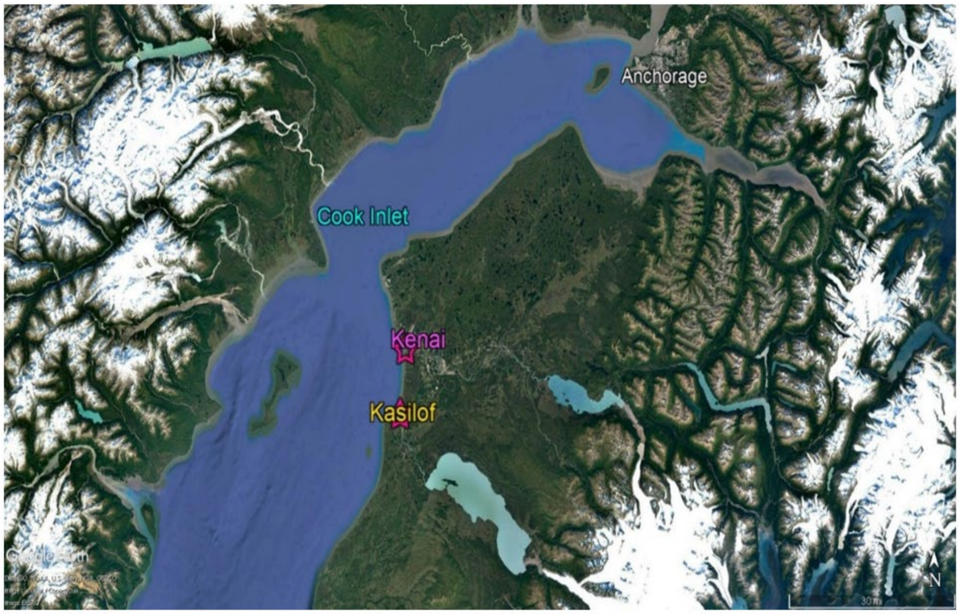

Figure 1. Map of Cook Inlet showing the Kenai and Kasilof Rivers.

The CIB population was listed as endangered in 2008 after sharp declines in the 1990s (Hobbs et al. 2015). In 1972, surveys estimated about 1,300 belugas in Cook Inlet (Hobbs et al. 2015); however, a 2019 study estimated the population to be 279, a decline of -2.3% per year (Shelden et al. 2019), steeper than a previously projected -0.4% per year (Shelden et al. 2017). In 2011, the National Marine Fisheries Service (NMFS) designated two areas comprising 7,800 km^2 as critical habitat for the endangered CIB (NMFS 2016). Prior studies have focused on CIB behavior, health, distribution, ecology, and population trends, but more research is needed to measure anthropogenic disturbance on beluga behavior (NMFS 2016). Since these whales live so close to humans, human activities may be contributing to population declines or delaying recovery.

To understand how anthropogenic activities may be impacting the CIB population, it is important to understand the whales' habitat and behaviors. Cook Inlet waters are dynamic, with extreme tidal changes and strong currents. Semidiurnal tides can be 8–10 meters and expose vast mudflats during the low tide (Ezer et al. 2008). Numerous glaciers and rivers feed into Cook Inlet and the basin receives a substantial amount of sediment that gets moved around to different channels (Sharma and Burell 1970). High turbidity makes it difficult to visually locate marine mammals unless they breach the surface, and even then it can be difficult to identify these small cetaceans.

Belugas have survived in the silty waters of Cook Inlet because they rely on sound to communicate, locate prey, and avoid predators (Chmelnitsky and Ferguson 2012). Different types of beluga calls have been documented, including whistles, pulsed tones, noisy calls, and echolocation clicks (Chmelnitsky and Ferguson 2012). Belugas primarily whistle and emit pulsed tones during social interactions and use echolocation clicks while navigating through the water and detecting prey (Chmelnitsky and Ferguson 2012). Whistles and echolocation clicks are notably different, with whistles having a lower frequency range. Echolocation clicks are directional broadband pulses that have a broader frequency range from 100 Hz to 120 kHz, with a peak frequency of 40 kHz or higher (Chmelnitsky and Ferguson 2012). As a cetacean moves in on its prey, it uses a burst of accelerated clicks to home in on it; this is also known as a feeding buzz (Verfuss et al. 2009). Understanding belugas' acoustic behavior is essential to quantifying their preferred foraging locations and seasonal patterns.

In the summer and fall, CIB feed on anadromous fish in the bays near river mouths and have been documented swimming up the rivers, likely following fish runs (Hobbs et al. 2015, Ovitz 2019). The Kenai River, Alaska's most heavily fished river, has shown an increase in human use since the late 1800s due to commercial, recreational, and sport fishing (ADFG 2015). Increased anthropogenic activity in the spring and summer months, resulting in a noisier marine environment, has the potential to alter beluga calls and spatial foraging behavior, especially if the animals cannot detect each other, prey, or predators (Small et al. 2017). Traditional knowledge holders have accounts of belugas frequenting the Kenai River between April and November, in groups of up to 50 animals (Huntington 2000). In recent years, the timing of beluga presence in the Kenai River has been truncated, with observers documenting belugas in March-April and

September-November (Ovitz 2019, AKBMP 2021). The entrance of the Kenai River falls under the critical habitat area designated by NMFS in 2011.

In 2016, NMFS created the Cook Inlet Beluga Recovery Plan which outlines different threats to population recovery; noise was listed in the top three threats along with catastrophic events (including natural disasters, pollutant spills, and mass strandings) and cumulative effects of multiple stressors (NMFS 2016). Examples of anthropogenic noise include propeller cavitation, pile driving, military detonation of high explosives, shore construction, fishing boats, recreational boats, and oil and gas exploration (NMFS 2016). The growing economic development in the Arctic and sub-Arctic could be affecting the recovery of this endangered species. Acoustic monitoring in areas that intersect with critical foraging habitat and anthropogenic use can lead to better management practices during times of high beluga usage and intense anthropogenic pressure.

This project builds upon and adds to recent work conducted by Castellote et al. (2020), wherein 14 moorings were maintained year-round within Cook Inlet to monitor CIB seasonal movements. The Kenai River was selected for this project because it is critical foraging habitat and presents an opportunity to study the potential impacts of anthropogenic activity on CIB distribution. Two types of PAM devices were deployed in the river: three F-PODs (Chelonia Ltd, UK) to detect high-frequency beluga echolocation, and one SoundTrap 500 hydrophone (Ocean Instruments, New Zealand) to record anthropogenic and environmental noise.

Objectives

1. Determine when Cook Inlet beluga whales are acoustically detected in the Kenai River.
2. Compare Cook Inlet beluga acoustic presence/absence with levels of anthropogenic and environmental noise in the Kenai River.

Methods

In June 2021, I deployed three continuously running F-PODs in the Kenai River (Figure 2). F-PODs are directional, detect high-frequency cetacean echolocation and have a range of up to 900 meters (Castellote et al. 2020). The projected 900-meter detection range is a conservative estimate because it is based on an older version (C-PODs) of the equipment used in previous Cook Inlet beluga acoustics studies(Castellote et al. 2016). F-PODs are more sensitive than C-PODs, and the detection range should be greater; however, at the time of this study, there were no data on the distance those instruments can detect cetaceans in Cook Inlet or the Kenai River. The detection range is limited because higher frequencies do not transmit as long a distance as lower frequency sound (Lammers et al. 2013). Additionally, due to the high sedimentation and the bends of the river, it is difficult to assess the exact detection range. Acoustic detections are categorized as detection positive minutes (DPM) and detection positive days (DPD) as described in Castellote et al. (2020), using the FPOD.exe software to analyze these acoustic recordings (https://www.chelonia.co.uk/fpod_downloads.htm) (Castelotte et al. 2020). After recovering the F-PODs, I visually validated the F-POD detections to confirm if the registered sounds were beluga clicks or if they were from another noise source.

Figure 2. Map of the 2021 Kenai River passive acoustic monitor locations.

In June 2021, I deployed one SoundTrap 500 hydrophone (ST-500) (Ocean Instruments, New Zealand) in the Kenai River to work in conjunction with the F-PODs. The primary purpose of this omnidirectional device was to continuously record lower frequency anthropogenic and environmental noise that the F-PODs will not detect, such as vessel traffic in the rivers, however, it also recorded lower frequency beluga vocalizations. The range of ST500s has not been studied in Cook Inlet before, but similar, older recorders were used in previous studies. The projected detection range is much longer than the F-PODs. The older recorders, called Ecological Acoustic Recorders (EARs), have an estimated range of 2–3km (Lammers et al. 2013). SoundTrap data was analyzed using the Raven Pro 1.4 software (2011, www.birds.cornell.edu/brp/raven). I classified 30-minute time frames every two hours into one of four noise categories: no noise (0), low noise (1), medium noise (2), and loud noise (3). These categories were classified based on visual assessment of acoustic activity in the spectrogram created in Raven using data from the ST500. I created a catalog of noise levels to use as a comparison when making these assessments. These levels of noise were compared to beluga presence to determine if there is a correlation between anthropogenic and environmental noise and presence of beluga whales. I also used hourly tidal data from water gauges in Nikiski, AK (~ 14 miles north of the Kenai River) to assess the influence of tides on beluga presence (NOAA Tides & Currents 2021).

Results

Beluga Acoustic Detections

Table 1 lists the deployment dates of the F-PODs in the Kenai River, the total number of days each detector was running, DPM, and DPD. The City Docks and Cannery Lodge F-PODs ran continuously throughout their deployments, whereas the Kenai Mouth F-POD experienced some technical problems and did not run July 18–25 and August 18–30.

Table 1. Kenai River F-Pod deployment dates and detection rates.

Location	Date deployed	Date removed	Days running	Detection positive days	Detection positive minutes
Kenai mouth	21 June 2021	7 November 2021	118	46	2831
City docks	15 June 2021	8 November 2021	146	47	3025
Cannery Lodge	18 June 2021	28 September 2021	102	10	247

Figure 3 shows a heat map of the number of minutes beluga whales were detected at each of the three F-PODs in the Kenai River. Belugas were first detected in the Kenai River at the City dock F-POD on August 28, with no detections from the initial deployment in mid-June up until that day. The highest number of detections on one F-POD occurred on October 1st at the Mouth F-POD, with 380 DPM, upwards of six hours. The day with the highest number of detections from all three devices was September 15, with 502 DPM registered. Belugas were detected 19 out of 30 days in September, 20 out of 31 days in October, and 6 out of 8 days of deployment in November. Between August 31 and September 27, all three F-PODs were successfully running. Of the 16 DPD within that time frame, belugas were detected at all three F-PODs for 6 days. During the other 10 days, detections occurred at the Mouth F-POD and the Kenai City Docks F-POD, but not the Cannery Lodge F-POD, which is further upriver than the other two locations.

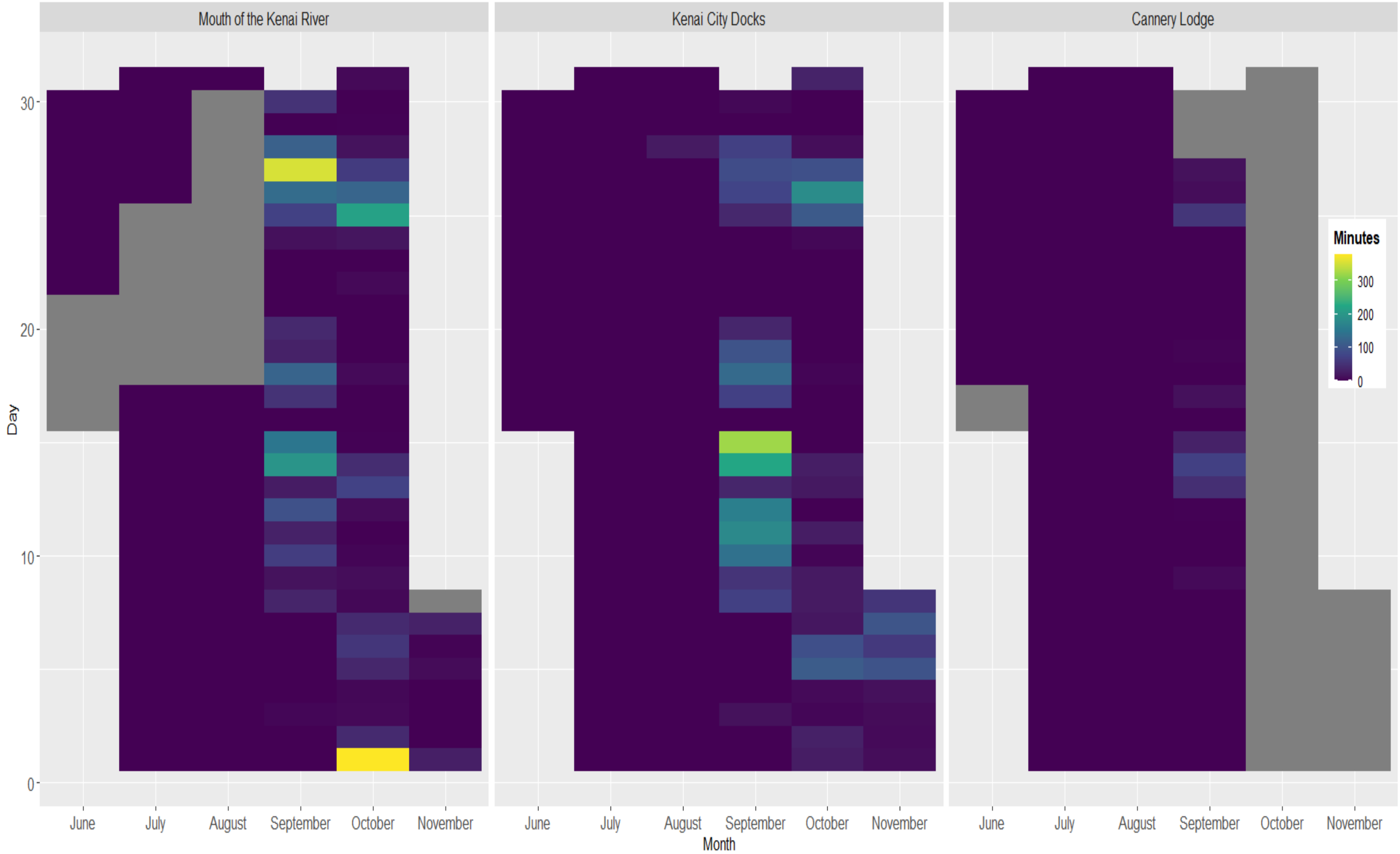

Figure 3. Heat maps of the number of minutes belugas were acoustically detected at each of the three F-PODs in the Kenai River. The spectrum starts at dark purple representing 0 minutes of detection and goes to bright yellow representing 380 minutes. Gray areas represent periods when the detector was not running.

Beluga Acoustic Detections Compared to Monthly Tidal Cycles

Figure 4 shows the comparison between beluga acoustic detections in the Kenai River at the three F-PODs and tide cycle using data from a water gauge in Nikiski. It should be noted that since the tide height was taken at a close, but different, location, the height is not exactly comparable to what might be observed in the Kenai River. I compared the predicted tides at the mouth of the Kenai River to the actual tides measured by the Nikiski water gauge and they were fairly comparable, with the high and low tides usually within an hour of each other, often much closer. Tide predictions from the Kenai River were not used because data from the Nikiski water gauge was more readily available. In Figure 4, there appears to be one detection at a tide height below zero in early November but that is likely explained by the location of the water gauge.

Beluga Acoustic Detections Compared with Anthropogenic and Environmental Noise

The ST-500 was deployed between June 7, 2021, and November 7, 2021, with equipment failure happening between June 25 and August 10, 2021, and September 19 and September 21, 2021. However, for the purposes of this report, the comparisons between anthropogenic and environmental noise and beluga detections are between August 11, 2021, and November 7, 2021. Figure 5 shows the relationship between beluga acoustic detections as registered by the three F-PODs in the Kenai River and anthropogenic and environmental noise recorded by the ST-500. The y-axis depicts the categories of the sound scale, with 0 representing no noise, 1 representing low noise, 2 representing medium noise, and 3 representing high noise. Belugas detected by the F-PODs during the few days in September when the ST500 was not recording are not included in the figure.

Generalized Additive Model

I used a generalized additive model (GAM) to examine the 2021 data. The model test concluded that beluga detections at a sound scale of 2 (medium noise) were significantly lower than beluga detections at a sound scale of 0 (no noise) (p-value =0.00782). The sound scales of 1 (low noise) and 3 (loud noise) showed no significant difference. The F-POD at the Cannery Lodge showed a significant difference in beluga detections compared to the Mouth F-POD (p-value ≈ 0), with fewer detections at the Cannery Lodge F-POD. The Kenai City Dock F-POD did not show a significant difference compared to the Mouth F-POD. Both smoothing terms, day of year and tide, were significant in explaining the variability in detection rates, (p-value ≈ 0 and p-value = 0.0307, respectively).

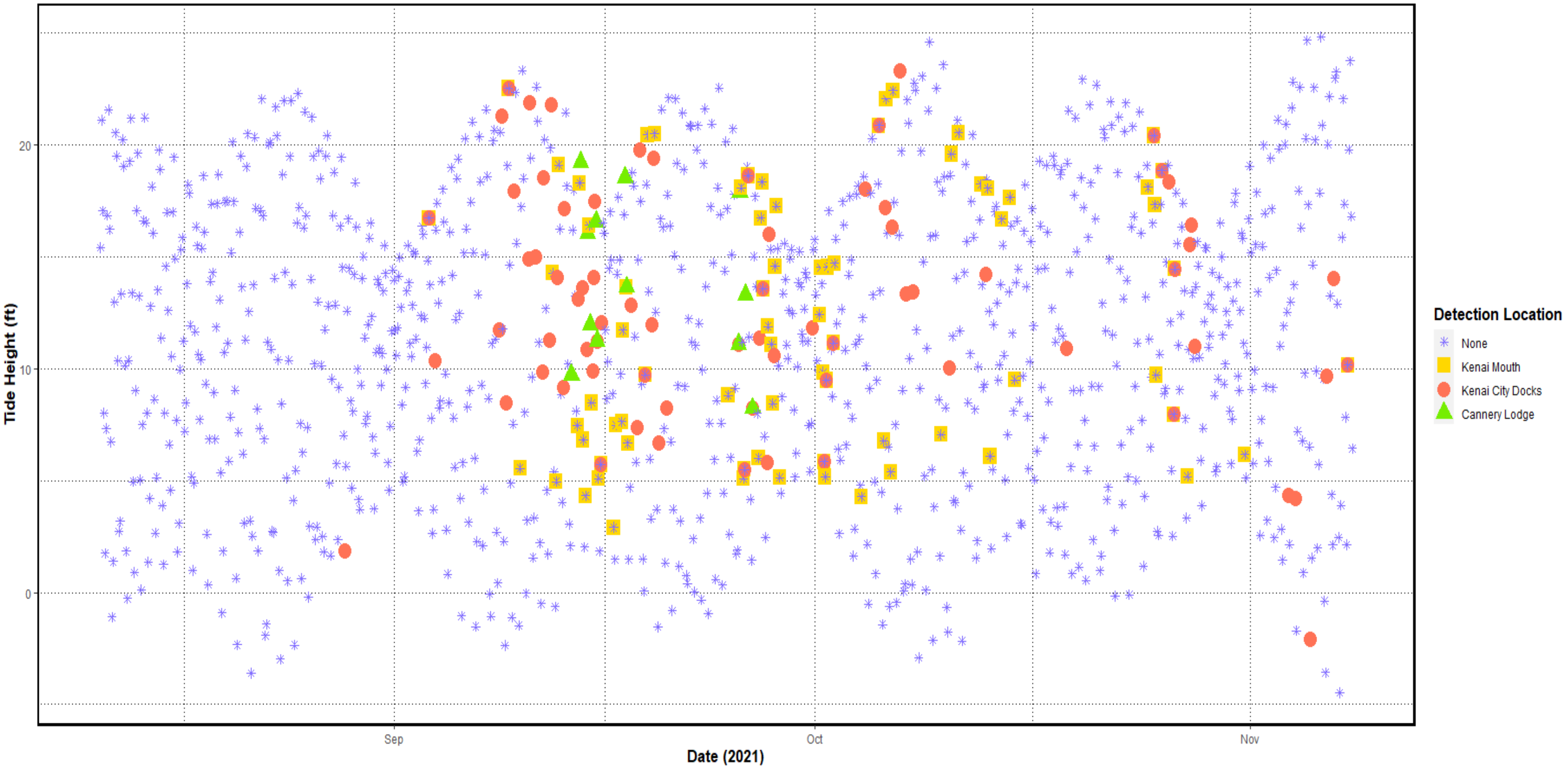

Figure 4. Beluga acoustic detections in the Kenai River compared to monthly tidal cycles in Fall 2021.

Figure 5. Comparison of beluga acoustic detections in the Kenai River (registered by F-PODs) and anthropogenic and environmental noise (recorded by ST-500). The anthropogenic and environmental noise scale was categorized into 4 different noise categories: 0 representing no noise, 1 representing low noise, 2 representing medium noise, and 3 representing loud noise.

Discussion

Initial deployment of the instruments was heavily dependent on the lack of sea ice in the river as well as the availability of deployment locations within the river. Ideally, each detector would have been attached to a dock piling at a fixed depth only accessible during a negative low tide, to ensure that the device did not float away, get buried by sediment, or be damaged by boats. Unfortunately, there are not very many structures within the first three river miles and the tide fluctuation in that region is so extreme that often even deeper sections of those structures are exposed during low tides or had the potential to be directly and physically impacted by boat traffic. The differences between deployment and recovery times of the devices were due to the accessibility and availability of different structures in the river.

Having three F-PODs in different locations within the first three river miles made it possible to assess belugas' preference of location within the river on given days and within certain periods of the tidal cycle. The bathymetry of the river is constantly changing due to high sediment loads and increasing volume of water throughout the summer as winter snow and glaciers melt, increasing the discharge into the river. Certain parts of the river may provide a more beneficial foraging habitat due to various features within the river. Beluga whales were acoustically detected in the Kenai River very consistently from the end of August through the beginning of November when the F-PODs were removed to prevent damage from sea ice that courses through the river in the winter. Belugas were detected less frequently at the Cannery Lodge, possibly because it was further upriver than the other F-POD locations. The Cannery Lodge F-POD was recovered two months earlier than the other F-PODs because the floating dock it was located on was removed from the river. Additionally, there was often a boat or two idling at the floating dock, potentially acoustically masking detections from the F-POD. Future work would include deploying a detector in the river channel in front of the dock instead of attached to the dock.

The commercial salmon fishing season ran from mid-June through mid-August with commercial fishers using the river as a staging area and essentially a harbor throughout the season. In addition, the salmon dip-netting fishery ran from July 10th to July 30th, with thousands of people using the Kenai River to fish from the riverbanks or various types of watercraft on the river. During these times, June, July, and most of August, the F-PODs had zero beluga detections. The first detection of beluga was a week and a half after the end of the fishing season, with consistent detections only occurring several weeks later, well after the last fishing boat was removed from the water.

In the spring and fall seasons, a dedicated group of volunteers through the Alaska Beluga Monitoring Partnership (AKBMP), a collaboration between several organizations, including NOAA Fisheries, conduct visual surveys for beluga whales at the Kenai River. The first fall 2021 documented sighting of a beluga whale in the Kenai occurred on September 3rd, six days after belugas were acoustically detected on August 28th. This is a strong indicator that continuing acoustic research in this region will be important in understanding beluga timing and usage of the river when compared with shore-based visual surveys alone. Unlike visual survey volunteers, the PAMs can record continuously and register beluga echolocation at all hours of the day.

Some results from the generalized linear model coincided with what I expected, and some were surprising. It was unsurprising that the tide was statistically significant (p-value = 0.0307) in explaining beluga detectability. The water levels in the Kenai River can be very low during low tides, with little room for belugas to maneuver, even though they are relatively small cetaceans. Additionally, belugas are often observed by AKBMP volunteers and other people within the community as coming in with the incoming tide. The significant (p-value ≈ 0) effect of the day of year was unsurprising since the summer is a time of high anthropogenic activity and noise, factors that might deter belugas from entering the river.

I was surprised to find that a noise level of 3 (loud noise) was not significantly different from a noise level of 0 (no noise) in detecting beluga presence. This might be due to the low number of time frames classified as a noise level of 3. Additional work will include processing the data at a finer scale by categorizing the sound 30 minutes every hour instead of every 2 hours, as was presented in this report, and including June in the analysis (the ST-500 was damaged and not running through July). I suspect that there will be a great number of periods with a noise level of 3 during those months.

During future field seasons, it would be beneficial to deploy the passive acoustic monitors as soon as there is no remaining sea ice coursing through the river. Being able to capture beluga presence and anthropogenic and environmental noise before the fishing season will give us a better understanding of how the noise level changes during the ice-free months. Ideally, the devices would be placed in the river year-round because there are periodic reports of belugas in the river throughout the winter and more consistent reports in March and April when ice is becoming less prevalent in the river.

Acknowledgments

I would like to thank the Alaska Coastal Marine Institute and the Bureau of Ocean and Energy Management for providing financial support for this project. Additional funding support from the Alaska Space Grant Program, Alaska EPSCoR, Northern Gulf of Alaska, AK UNiTE, Rasmuson Fisheries Research Center, and the University of Alaska Fairbanks made this project possible. I thank Verena Gill and Dr. Manuel Castellote (NOAA Fisheries Division) for their guidance, mentorship, and support of my research. I appreciate the support that Chris Garner provided before the commencement of my fieldwork and ongoing feedback throughout my field season. Thank you to Dr. Lara Horstmann for going above and beyond her role as my graduate advisor and for constantly being a positive and supportive person in my life. I also thank my committee members, Drs. Curry Cunningham and Brenda Konar, for providing feedback on my methods, proposal, and analytical approaches. I am incredibly grateful to Pacific Star Seafoods, Copper River Seafoods, Rogue Wave Seafoods, the Cannery Lodge, Ron Hyde, the City of Kenai, and Randy Vasko for allowing me to use their docks and equipment to deploy my passive acoustic monitoring devices. I am also sincerely appreciative of the many volunteers who helped me deploy my devices and conduct visual surveys.

References

Alaska Beluga Monitoring Partnership (AKBMP). 22 Oct. 2020. Sighting Log. Online: http//akbmp.org/beluga-observation-log.

Alaska Department of Fish and Game (ADFG). (2015). The Kenai River. Recreational fishing series, division of sport fish, Southcentral Region, Anchorage, Alaska. Online: http://www.adfg.alaska.gov/static/fishing/pdfs/sport/byarea/southcentral/northkenai2.pdf

Raven Pro 1.4. (2011). Raven Pro: Interactive Sound Analysis Software. K. Lisa Yang Center for Conservation Bioacoustics at the Cornell Lab of Ornithology, Ithaca, NY.

Castellote M., Small R. J., Lammers M. O., Jenninges J. J., Mondragon J., Garner C. D., Atkinson S., Delevaux J. M. S., Graham R., and Westerhold D. (2020). Seasonal distribution and foraging occurrence of Cook Inlet beluga whales based on passive acoustic monitoring. Endangered Species Research. 41:225-243.

Chmelnitsky G. E., and Ferguson S. H. (2012). Beluga whale, *Delphinapterus leucas*, vocalizations from the Churchill River, Manitoba, Canada. The Journal of the Acoustical Society of America. 131:4821-4835.

Ezer T., Hobbs R. C., and Oey L. Y. (2008). On the movement of beluga whales in Cook Inlet, Alaska. Oceanography (21):186-196.

Hobbs R., Sheldon K. E. W., Rugh D. J., Sims C. L., and Waite J. M. (2015). Estimated abundance and trend in aerial counts of beluga whales, *Delphinapterus leucas*, in Cook Inlet, Alaska, 1994-2012. Marine Fisheries Review. 77(1):11-31.

Huntington H. P. (2000). Traditional knowledge of the ecology of beluga, *Delphinapterus leucas*, in Cook Inlet, Alaska. Marine Fisheries Review. 62:134-140.

Lammers M. O., Castellote M., Small R., Atkinson S., Jenniges J., Rosinski A., Oswald J. N., and Garner C. (2013). Passive acoustic monitoring of Cook Inlet beluga whales (*Delphinapterus leucas*). The Journal of the Acoustical Society of America. 134:2497-2504.

Lesage V., Kingsley M. C. S., and Siare B. (1999). The effects of vessel noise on the vocal behavior or belugas in the St. Lawrence River Estuary, Canada. Marine Mammal Science. 15(1):65-84.

Mahoney B., and Shelden K. (2000). Harvest history of belugas, *Delphinapterus leucas*, in Cook Inlet, Alaska. Marine Fisheries Review. 62(3):124-133

NMFS (National Marine Fisheries Service). (2016). Recovery Plan for the Cook Inlet beluga whale (*Delphinapterus leucas*). National Marine Fisheries Service, Alaska Region, Protected Resources Division, Juneau, AK.

NOAA Tides & Currents (2021). Station Home Page: Nikiski, AK – Station ID: 9455760. Online: https://tidesandcurrents.noaa.gov/stationhome.html?id=9455760#sensors.

O’Corry-Crowe G., Suydam S., Rosenberg A., Frost K., and Dizon A. (1997). Phylogeography, population structure and dispersal patterns of the beluga whale *Delphinapterus leucas* in the western Nearctic revealed by mitochondrial DNA. Molecular Ecology. 6:955-970.

Sharma G., and Burrell D. (1970). Sedimentary environment and sediments of Cook Inlet, Alaska. American Association of Petroleum Geologists. 54:647-654.

Shelden K. E. W., Hobbs R. C., Sims C. L., Vate Brattström L., Mocklin J.A., Boyd C., and Mahoney B. A. (2017). Aerial surveys of beluga whales (*Delphinapterus leucas*) in Cook Inlet, Alaska, June 2016. AFSC Processed Rep. 2017-09, 62 p. Seattle, WA

Shelden K. E. W., and Wade P. R. (editors). (2019). Aerial surveys, distribution, abundance, and trend of belugas (*Delphinapterus leucas)* in Cook Inlet, Alaska, June 2018. AFSC Processed Rep. 2019-09, 93 p. Seattle, WA

Small, R .J., Brost B., Hooten M., Castellote M., and Mondragon J. (2017). Potential for spatial displacement of Cook Inlet beluga whales by anthropogenic noise in critical habitat. Endangered Species Research. 32:43-57.

Verfuss U. K., Miller L. A., Pilz P. K. D., and Schnitzler H. U. (2009). Echolocation by two foraging harbor porpoises. Journal of Experimental Biology. 212:823-834.

Lindsey Stadler

Feeding Ecology of Nearshore Fishes along a Gradient of Glacially-influenced Watersheds in Kachemak Bay, Alaska

Contents

List of Figures

List of Tables

Abstract

Changes in marine ecosystem functioning can be driven by climatic influences and the effects of human activities such as oil and gas exploration and development. High-latitude systems experience magnified effects from climate change including rising temperatures, increasing precipitation, and receding glaciers. Impacts linked with these changes, such as increased glacial discharge into nearshore estuaries, may impact food web dynamics and overall ecosystem functioning. This project focused on fish as important integrators of energy flow and ecosystem processes within the nearshore environment. Stable carbon and nitrogen isotope analyses were applied to examine resource use by fishes in Kachemak Bay watersheds with varying glacial coverage. Resource use by the crescent gunnel, a resident nearshore fish, was assessed across a gradient of glacial coverage and during different glacial discharge periods. The spatial patterns of resource use by gunnels were compared with those of more mobile nearshore fish species, starry flounder and staghorn sculpin, during the post-peak discharge period. Crescent gunnels exhibited significant spatial (sites of varying glacial coverage) (ANOVA, $p\text{-value} < 0.001$) and temporal (discharge periods) (ANOVA, $p\text{-value} < 0.05$) differences in their isotopic signatures, suggesting resource use was specific to site and discharge period, although patterns were not always linearly aligned with watershed glaciation. Alternatively, differences in baseline primary producer isotopic signatures relative to differing watershed glaciation and discharge rates may transfer to higher trophic levels such as fish. Compared to moderately-mobile staghorn sculpins and highly-mobile starry flounder, crescent gunnels showed much higher watershed-specific levels of significance (lowest p-values through ANOVA, pairwise comparisons) during the post-peak discharge period. This study supports the notion that crescent gunnels are useful mid-trophic level indicators of local conditions and can be used to track environmental changes. While staghorn sculpins and starry flounders may also respond to local watershed conditions in their resource use, they are not as useful as crescent gunnels as indicator species.

Introduction

Nearshore marine ecosystems provide important breeding grounds, nursery grounds, and feeding habitats for fish. Estuarine fishes employ a number of habitat uses and feeding strategies (Potter et al. 2013), making them good integrators of multiple ecosystem processes since they often occupy intermediate trophic levels. They may, thus, provide insight into how energy flow from a variety of basal resources interconnects through the trophic web (Possamai et al. 2020).

In high-latitude systems such as Kachemak Bay, Alaska, glacial melt may influence habitat structure and productivity of nearshore systems. Glacial discharge influences physical-chemical habitat conditions (Arimitsu et al. 2016) and resource availability for fishes in these habitats, with varying contributions from terrestrial and marine production sources (Whitney et al. 2018). The local resource use by fishes in such glacially-influenced systems will likely differ between largely location-bound nearshore fish species versus those that are more mobile and/or employ a variety of feeding strategies. Sedentary species will likely depend more on local food resources that are directly influenced by glacial discharge. More mobile species, however, will have expanded spatial resource use and will be less influenced by glacial effects on energy pathways in glacial estuaries. In addition, resident, location-bound species such as gunnels (*Pholidae*), may serve as an excellent proxy for measuring not only spatial (degrees of glacial discharge) but also temporal effects of glacial melt on nearshore food web structure and energy flow. In combination, a multispecies approach can inform about how tightly linked nearshore fishes are to local resources, and, thus, about their vulnerability to changes in the glacial landscape (Whitney et al. 2018).

The nearshore environment and its trophic connections are particularly vulnerable to climatic and anthropogenic drivers. Being adjacent to Cook Inlet exposes Kachemak Bay to potential impacts from shipping, oil and gas oil production, and population centers. The susceptibility of nearshore food webs to the effects of anthropogenic activities such as oil and gas development became abundantly clear in Alaska in 1989 when the *Exxon Valdez* oil spill contaminated over 2000 km of shoreline. The event devastated much of the nearshore habitat in the region and disrupted essential food web links to higher trophic levels such as fish (Peterson, 2001). Advancing our understanding of nearshore food web ecology in variable environmental settings, such as those with glacial influence, can help inform the management of these important habitats. Toward this goal, I specifically investigated (1) the differences in the diet of nearshore sedentary fishes (gunnels) across glacial discharge periods, (2) the differences in diet across watersheds with varying glacial influence, and (3) the differences in resource use by nearshore fishes with more mobile feeding strategies and ecologies.

Objectives

1. Assess whether the percent of glacial coverage in a watershed affects the resource use by nearshore fishes,
2. Assess whether resource use varies seasonally (by discharge period), and
3. Compare resource use by nearshore fish species with different mobility and behavior to discern specific habitat uses.

To address these objectives, I used stable isotope analyses of nearshore resident crescent gunnels (*Pholis laeta)* to understand dietary resource use across glacial discharge periods (pre-peak, peak, post-peak) and from five watersheds with differing glacial influence in Kachemak Bay. I compared crescent gunnels' trophic position and resource use with those of two other benthic species: staghorn sculpin (*Leptocottus armatus*), which typically remain in the nearshore environment but are more mobile than gunnels, and starry flounder (*Platichthys stellatus*)*,* which are highly mobile and venture into deeper waters. These mobile species may use resources differently in these watersheds.

Stable isotope analysis is a useful way to track the long-term diet over weeks to months during which animals incorporate the isotopic composition of their diet (Peterson and Fry, 1987; Post, 2002). The most typically used isotopes in diet studies are carbon and nitrogen; carbon informs about the assimilation of organic matter sources by consumers and nitrogen informs about trophic levels (DeNiro and Epstein, 1978; Peterson and Fry, 1987). For example, carbon of terrestrial origin possibly deposited into the nearshore environment with glacial discharge is isotopically lighter than carbon of marine origin; similarly, carbon isotope values from pelagic marine primary producers are lighter than those from benthic producers. The use of such different resources typically causes a distinguishable carbon stable isotope signature in the consumer, based on their reliance on these various trophic pathways (Post, 2002). The stable isotope approach can assess how tightly the feeding ecology of nearshore fishes is connected to the variable food sources in glacially-influenced watersheds, particularly marine-derived versus terrestrial resources. The specific hypotheses tested were that nearshore fishes will exhibit distinct trends in resource use depending on the degree of glacial influence in the respective watershed and that this resource use will be related to seasonal changes in glacial discharge rates. In addition, it was hypothesized that habitat use (sedentary vs. mobile) and feeding mode will play a role in resource use.

Methods

This study was completed in collaboration with the NSF-funded EPSCoR Fire and Ice program at UAF, which provided the logistics and access to five estuaries in Kachemak Bay: Grewingk Halibut, Wosnesenski (Wos), Jakolof, and Tutka. The watersheds ranged from 0-60% glacial coverage (Figure 1). Three nearshore fish species were collected, including highly resident crescent gunnels, nearshore but mobile staghorn sculpin, and wide-ranging and mobile starry flounder. Crescent gunnels were collected in June and July 2020, and April and May 2021, to allow temporal comparisons of resource use during pre-peak (Apr/May), peak (Jun/Jul), and post-peak (Aug/Sept) glacial discharge conditions (Figure 2). Collections of all three species were also done in August and September 2020 for spatial comparisons of resource use by different fish species across glacial watersheds during the post-peak discharge regime.

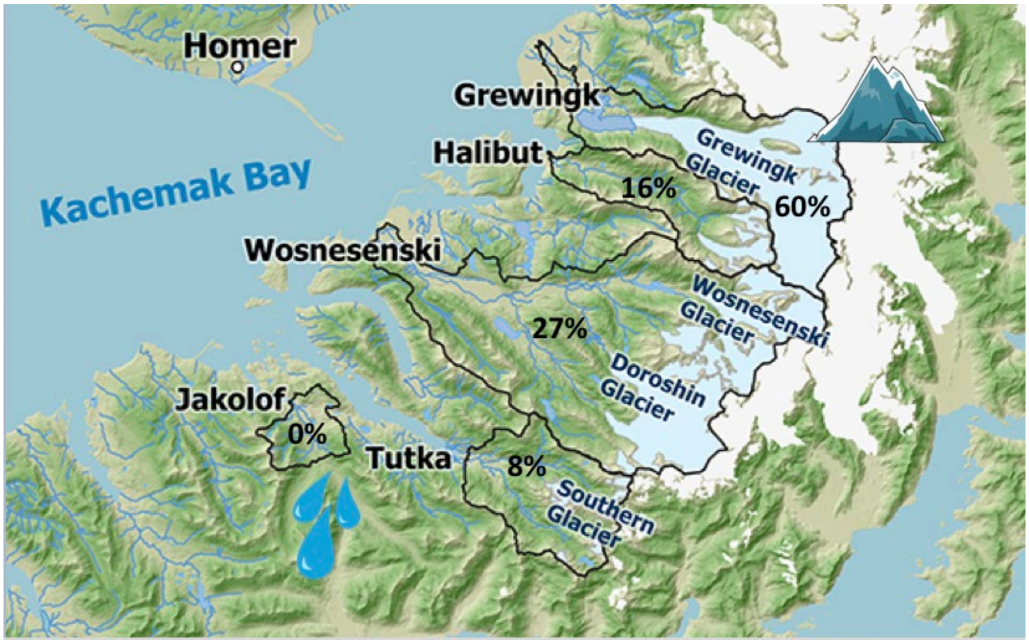

Figure 1. Map of Kachemak Bay study sites showing percent glacial cover of the respective watershed.

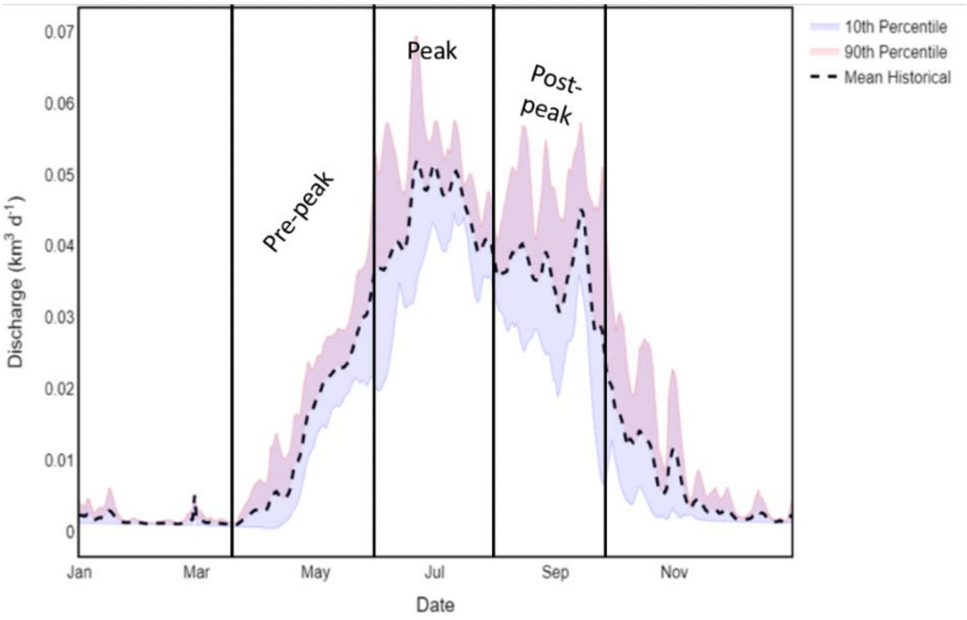

Figure 2. Modeled glacial discharge in Kachemak Bay from 2012-2019 (figure from J. Jenckes, UAA, data from Beamer et al, 2016).

To distinguish fish resource use and reliance on energy pathways from different basal producers (Herzka, 2005; von Biela et al., 2015), I employed bulk stable isotope analysis using liver tissues. Liver tissue has a fast turnover rate, reflecting the diet of the prior 2-4 weeks, and thus is a particularly useful tissue type to resolve shorter-term (i.e., monthly or discharge period) changes in resource use (Mohan et al., 2016). Liver samples were dried at 60°C until constant weight (about 24 h) and then homogenized. Because lipids can be depleted in ^{13}C relative to protein or carbohydrate and can significantly confound stable carbon isotope interpretation in lipid-rich tissues such as liver (Mintenbeck et al., 2008), I subjected a subset of samples to chemical lipid removal with repeated treatment of 2:1 chloroform:methanol to assess the effects of lipid content on stable isotope values (Mohan et al., 2016). A mathematical correction for lipid content was then derived from these test samples. Dried liver samples were measured at the Alaska Stable Isotope Facility (ASIF) at UAF for carbon and nitrogen stable isotope values. Stable isotope values were expressed in the common delta (δ) notation as parts per thousand (‰) according to the equation: $\delta X = [(R_{sample}/R_{standard}) - 1] \bullet 1000$, where X is ^{13}C or ^{15}N of the sample and R is the corresponding ratio $^{13}C/^{12}C$ or $^{15}N/^{14}N$. Pee Dee Belemnite and atmospheric N_2 served as standards for carbon and nitrogen, respectively.

To assess resource use in these fish species, fish liver isotope data were positioned in the resource isotope space of various primary producers. Specifically, phytoplankton (as particulate organic matter, POM.mix), various common macroalgae, select marsh plants, and upland plants were collected to delineate the available resource space. Many of these data were obtained from a partner project within the EPSCoR program studying nearshore food web dynamics involving lower trophic levels in 2020 (Schloemer, 2022).

Resource use represented by isotope values of the fishes was compared among species, by site and sampling event (for gunnels), using univariate statistics in RStudio (v. 1.4.1103). These analyses included Analysis of Variance (ANOVA) to compare isotope values among fish species or to detect changes in stable isotope values over time.

Results

A total of 449 fish from three species were collected from June – September 2020, March – May 2021, and August 2021. Crescent gunnels were collected from all five sites and during all three discharge rates (Table 1). Staghorn sculpin and starry flounder were collected during the "post-peak" discharge rate (i.e., August and September) in 2020 at all five sites (Table 2).

A total of 132 fish were analyzed for lipid effects: 70 crescent gunnel, 40 staghorn sculpin, and 22 starry flounder. Up to two individual fish from each site during each sampling event were chosen. Paired samples were analyzed for bulk carbon and nitrogen stable isotopes before and after chemical lipid extraction. The before and after values showed a tighter distribution (Figure 3), indicating that lipid extraction was useful. The following mathematical equation was used for lipid correction:

$L=93/[1 + (0.246\ C/N - 0.775) -1]$ $\delta' = \delta + D\ [-0.207 + 3.90/(1+287/L]$

where L is lipid, and D is the isotopic difference between protein and lipid (McConnauhey and McRoy, 1979).

Table 1. Number of crescent gunnels collected by discharge rate, pre-peak (March-May), peak (June-July), and post-peak (August-September).

	Grewingk	Wos	Halibut	Tutka	Jakolof
Pre-Peak	14	8	14	19	11
Peak	15	22	19	21	24
Post-Peak	28	22	26	29	23

Table 2. Numbers of fish species collected during post-peak discharge rate (August and September) by site and individual primary producer samples separated into groups that encompass various species collected by a partner project during the same discharge period (Schloemer, 2022). Macroalgal, marsh plant, and upland plant samples represent the total number of samples derived from replicates from multiple species. POM.mix represents particulate organic matter.

	Grewingk	Wos	Halibut	Tutka	Jakolof
Crescent Gunnels (*P. laeta*)	28	26	23	29	22
Staghorn Sculpin (*L. armatus*)	24	19	20	21	18
Starry Flounder (*p. stellatus*)	3	20	8	12	9
Macroalgae	32	36	23	18	21
POM.mix	6	6	6	6	6
marsh plant	21	24	24	12	21
upland plant	15	6	6	6	15

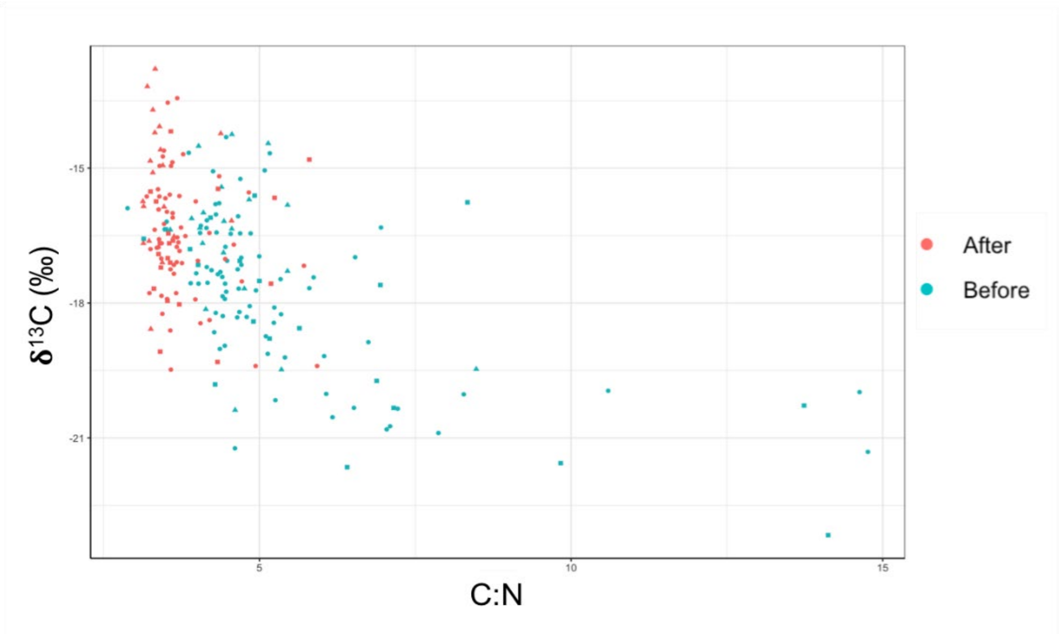

Figure 3. Crescent gunnel, staghorn sculpin, and starry flounder isotope values before and after chemical lipid extraction. Values plotted by δ^{13}C on the y-axis and C:N ratio on the x-axis.

Spatial Resource Use by Crescent Gunnels Relative to Watershed Glacial Coverage

Crescent gunnels showed significant differences in δ^{13}C and δ^{15}N values among the five sites of varying glacial cover (Figure 4) (ANOVA, p-value <0.001) when samples were combined across all sampling periods. A posthoc pairwise comparison (Tukey Honest Significant Difference (HSD) showed that all sites were significantly different from each other (all p-values <0.03) in their δ^{13}C values except for Wos (27% glacial cover) and Tutka (8% glacial cover) (Table 3). In contrast, differences in δ^{15}N values by site were mostly non-significant except for the comparisons of Tutka (8%) and Grewingk (60%), Jakolof (0%) and Halibut (16%), and Tutka (8%) and Jakolof (0%) (p-values <0.05). Gunnels at the Jakolof, which had no glacial cover, had heavier (or less negative) δ^{13}C values and higher δ^{15}N values. Gunnels at Wos (27% glacial cover) had relatively lighter (or more negative) δ^{13}C values and lower δ^{15}N values. The δ^{13}C values for gunnels at other sites, including the highest glaciated site (Grewingk), fell between Jakolof and Wos endpoints. Gunnels at Tutka Bay (8% glacial coverage) also were notable, as they grouped more closely to gunnels from sites of higher glacial coverage.

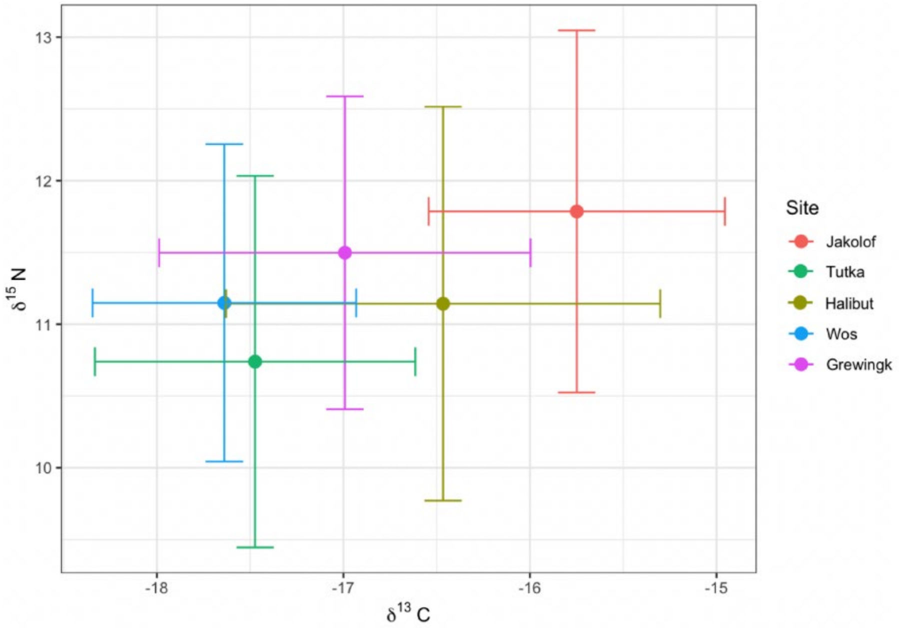

Figure 4. Crescent gunnel isotope biplot showing average δ^{13}C and δ^{15}N values (± standard deviation) by site, combined across all discharge conditions. Sites are listed in order of glacial cover starting with Jakolof (0%), Tutka (8%), Halibut (16%), Wos (27%), and Grewingk (60%).

Table 3. Tukey Honest Significant Difference (HSD) pairwise comparisons between each site pair. The symbol * represents significant adjusted p-values (p adj, < 0.05). DIFF represents the difference between the lower (LWR) and upper (UPR) bounds of the adjusted p-value (p-ADJ).

	DIFF	LWR	UPR	p-ADJ
$\delta^{13}C$				
Halibut (16%) – Grewingk (60%)	0.526	0.0570	0.996	0.019*
Jakolof (0%) – Grewingk (60%)	1.243	0.772	1.714	<0.0001*
Tutka (8%) – Grewingk (60%)	-0.482	-0.934	-0.029	0.030*
Wos (27%) – Grewingk (60 %)	-0.646	-1.131	-0.162	0.002*
Jakolof (0%) – Halibut (16%)	0.717	0.250	1.184	0.0003*
Tutka (8%) – Halibut (16%)	-1.008	-1.456	-0.560	<0.0001*
Wos (27%) – Halibut (16%)	-1.173	-1.653	-0.692	<0.0001*
Tutka (8%) – Jakolof (0%)	-1.725	-2.175	-1.275	<0.0001*
Wos (27%) – Jakolof (0%)	-1.889	-2.372	-1.407	<0.0001*
Wos (27%) – Tutka (8%)	-0.165	-0.629	0.299	0.866
$\delta^{15}N$				
Halibut (16%) – Grewingk (60%)	-0.355	-0.985	0.275	0.533
Jakolof (0%) – Grewingk (60%)	0.288	-0.345	0.920	0.723
Tutka (8%) – Grewingk (60%)	-0.759	-1.366	-0.152	0.006*
Wos (27%) – Grewingk (60 %)	-0.350	-0.999	0.301	0.579
Jakolof (0%) – Halibut (16%)	0.642	0.015	1.270	0.042*
Tutka (8%) – Halibut (16%)	-0.404	-1.005	0.197	0.350
Wos (27%) – Halibut (16%)	0.005	-0.640	0.650	0.999
Tutka (8%) – Jakolof (0%)	-1.046	-1.651	-0.442	<0.0001*
Wos (27%) – Jakolof (0%)	-0.637	-1.285	0.011	0.056
Wos (27%) – Tutka (8%)	0.409	-0.214	1.032	0.373

Variability in Resource Use by Crescent Gunnels in Relation to Glacial Discharge Regime

Crescent gunnels showed significant differences in $\delta^{13}C$ values and $\delta^{15}N$ values between discharge rates (ANOVA, $\delta^{13}C$ p-value = 0.0112, $\delta^{15}N$, p <0.0001). There was a decrease in $\delta^{13}C$ (toward more negative values) and in $\delta^{15}N$ values throughout consecutive discharge rates (from pre-peak to post-peak) when data were combined across all sites (Figure 5).

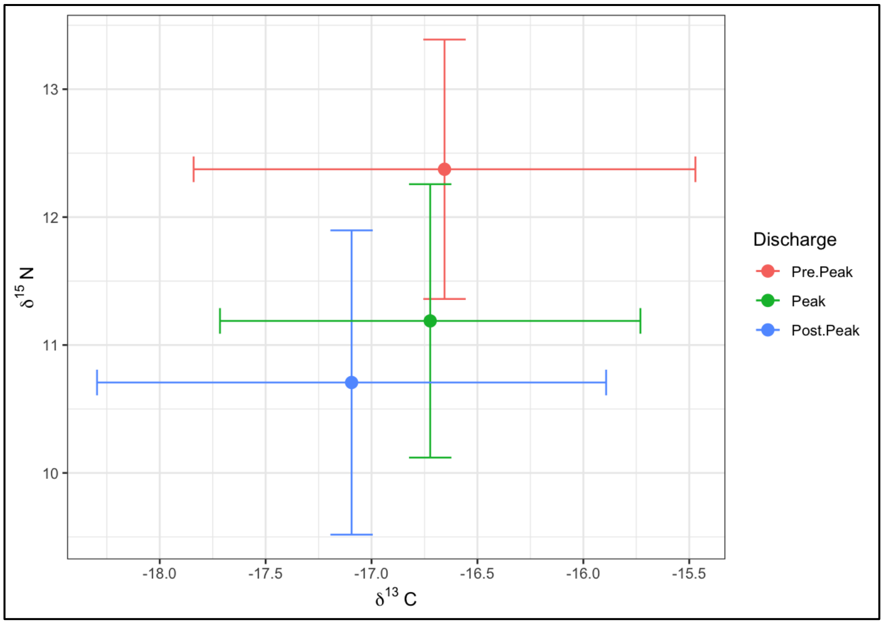

Figure 5. Averaged $\delta^{13}C$ and $\delta^{15}N$ isotope values (± standard deviation) for crescent gunnels by discharge rates, combined for all sites. Pre-peak discharge (March-May), peak discharge (June-July), post-peak discharge (August-September).

Table 4. Tukey Honest Significant Difference (HSD) pairwise comparisons between each discharge periods. The symbol * represents significant adjusted p-value (p adj < 0.05). DIFF represents the difference between the lower (LWR) and upper (UPR) bounds of the adjusted p-value (p-ADJ).

	DIFF	LWR	UPR	p-ADJ
$\underline{\delta^{13}C}$				
Pre-Peak – Post-Peak	0.439	0.035	0.842	0.029*
Pre-Peak – Peak	0.068	-0.354	0.489	0.924
Post-Peak – Peak	-0.371	-0.726	-0.017	0.029*
$\underline{\delta^{15}N}$				
Pre-Peak – Post-Peak	1.667	1.270	2.063	<0.0001*
Pre-Peak – Peak	1.185	0.771	1.599	<0.0001*
Post-Peak – Peak	-0.482	-0.830	-0.133	0.004*

Resource Use by Three Nearshore Fish Species along Glaciated Watersheds during the Post-peak Discharge Period

The three fish species showed significant differences in $\delta^{13}C$ values (ANOVA, $p = 0.0162$) by site and were not significantly different among sites for $\delta^{15}N$ (ANOVA, $p = 0.095$). Staghorn sculpins, on average, had the highest $\delta^{15}N$ values, while starry flounders had the highest $\delta^{13}C$ values (Figure 6). Crescent gunnels had similar $\delta^{13}C$ values as staghorn sculpins and similar $\delta^{15}N$ values as starry flounders. The $\delta^{13}C$ and $\delta^{15}N$ values for each fish species were significantly different by site (ANOVA, $p > 0.05$) (Table 5). For crescent gunnels, most site comparisons were significantly different for both δ^{13}C and δ^{15}N values. Staghorn sculpin and starry flounder, however, were significantly different for both δ^{13}C and δ^{15}N at fewer (less than half) site combinations (Table 6).

Crescent gunnels and starry flounders showed decreasing δ^{13}C values with increasing glacial cover (Figure 7), except for the site with 60% glacial cover, which had a higher δ^{13}C value than the other sites (e.g., Wos at 27%) with higher glacial cover. Staghorn sculpins showed no distinct trends except for the low δ^{13}C values at the intermediate glaciation site, Halibut (16%). Primary producers (macroalgae, POM.mix, marsh plant, and upland plant) did not differ among sites except for a slight trend of decreasing δ^{13}C values with increasing glacial cover in POM.mix (Figure 7). No patterns are visible in δ^{15}N values by site except for marsh plants, which exhibited decreasing δ^{15}N values with increasing glacial cover (Figure 8).

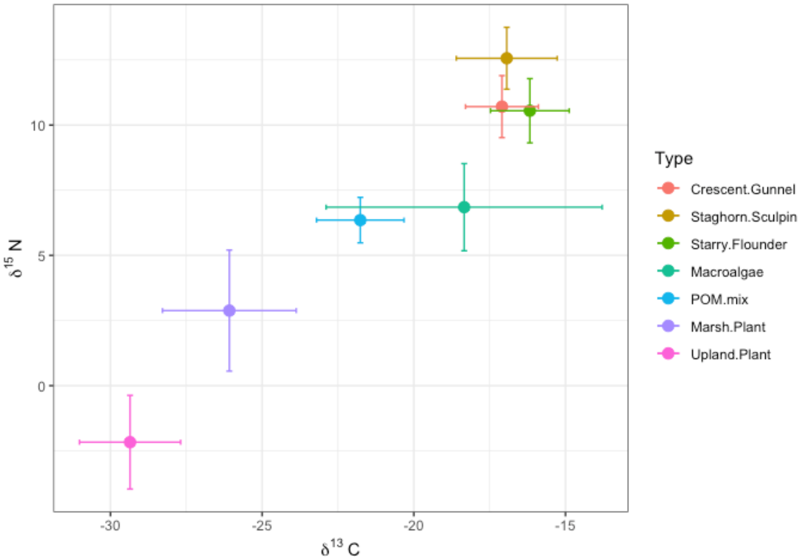

Figure 6. Average δ^{13}C and δ^{15}N isotope values for crescent gunnels (CG), staghorn sculpin (SS), starry flounder (SF), and various primary producers during the post-peak discharge period, combined across all sites.

Table 5. Results from a one-way analysis of variance (ANOVA) for each fish species, by site, during the post-peak discharge period. The * symbol indicates a significant p-value (< 0.05).

	DF	Sum Sq	Mean Sq	F-value	Pr(>F)
δ^{13}C					
Crescent Gunnels (*P. laeta*)	4	65.51	16.378	17.08	<0.0001*
Staghorn Sculpin (*L. armatus*)	4	78.14	19.535	9.413	<0.0001*
Starry Flounder (*p. stellatus*)	4	41.65	10.41	11.08	<0.0001*
δ^{15}N					
Crescent Gunnels (*P. laeta*)	4	49.32	12.33	11.64	<0.0001*
Staghorn Sculpin (*L. armatus*)	4	24.36	6.090	5.005	0.00104*
Starry Flounder (*p. stellatus*)	4	23.60	5.899	5.146	0.0016*

Table 6. Tukey Honest Significant Difference (HSD) pairwise comparisons of δ^{13}C and δ^{15}N among sites for each species (crescent gunnels, staghorn sculpins, and starry flounders). The symbol * represents significant p-value (< 0.05). DIFF represents the difference between the lower (LWR) and upper (UPR) bounds of the adjusted p-value (p-ADJ).

	DIFF	LWR	UPR	p-ADJ
Crescent gunnel				
δ^{13}C				
Halibut (16%) – Jakolof (0%)	-0.921	-1.697	-0.145	0.011*
Tutka – Jakolof (0%)	-1.905	-2.662	-1.148	<0.0001*
Wos (27%) – Jakolof (0%)	-2.057	-2.865	-1.248	<0.0001*
Grewingk (60 %) – jakolof (0%)	-1.223	-1.986	-0.460	0.0001*
Tutka (8%) – Halibut (16%)	-0.984	-1.716	-0.251	0.003*
Wos (27%) – Halibut (16%)	-1.135	-1.921	-0.350	0.001*
Grewingk (60%) – Halibut (16%)	-0.302	-1.041	0.437	0.790
Wos (27%) – Tutka (8%)	-0.152	-0.918	0.615	0.982
Grewingk (60%) – Tutka (8%)	0.682	-0.036	1.400	0.072
Grewingk (60%) – Wos (27%)	0.834	0.061	1.606	0.027*
δ^{15}N				
Halibut (16%) – Jakolof (0%)	-1.222	-2.038	-0.406	0.001*
Tutka – Jakolof (0%)	-1.692	-2.487	-0.896	<0.0001*
Wos (27%) – Jakolof (0%)	-0.744	-1.593	0.106	0.116
Grewingk (60 %) – jakolof (0%)	-0.303	-1.105	0.499	0.834
Tutka (8%) – Halibut (16%)	-0.469	-1.239	0.300	0.445
Wos (27%) – Halibut (16%)	0.479	-0.347	1.304	0.497
Grewingk (60%) – Halibut (16%)	0.920	0.143	1.696	0.012*
Wos (27%) – Tutka (8%)	0.948	0.142	1.754	0.012*
Grewingk (60%) – Tutka (8%)	1.389	0.634	2.144	<0.0001*
Grewingk (60%) – Wos (27%)	0.441	-0.371	1.253	0.562*
Staghorn Sculpin				
δ^{13}C				
Halibut (16%) – Jakolof (0%)	-0.891	-2.174	0.392	0.308
Tutka (8%) – Jakolof (0%)	-2.462	-3.713	-1.211	<0.0001*
Wos (27%) – Jakolof (0%)	-0.465	-1.766	0.836	0.858
Grewingk (60 %) – jakolof (0%)	-0.331	-1.544	0.881	0.941
Tutka (8%) – Halibut (16%)	-1.571	-2.839	-0.303	0.007*
Wos (27%) – Halibut (16%)	0.426	-0.891	1.743	0.897
Grewingk (60%) – Halibut (16%)	0.560	-0.670	1.790	0.713
Wos (27%) – Tutka (8%)	1.997	0.710	3.283	0.0004*
Grewingk (60%) – Tutka (8%)	2.131	0.934	3.327	<0.0001*
Grewingk (60%) – Wos (27%)	0.134	-1.115	1.382	0.998

	DIFF	LWR	UPR	p-ADJ
Staghorn Sculpin con't				
$\delta^{15}N$				
Halibut (16%) – Jakolof (0%)	-0.993	-1.98	-0.011	0.0462*
Tutka – Jakolof (0%)	-1.229	-2.187	-0.271	0.005*
Wos (27%) – Jakolof (0%)	-0.327	-1.323	0.669	0.891
Grewingk (60 %) – jakolof (0%)	-0.139	-1.068	0.789	0.994
Tutka (8%) – Halibut (16%)	-0.236	-1.207	0.735	0.961
Wos (27%) – Halibut (16%)	0.666	-0.343	1.675	0.359
Grewingk (60%) – Halibut (16%)	0.854	-0.088	1.795	0.094
Wos (27%) – Tutka (8%)	0.902	-0.083	1.887	0.089
Grewingk (60%) – Tutka (8%)	1.090	0.174	2.006	0.011*
Grewingk (60%) – Wos (27%)	0.188	-0.768	1.144	0.982
Starry Flounder				
$\delta^{13}C$				
Halibut (16%) – Jakolof (0%)	-1.068	-2.218	0.083	0.081
Tutka – Jakolof (0%)	-1.971	-3.227	-0.716	0.0004*
Wos (27%) – Jakolof (0%)	-2.793	-4.129	-1.456	<0.0001*
Grewingk (60 %) – jakolof (0%)	-2.360	-4.222	-0.498	0.007*
Tutka (8%) – Halibut (16%)	-0.904	-1.908	0.101	0.096
Wos (27%) – Halibut (16%)	-1.725	-2.829	-0.621	0.0005*
Grewingk (60%) – Halibut (16%)	-1.292	-2.994	0.410	0.216
Wos (27%) – Tutka (8%)	-0.821	-2.034	0.391	0.321
Grewingk (60%) – Tutka (8%)	-0.389	-2.164	1.387	0.971
Grewingk (60%) – Wos (27%)	0.433	-1.401	2.266	0.962
$\delta^{15}N$				
Halibut (16%) – Jakolof (0%)	0.875	-0.396	2.145	0.305
Tutka – Jakolof (0%)	-0.541	-1.927	0.845	0.802
Wos (27%) – Jakolof (0%)	-0.338	-1.814	1.138	0.966
Grewingk (60 %) – jakolof (0%)	1.500	-0.556	3.556	0.250
Tutka (8%) – Halibut (16%)	-1.415	-2.524	-0.306	0.006*
Wos (27%) – Halibut (16%)	-1.212	-2.431	0.007	0.052
Grewingk (60%) – Halibut (16%)	0.626	-1.255	2.506	0.878
Wos (27%) – Tutka (8%)	0.203	-1.136	1.542	0.993
Grewingk (60%) – Tutka (8%)	2.041	0.080	4.001	0.0376*
Grewingk (60%) – Wos (27%)	1.838	-0.187	3.862	0.092

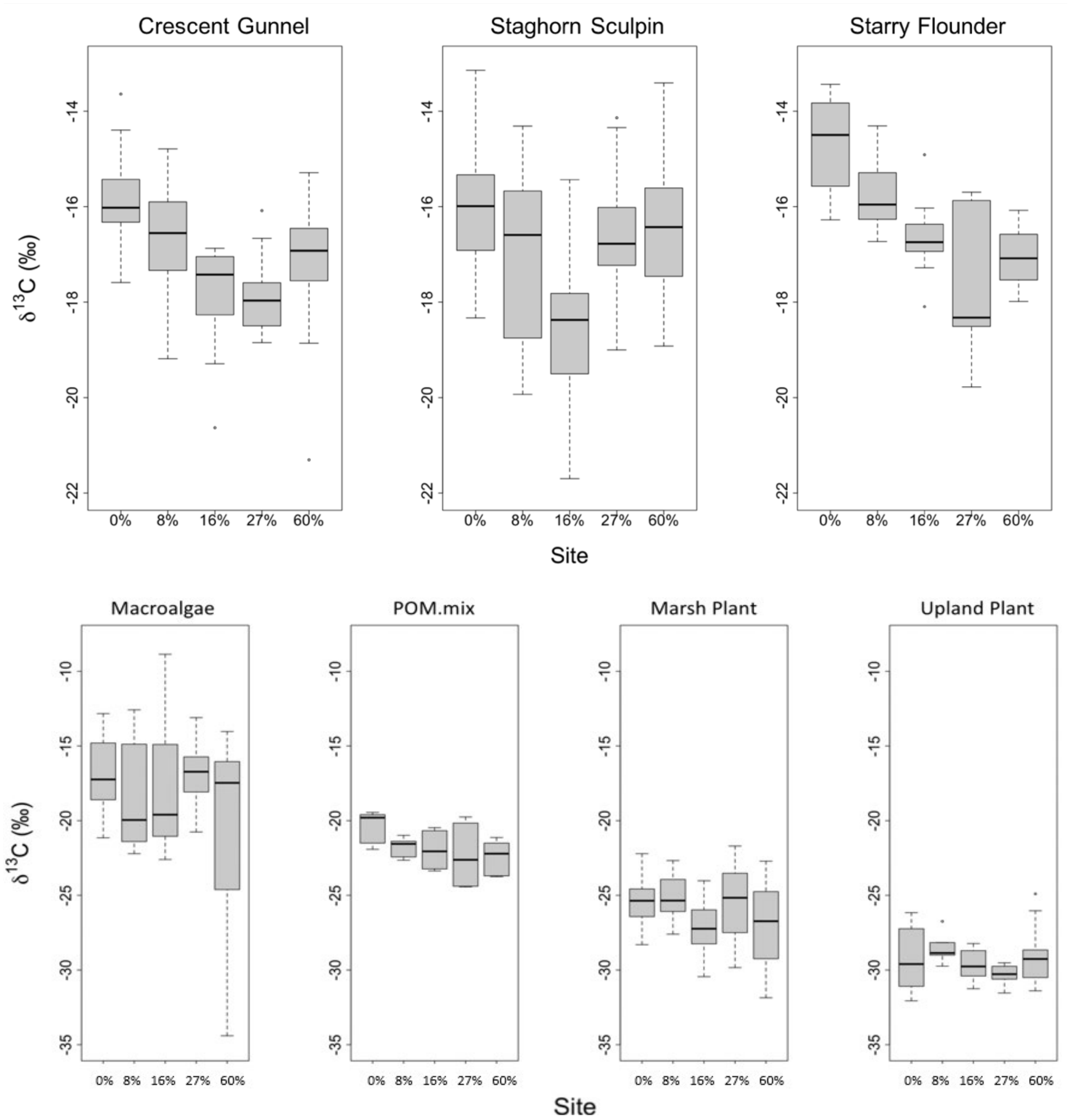

Figure 7. Boxplots showing δ^{13}C values of the three fish species and the primary producers across sites. Sites are denoted by their percent glacial cover (0% = Jakolof, 8% = Tutka, 16%= Halibut, 27% = Wos, 60% = Grewingk).

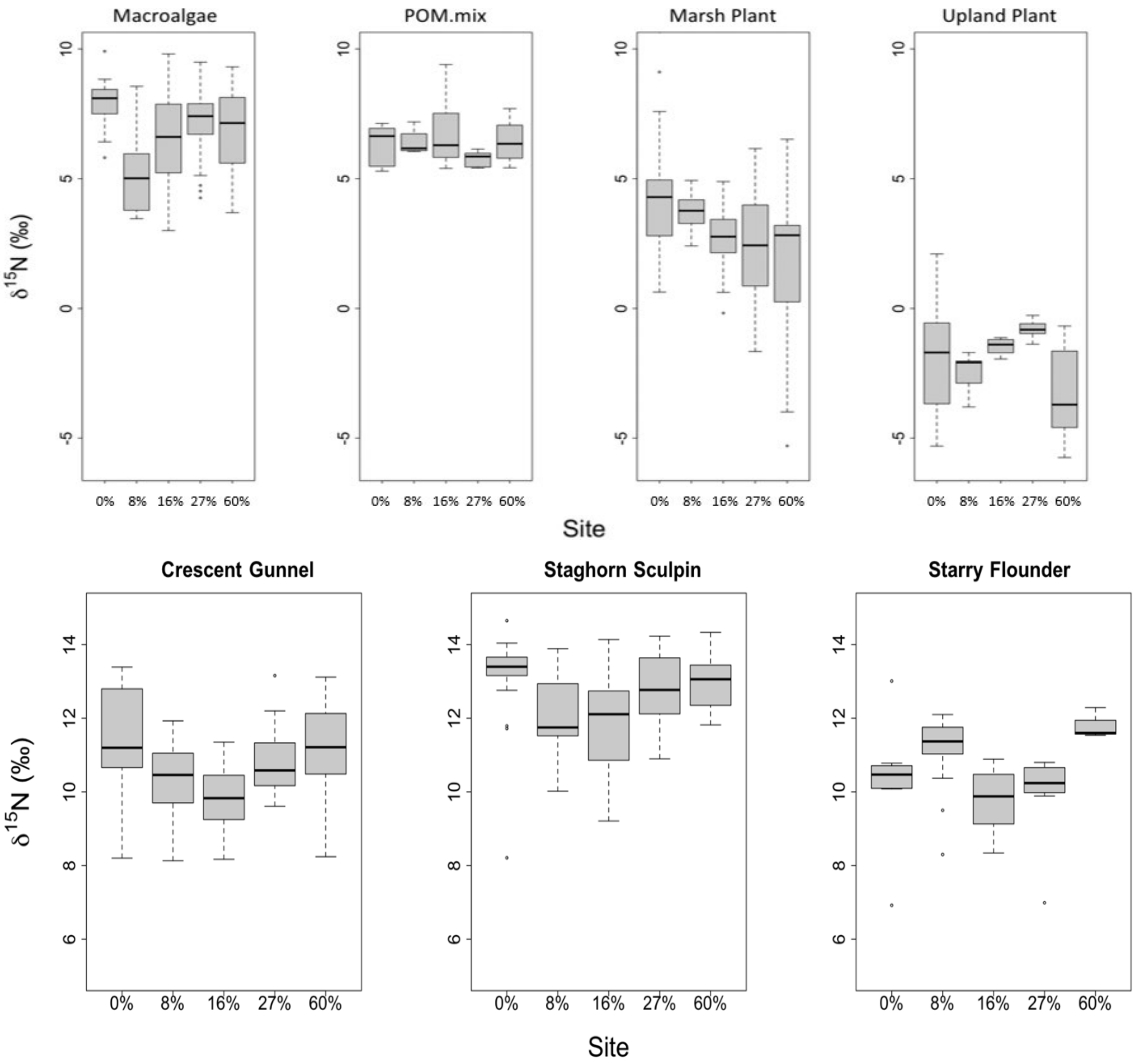

Figure 8. Boxplots showing $\delta^{15}N$ values of the three fish species and the primary producers across sites. Sites are denoted by their percent glacial cover (0% = Jakolof, 8% = Tutka, 16%= Halibut, 27% = Wos, 60% = Grewingk).

Discussion

Spatial Resource Use by Crescent Gunnels Relative to Watershed Glacial Coverage

Crescent gunnels, a resident location-bound species, may be good indicators of local conditions. The crescent gunnel stable isotope values differed by site, with higher $\delta^{13}C$ values in gunnels at sites with low glacial cover (especially Jakolof with 0% cover) than those at sites with higher glacial cover (especially Wos with 27% glacial cover). $\delta^{13}C$ values of crescent gunnels at other sites were in between these two endpoints. These results indicate that watershed characteristics such as glacial cover seem to play a role in resource use of crescent gunnels but not in a linear fashion with the percentage of glaciation of a watershed. If percent glaciation was the main driver of gunnel stable isotope values, then the highly glaciated Grewingk site (60%) should have shown the lowest δ^{13}C values. Instead, other watershed characteristics may affect nearshore conditions and resource use by gunnels. For example, while the Wos watershed only had 27% glaciation compared to the 60% at Grewingk, the discharge volume of the Wos watershed is the highest of all sites. This could reflect more reliance on trophic pathways linked to higher terrestrial matter inputs in a watershed with greater glacial coverage and high discharge volume. Terrestrial matter is typically depleted in ^{13}C compared to marine sources (Petersen 1999), and considering that glacial discharge is expected to transport high amounts of terrestrial matter into the nearshore environment (Ren et al. 2019), this could be a more significant basal resource in higher glaciated watersheds. Similar findings of lighter δ^{13}C values in consumers in these more glaciated watersheds were found for intertidal invertebrate consumers (Schloemer 2022). However, in that study, mixing model outputs determined that terrestrial matter was not a significant contributor to trophic pathways. Also, other watershed characteristics that were not linear with watershed glaciation, such as river length, vegetation percentage, and total suspended solids (TSS), were drivers in the isotope composition of invertebrate consumers in these watersheds (Schloemer 2022). Rather than terrestrial matter and glaciation itself, the author suggested that certain characteristics of glacial discharge (volume, TSS) influences the stable isotope composition of the marine primary producers, which was then reflected in the consumers. Another watershed characteristic that could be considered is coastline morphology, which would differentiate sites inside fjords (e.g., Tutka) from those that are more exposed (e.g., Wos and Grewingk). As a next step, I plan on testing various watershed attributes as drivers of fish stable isotope values and involving isotope mixing models, which would allow testing if fish consumers are similarly impacted by these watershed attributes or if fishes indeed rely on terrestrial-based trophic pathways as has been determined elsewhere in Alaskan glaciated watersheds (Whitney et al. 2018).

Changes in habitat such as fluxes in salinity, temperature, turbidity, and dissolved oxygen may cause shifts in horizontal biodiversity (Gabara et al., 2021). In other words, organisms at the base of the food chain (i.e., multiple primary producer groups of the same trophic level) may experience changes in composition (i.e., biodiversity). Therefore, isotopic signatures at the base of the food web can change accordingly, driven by changes in their environment. This change in baseline isotopic signatures impacts the organisms in higher trophic levels that directly or indirectly consume these primary producers. Such horizontal shifts in basal producer composition, which would have been transferred to crescent gunnels through intermediate invertebrate consumers, may have played a role in the differing δ^{13}C values observed. Since marsh and upland plants are associated with lower δ^{13}C values than marine-based primary producers (Figure 7, Peterson 1999), it is possible that a shift in producer biodiversity results in more availability of terrestrially-derived nutrients at sites with higher glacial influence. An example of this kind of shift is in coral reef systems; when reef habitat is lost, the base of the food web experiences a horizontal biodiversity shift (i.e., δ^{13}C shift) of the producer baseline value (Morillo-Velarde, et al., 2018) associated with a move from turf algae and epiphytes to particulate organic matter, which have different isotopic signatures. It is uncertain whether such changes have an impact on the length of the food chain or vertical biodiversity shifts (i.e., inter-trophic level). While the basal resource composition of watersheds may influence resource use by gunnels (as reflected by stable isotope composition), these nearshore fish were mostly associated with marine resources (Figure 6, macroalgae, POM.mix), at least during the post-discharge period. Using a mixing model approach separately for all three discharge periods would be able to shed light on the importance of basal producer diversity on the resource use by crescent gunnels. Understanding the use of different primary producer resources by consumers of mid-level trophic positions in high-latitude systems can help further our understanding of ecosystem resilience and the importance of biodiversity in resource use.

Variability in Resource Use by Crescent Gunnels in Relation to Glacial Discharge Regime

In addition to spatial differences associated with glacial coverage, crescent gunnels showed significant differences (ANOVA, $p < 0.05$) in their isotope values among different discharge regimes. This further supports the idea that crescent gunnels may be good indicators of local conditions. Glacial discharge in the Kachemak Bay study region undergoes distinct changes from pre-peak, to peak, to post-peak discharge over the course of the spring and summer (Figure 2). However, although both $\delta^{13}C$ and $\delta^{15}N$ values of crescent gunnels were significantly different among discharge periods, these differences were stronger in $\delta^{15}N$ than $\delta^{13}C$. While a decrease in $\delta^{15}N$ values from pre- to post-peak is typically viewed as a signal of a consumer shift to a lower trophic level, it is important to remember that the fish species in this study are generalists, and a more likely scenario is a shift in changing habitat conditions that favor certain primary producers over others. The changes in conditions are related to the distinct glacial discharge regimes these high-latitude estuarine systems experience (Beamer et al. 2016). Snow and glacier melt contributions in the late summer months cause changes in temperature, salinity, turbidity, dissolved oxygen, and water column structure (stratification) (Doroff and Holderied, 2018). Summer is also associated with the peak of the "spring bloom" of primary producers like diatoms in Kachemak Bay that begins in late April or early May and peaks in July (Doroff and Holderied, 2018), continuing through August when the biomass of diatoms begins to decline. This temporal trend is directly in line with the shift in $\delta^{15}N$ of gunnels and may reflect changing $\delta^{13}C$ baseline (primary producer) values. This shows that horizontal biodiversity (i.e., primary producer biodiversity available for consumers) may also impact vertical diversity (i.e., $\delta^{15}N$ values of consumers) in different habitats.

Resource Use by Three Nearshore Fish Species along Glaciated Watersheds during the Post-peak Discharge Period

All three fish species differed significantly (ANOVA, $p < 0.05$) in their isotope composition among the five sites of varying glacial influence. Spatial differences were most pronounced in crescent gunnels, again supporting the notion that gunnels may serve as sentinel species to detect changes in local conditions. Staghorn sculpin are moderately mobile in the nearshore and stay subtidal during low tide, but remain relatively close to the watershed resources. This mobility makes them more resilient to changing conditions as they can move to different locations or systems for feeding (Whitney et al., 2017). Starry flounder are considered highly mobile and inhabit the nearshore and move to the deeper subtidal. This allows them to avoid unfavorable food conditions in these estuaries, which was reflected in the more homogenous isotope composition across sites.

When compared to the resource space provided by the primary producer groups, the three fish species, were most closely related to the marine resources (macroalgae and POM.mix). Terrestrial producers were far removed from all three fish species, indicating that they likely contribute little to the trophic pathways sustaining these nearshore fish species. This further supports the idea that sites with more glacial influence or other watershed characteristics such as discharge volume may be experiencing a shift in baseline $\delta^{13}C$ values that influence resource use by nearshore fishes.

Acknowledgments

I would like to thank the Coastal Marine Institute and the Bureau of Ocean and Energy Management for supporting this project, a valuable addition to my master's thesis that contributed to a more well-rounded research endeavor. I would also like to thank Alaska EPSCoR Fire and Ice for collaboration and support and the Kasitsna Bay Laboratory for providing space to conduct my research. I would like to thank the College of Fisheries and Ocean Sciences for academic guidance during my graduate studies. I am very grateful to my advisor, Dr. Katrin Iken, who has provided endless advice and support, and to my committee members Dr. Vanessa von Biela, Dr. Kristen Gorman, and Dr. Andy Seitz for providing invaluable input and contributions to my project. Finally, I would like to thank my lab team and colleagues for their help collecting samples, developing ideas, troubleshooting, and providing support.

References

Arimitsu ML, Piatt JF, Mueter F. 2016. Influence of glacier runoff on ecosystem structure in Gulf of Alaska fjords. Marine Ecology Progress Series, 560:19-40.

Beamer JP, Hill DF, Arendt A, Liston GE. 2016. High-resolution modeling of coastal freshwater discharge and glacier mass balance in the Gulf of Alaska watershed. Water Resources Research, 52(5), 3888-3909.

DeNiro MJ, Epstein S. 1978. Influence of diet on the distribution of carbon isotopes in animals. Geochimica et Cosmochimica Acta, 42:495-506.

Doroff A, Holderied K. 2018. Exxon Valdez Oil Spill Long-Term Monitoring Program (Gulf Watch, Alaska) Final Report. Exxon Valdez Oil Spill Trustee Council Project, 16120114-G.

Gabara SS, Konar BH, Edwards MS. 2021. Biodiversity loss leads to reductions in community-wide trophic complexity. Ecosphere, 12(2):e03361. doi:10.1002/ecs2.3361.

Herzka SZ. 2005. Assessing connectivity of estuarine fishes based on stable isotope ratio analysis. Estuarine, Coastal and Shelf Science, 64(1):58-69.

Mintenbeck K, Brey T, Jacob U, Knust R, Struck U. 2008. How to account for the lipid effect on carbon stable-isotope ratio ($\delta^{13}C$): sample treatment effects and model bias. Journal of Fish Biology, 72(4): 815-830.

Mohan JA, Smith SD, Connelly TL, Attwood ET, McClelland JW, Herzka SZ, Walther BD. 2016. Tissue-specific isotope turnover and discrimination factors are affected by diet quality and lipid content in an omnivorous consumer. Journal of Experimental Marine Biology and Ecology, 479:35-45.

Morillo-Velarde PS, Briones-Fourzan P, Alvarez-Filip L, Aguiniga-Garcia S, Sanchez-Gonzalez A, Lozano-Alvarez E. 2018. Habitat degradation alters trophic pathways but not food chain length on shallow Caribbean coral reefs. Scientific Reports, 8(4109).

Neal EG, Hood E, Smikrud K. 2010. Contribution of glacier runoff to freshwater discharge into the Gulf of Alaska. Geophysical Research Letters, 37(6):L06404.

Peterson BJ. 1999. Stable isotopes as tracers of organic matter input and transfer in benthic food webs: a review. Acta Oecologica, 20(4):479-487.

Peterson CH. 2001. The “Exxon Valdez” oil spill in Alaska: acute, indirect and chronic effects on the ecosystem. Advances in Marine Biology, 39:1-103.

Peterson BJ, Fry B. 1987. Stable isotopes in ecosystem studies. Annual Review Ecology, Evolution and Systematics, 18:293-320.

Possamai B, Hoeinghaus DJ, Odebrecht C, Abreu PC, Moraes LE, Santos ACA, Garcia AM. 2020. Freshwater inflow variability affects the relative importance of allochthonous sources for estuarine fishes. Estuaries and Coasts, 43:880-893.

Post DM. 2002. Using stable isotopes to estimate trophic position: models, methods, and assumptions. Ecology Society of America, 83(3):703-718.

Potter IC, Tweedley JR, Elliott ME, Whitfield AK. 2013. The ways in which fish use estuaries: a refinement and expansion of the guild approach. Fish and Fisheries, 16(2):230-239.

Ren Z, Martyniuk N, Oleksy IA, Swain A, Hotaling S. 2019. Ecological stoichiometry of the mountain cryosphere. Frontiers in Ecology and Evolution,7:360.

Schloemer J. 2022. Marine and not terrestrial resources support nearshore food webs across a gradient of glacial watersheds in the northern Gulf of Alaska. M.Sc. Thesis, University of Alaska Fairbanks.

von Biela VR, Newsome SD, Bodkin JL, Kruse GH, Zimmerman CE. 2015. Widespread kelp-derived carbon in pelagic and benthic nearshore fishes suggested by stable isotope analysis. Estuarine, Coastal and Shelf Science, 181:364-374.

Whitney EJ, Beaudreau AH, Duncan DH. 2017. Spatial and Temporal Variation in the Diets of Pacific Staghorn Sculpins Related to Hydrological Factors in a Glacially Influenced Estuary. Transactions of the American Fisheries Society, 146(6):1156-1167.

Whitney EJ, Beaudreau AH, Howe ER. 2018. Using stable isotopes to assess the contribution of terrestrial and riverine organic matter to diets of nearshore marine consumers in a glacially influenced estuary. Estuaries and Coasts, 41(1):193-205.

The Department of the Interior Mission

As the Nation’s principal conservation agency, the Department of the Interior has responsibility for most of our nationally owned public lands and natural resources. This includes fostering the sound use of our land and water resources, protecting our fish, wildlife and biological diversity; preserving the environmental and cultural values of our national parks and historical places; and providing for the enjoyment of life through outdoor recreation.The Department assesses our energy and mineral resources andworks to ensure that their development is in the best interests of all our people by encouraging stewardship and citizen participation in their care. The Department also has a major responsibility for American Indian reservation communities and for people who live in island communities.

The Bureau of Ocean Energy Management

The Bureau of Ocean Energy Management (BOEM) works to manage the exploration and development of the nation's offshore resources in a way that appropriately balances economic development, energy independence, and environmental protection through oil and gas leases, renewable energy development and environmental reviews and studies.